Eidgenössische Technische Hochschule Zürich
Swiss Federal Institute of Technology Zurich

Mikhail Shein

Spin trapping of radicals in smoke and aerosols of various tobacco products

Master's Thesis

Laboratory of Physical Chemistry
EPR Group
Swiss Federal Institute of Technology (ETH) Zurich

Supervision

Prof. Dr. Gunnar Jeschke

11th February 2018

Abstract

Free radicals in cigarette smoke cause oxidative damage and contribute to smoke related diseases. New smoking and vaping products are marketed as a safer alternative. Electron paramagnetic resonance (EPR) studies of radical and nitric oxide (NO) levels and kinetics in mainstream smoke or aerosols created by different smoking/vaping products have been performed. The products were chosen to represent a broad variety of smoking products, including a conventional cigarette (3R4F research cigarette), a heat-not-burn product (*IQOS*) and two e-cigarettes with different liquid heating mechanisms (*Solaris* and *MESH*). Short-lived gas phase radicals have been spin trapped by *N*-*tert*-butyl-α-phenylnitrone (PBN) and 5-*tert*-butoxycarbonyl-5-methyl-1-pyrroline-*N*-oxide (BMPO), while toluene extracts containing long-lived particulate phase radicals were measured directly. NO was trapped from whole smoke by iron dithiocarbamate (Fe(II)-$(DETC)_2$) complexes. Overall, radical levels produced by the HNB-product *IQOS* and by the e-cigarettes *MESH* and *Solaris* were 94-99% lower than that of the research cigarette 3R4F and generally similar to background levels. No nitric oxide was found in aerosols of the e-cigarettes and only 6-7% of the 3R4F level was found in *IQOS* aerosol. These results pair well with the previously published findings of reduction in levels of Harmful and Potentially Harmful Constituents (HPHCs) in aerosols of HNB-products and e-cigarettes. The toxicological implications of reduced radical levels remain unclear.

Contents

List of Figures

List of Tables

List of Schemes

Chapter 1

Introduction

In 1999 Baker spoke of 2000 known substances in cigarette smoke.[1] This number rose to 4800 until 2006[2] and in 2013 Rodgman and Perfetti report of more than 6000 chemical compounds, divided in four broad classes: hydrocarbons, oxygen-containing components, nitrogen-containing components and miscellaneous components.[3] Many of these substances are carcinogen, toxic, mutagen or addictive. The most comprehensive list of *Harmful and Potentially Harmful Constituents in Tobacco Products and Tobacco Smoke* (HPHCs) is established by the US Food and Drug Administration (FDA) and names 93 substances.[4] The presence of these (and possibly further) dangerous chemicals in smoke leads to an estimated death toll of approximately 480,000 annually in the United States alone.[5] It is a great desire of health scientists and regulatory administrations to give better toxicity estimates to the public and the smokers. For many decades, CO, tar and nicotine levels were used as standard toxicity indicators, although these advertisements are often criticized for being deceiving.[1, 6] Nowadays, scientists hope to give better estimates by using biomarkers, however, such indicators suffer from individual characteristics of the human and the product.[6] On the other hand, the desire to better grasp the chemistry of cigarettes and create safer products is the driving force behind tobacco research.[7]

In the last decade tobacco companies have introduced a variety of new "safer", smoke-free products. Most prominent are electronic cigarettes, or shorter e-cigarettes - and Modified-Risk Tobacco Products (MRTPs) such as heat-not-burn (HNB) products. While the popularity of such alternative tobacco(-free) smoking devices is growing fast, neither of these types of products are exactly new. The first e-cigarette was developed by Herbert A Gilbert in 1963.[8] However, the product did not catch on and the invention was only rediscovered in China in the beginning of the 2000s.[9, 10] Similarly, although not a commercial success, heat-not-burn products have been introduced in 1988 and were even studied for their radical production.[11, 12]

The now growing popularity of these products is explained by the fact that many users consider "vaping" safe or at least generally less toxic than smoking.[10] However, there is insufficient data to support such claims. A recent report *Public Health Consequences of E-Cigarettes* by an expert committee of the National Academies of Sciences, Engineering, and Medicine from January 2018 summarized findings on e-cigarette toxicology.[13] While they found substantial evidence that e-cigarettes emit significantly lower amounts of HPHCs (except for nicotine) and completely switching from usual combustible cigarettes reduces adverse health-effects, the report also supports the worries of many Anti-Smoking advocates that e-cigarettes may act as a gateway to normal cigarettes for the youth and young adults. In a similar fashion, an FDA advisory panel assessed in January 2018 a HNB-product by Philip Morris International (PMI) called *IQOS*. The panel ruled 8 to 1 in favor of the claim that switching from common cigarettes to *IQOS* decreases exposure to HPHCs, however, since lower toxic levels do not necessarily translate to a reduced health hazard, the panel found studies presented by PMI insufficient to claim reduced 'risk of harm'.[14] Some of the uncertainties in regard to MRTPs stems from the use of new substances such a glycerol

and propylene glycol for aerosol production. Although these substances are FDA approved, their toxicological implications upon inhalation are poorly known.[15]

Cigarette smoke, a highly concentrated aerosol system consisting of a particulate and a gas phase, is produced in a dynamic tobacco burning process with various oxygen-concentrations along the cigarette rod.[1] The temperatures in the combustion zone range from 200 to 950°C, allowing a variety of reactions to take place, such as pyrolysis, combustion and distillation. When the smoke cools down below 350°C, smoke particulate forms with 30-50% of the particles being neutral and the remainder equally divided in positively and negatively charged.[1] Further, the particulate phase of the smoke plays a key role in the delivery of several substances, for instance, nicotine and glycerol. Studies found, that only 70% of nicotine is recovered in smoke, emphasizing decomposition processes taking place in the cigarette. Decomposition leads to toxic side products and to reactive species such as radicals.[1, 3]

Radicals in the cigarette smoke were thought for many years to be too short-lived to be toxicologically relevant. It was not until the work of Lyons *et al.* [16] in which the existence of persistent radicals in tobacco smoke was proven that scientists started to consider a link between radicals and smoke related diseases. Major contributions in the field include the study by Bluhm *et al.* [17], where for the first time short-lived radicals were analyzed and that of the group of Pryor which showed that radicals of cigarette tar cause DNA damage.[18] Nowadays many smoke-related diseases, such as cardiovascular diseases, cancer, lung diseases and neurodegeneration can be linked to oxidative stress created by the presence of radicals.[19–23] Nevertheless, radicals are presently not part of the FDA 93-list and thus, no maximal radical levels are defined for cigarette smoke.

In tobacco smoke, two types of radicals can be found: short-lived radicals which are predominantly found in the gas phase and can only be analyzed if they are spin trapped and long-lived ones, which exist in the particulate phase and whose signal intensity stays constant over several days.[24] Both groups of radicals have been studied extensively; important findings on the particulate phase radicals are summarized in a review by Dellinger *et al.* [25] and a comprehensive review on smoke spin trapping experiments is presented by Robinson and Johnson[26]. In this context, the fundamental work of the group of Pryor from the 1980s and 1990s should be pointed out.[18, 24, 27]

The constant production of gas phase radicals was thought for a long time to be directly connected to nitric oxide[27]: NO is slowly oxidized to NO_2 which then readily reacts with unsaturated carbohydrates in the smoke, creating new carbon-centered radicals. NO itself, however, is rather unreactive. It is an important neurotransmitter and thus its presence in the cigarette smoke is connected to adverse health effects.[28, 29] NO is abundant in smoke (500–600 μg per cigarette[30–32]) and originates mainly from nitrates in tobacco, and partially from oxidation of gaseous nitrogen and of nitrogenous proteins and amino acids.[1]

For many years, tobacco companies funded research into the role of NO in radical chemistry. Particularly the rates of oxidation in the gas phase and in whole smoke have been studied for many years in hopes of eventually connecting all pieces to a bigger picture and, for instance, to update the "steady-state model" of Pryor.[27] Typically, methods of choice to study NO radicals have been Infrared (IR) spectroscopy or tunable infrared laser differential absorption spectroscopy (TILDAS).[33, 34]

Another possibility to study NO is spin trapping using iron(II)-dithiocarbamate complexes.[35, 36] The paramagnetic mononitrosyl complexes can be measured with Electron Paramagnetic Resonance (EPR) spectroscopy. EPR is a selective and sensitive method for radical research and in combination with the spin trapping technique, even short-lived radicals can be examined and potentially identified and quantified.

The majority of cigarette smoke radical research has been performed using EPR. However, while the understanding of reactions taking place inside a burning cigarette has gradually improved, research into new (tobacco) products is mostly uncharted. In several studies chemical composition of the produced aerosols has been analyzed and radical emissions briefly addressed[30, 31, 37,

38]. To the best of our knowledge, no study so far has directly compared radical levels between conventional cigarettes and different types of smoking/vaping products. The goal of this thesis is to establish a methodology for spin trapping experiments and to compare quantitatively radical and NO levels and kinetics between a 3R4F research cigarette, a heat-not-burn product and two different e-cigarettes.

Chapter 2

Theoretical background

2.1 EPR spectroscopy

Electron paramagnetic resonance (EPR) spectroscopy, also known as electron spin resonance (ESR) spectroscopy, is a technique with the underlying principle of the absorption of electromagnetic waves in the microwave frequency range by paramagnetic species in a magnetic field.[39] This technique is closely related to nuclear magnetic resonance (NMR) with the difference that in the case of EPR electrons instead of nuclei absorb electromagnetic energy. The degenerate energy levels of electrons are Zeeman split in the presence of a magnetic field due to the intrinsic spin property of the elementary particles. By varying either the frequency of the electromagnetic radiation or the strength of the magnetic field, electrons can be brought to resonance and can absorb energy to transition between the α and β states. The energy level splitting between the two states ΔE in a static magnetic field B_0 can be described as

$$\Delta E = g\mu_B B_0 = |\vec{\mu}|B_0 \tag{2.1}$$

with g being the Landé factor (or the g factor), μ_B the Bohr magneton and $\vec{\mu}$ the magnetic moment of the electron, which is equal to

$$\vec{\mu} = -g\mu_B \vec{S} \tag{2.2}$$

where $\vec{S}$ is the electron spin angular momentum. For a free electron, g has a value of $g = 2.0023$. The energy difference can also be described in terms of angular frequency ω_0, also called *Larmor frequency*:

$$\omega_0 = \frac{g\mu_B B}{\hbar} \tag{2.3}$$

In the proximity of nuclei with spin $I \neq 0$, the energy levels of the electron are further split due to hyperfine coupling. In the fast tumbling regime of the paramagnetic species (which is a good approximation for liquid solutions)[39] the hyperfine contribution (also known as Fermi-contact contribution) E_{hf} can be described as

$$E_{hf} = a\vec{S} \cdot \vec{I} \tag{2.4}$$

with $\vec{I}$ being the nuclear spin angular momentum and a the isotropic hyperfine coupling constant. This formula explains that a coupling to a nucleus with a spin quantum number $I = 1/2$ (e.g. ^{1}H) leads to a splitting into two lines while a coupling to a nucleus with $I = 1$ (such as ^{14}N) creates a

three-line splitting. The total number of electron Zeeman levels (and thus total number of lines) N is described by

$$N = \prod_k (2I_k + 1), \tag{2.5}$$

where I_k is spin quantum number of the k-th nucleus coupling to the electron spin. This principle is shown in Figure 2.1 with a simulated CW-EPR spectrum (see below) of a nitroxide (PBN adduct) where the electron couples to the nitrogen and the β-hydrogen atoms.

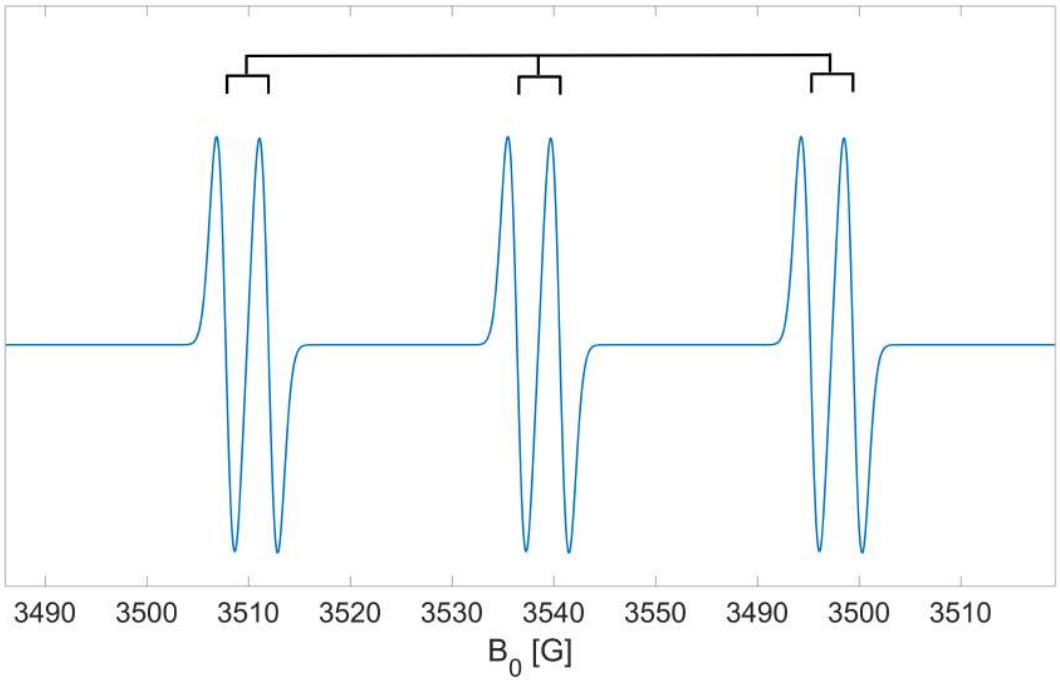

Figure 2.1: Simulated spectrum of the *N-tert*-butyl-α-phenylnitrone (PBN) adduct with a carbon-centered radical in toluene at room temperature. Simulation parameters: $g = 2.006$, $a_N = 14.4$ G, $a_H = 2.1$ G, microwave frequency 9.88 GHz and line-width 0.9 G (according to [40] and [41]). The long horizontal bar indicates the line splitting due to coupling to nitrogen and the three small horizontal bars show splitting due to β-hydrogen.

A real sample, however, consists of a multitude of spins which can be described macroscopically.[39] Magnetic polarization of a spin ensemble can be depicted by the magnetization vector $\vec{M}$ and its respective Cartesian components M_x, M_y and M_z. In a static magnetic field B_0 along the z-axis, the equilibrium magnetization vector M_0 is aligned along the positive z-direction. The equilibrium is disturbed by oscillating microwaves of angular frequency ω_{mw} acting along the x-axis and creating a small time-dependent field B_1. The magnetization vector is then rotated towards the x/y-plane and starts rotating (precessing) about the large B_0 field with the Larmor frequency ω_0 and about the small B_1 field with an angular frequency ω_1.

Over time, spins tend to relax and restore the equilibrium magnetization M_0 by interacting with the surrounding lattice (spin-lattice or longitudinal relaxation) or with each other (spin-spin or transverse relaxation). Phenomenologically, combining the motion of the magnetization with spin

relaxation terms in a rotating coordinate frame yields the *Bloch-equations*:

$$\begin{aligned}\frac{\mathrm{d}M_x}{\mathrm{d}t} &= M_y(\omega_{\mathrm{mw}} - \omega_0) - \frac{M_x}{T_2} \\ \frac{\mathrm{d}M_y}{\mathrm{d}t} &= M_z\omega_1 - M_x(\omega_{\mathrm{mw}} - \omega_0) - \frac{M_y}{T_2} \\ \frac{\mathrm{d}M_z}{\mathrm{d}t} &= -M_y\omega_1 - \frac{M_z - M_0}{T_1}\end{aligned} \tag{2.6}$$

T_1 and T_2 represent the longitudinal and transverse relaxation time, respectively. Spin relaxation directly influences spectral qualities, as the observed line width is proportional to $1/T_2$. However, several relaxation mechanisms can contribute to or one mechanism can dominate the total relaxation rate. In solutions, broadening of the line can be caused by the presence of oxygen: through collisions between the paramagnetic oxygen molecules and other radical species spin exchange can occur and thus contribute to spin-spin relaxation. This effect is commonly referred to as oxygen broadening.[42]

2.2 Spin trapping

Measurements of free radicals by EPR are often limited by their reactivity and thus short lifetimes and low concentrations. While direct EPR can not be applied in such cases, a technique known as spin trapping often allows the study of these reactive radicals.

Spin trapping has been developed in the second half of the 1960s. One of the pioneers of spin trapping, Edward G. Janzen, wrote in 1971:

> *"The possibility that a radical addition reaction might provide a means of detecting short-lived radicals had initially been considered during mechanistic studies of the dehydrogenation of hydroaromatics with hot nitro-benzene and thermal decomposition of nitro aromatics."*[43]

This statement summarizes the idea and principle behind spin trapping. As depicted in the following scheme

$$\underset{\substack{\text{(paramagnetic)}\\ \text{short-lived}}}{\mathrm{R}\cdot} + \underset{\text{(diamagnetic)}}{\mathrm{ST}} \longrightarrow \underset{\substack{\text{(paramagnetic)}\\ \text{long-lived}}}{\mathrm{R}-\mathrm{ST}\cdot} \tag{2.7}$$

where the free radical is abbreviated with R and the spin trap with ST, a (radical) spin adduct $\mathrm{R}-\mathrm{ST}$ is formed by the covalent bonding of radical and the spin trap.[44] By trapping the radical, the paramagnetism of the short-lived radical is transferred to the diamagnetic spin trap forming the relatively stable spin adduct. A major advantage is that the spin trapping reagents themselves are generally EPR silent and do not disturb the measurement. A notable downside of the spin trapping technique is that after the trapping reaction the unpaired electron is located on the spin trap, far away from the radical of interest itself. This limits the structural information gain: the great distance between the nitroxide functionality and the bound radical often makes resolution of the small coupling constants impossible and variation of the g value minimal. Additionally, the coupling constant of the nitrogen atom is often only weakly dependent on the bound radical which leaves structural information gain mostly to hyperfine coupling to adjacent protons of the spin adduct.[45, 46]

Typically, nitrone and nitroso compounds have been employed as spin traps (see Scheme 2.1).[44–46] The advantage of nitroso compounds over nitrone traps are generally faster reaction rates with

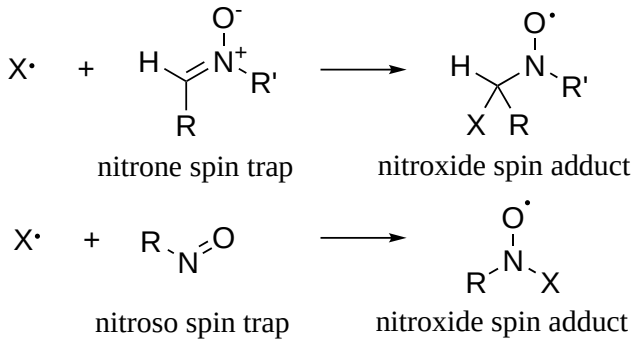

Scheme 2.1: General reaction scheme of nitrone and nitroso spin traps with radicals to form a nitroxide spin adduct. The radical is abbreviated with X.

radicals and greater information gain due to the proximity of the trapped radical to the nitroxide group. However, these chemicals are considered to be less stable (photochemically and thermally) than nitrone based adducts, usually do not form stable adducts with oxygen-centered radicals, are highly toxic and tend to form dimers.[28]

In the past, standard spin traps of choice were the nitrone traps *N*-*tert*-butyl-α-phenylnitrone (PBN) and 5,5-dimethyl-1-pyrroline-*N*-oxide (DMPO) (see scheme 2.2). In comparison to the linear PBN, the latter is a representative of pyrroline-based cyclic nitrones which show a greater dependence of the β-hydrogen coupling constant on bound species.[46] Coupling constants of spin adducts with numerous chemicals have been measured in the past and can help to identify unknown detected species. Especially adducts with PBN and DMPO have been well characterized and tabulated data was published already in 1987[47]. Nowadays the National Institute of Environmental Health Sciences (USA) provides a large database for spin adduct data[48]. A simulated spectrum of an adduct of PBN with a carbon-centered radical is shown in Figure 2.1.

Although both spin traps are still often used in modern research, early studies showed disadvantages of these traps. Fast decay of adducts to EPR silent compounds, degradation of adducts to different nitroxide species (as it is the case for DMPO-OOH which converts to DMPO-OH[49]), low reaction rates with radicals, cytotoxicity (relevant for biological studies), artifacts due to competing reactions with non-radical species (e.g. Forrester-Hepburn reaction[28]), oxidation and thus deactivation of the spin trap itself and difficulties in signal separation due to similar coupling constants were major issues associated with these early traps.[28, 46, 50] Several of these problems were resolved with development of new spin traps, specifically designed to address different issues. Nitrone spin traps such as 5-*tert*-butoxycarbonyl-5-methyl-1-pyrroline-*N*-oxide (BMPO), 5-(diethoxyphosphoryl)-5-methyl-1-pyrroline-*N*-oxide (DEPMPO), 2,2-dimethyl-4-phenyl-2*H*-imidazole-1-oxide (DMPIO), 5-(diisopropoxyphosphoryl)-5-methyl-1-pyrroline-*N*-oxide (DIPPMPO), 2,2,4-trimethyl-2*H*-imidazole-1-oxide (TMIO) and α-(4-pyridyl 1-oxide)-*N*-tert-butylnitrone (POBN) have been synthesized to facilitate line separation through stronger variation in coupling constants[51, 52], to enhance stability of adducts with the superoxide radical $O_2^{\cdot-}$ [51, 53], to improve solubility properties[44] or to add a new source of information through introduction of a phosphor-centered group (which provides an additional coupling). In Scheme 2.2 **A**, spin traps which were used in quantitative measurements of this work, PBN and BMPO, are presented and their general reaction scheme with a radical R is shown. Other spin traps which were tested in initial experiments are displayed in Scheme 2.2 **B**.

Nitric oxide (NO) is a rather unreactive radical and does not form adducts with common spin traps.[44] Instead, NO can be trapped by Fe(II) thiocarbamate complexes by forming a coordination bond.[28, 35, 54, 55] This spin trapping experiment has also been previously performed on cigarette smoke.[36]

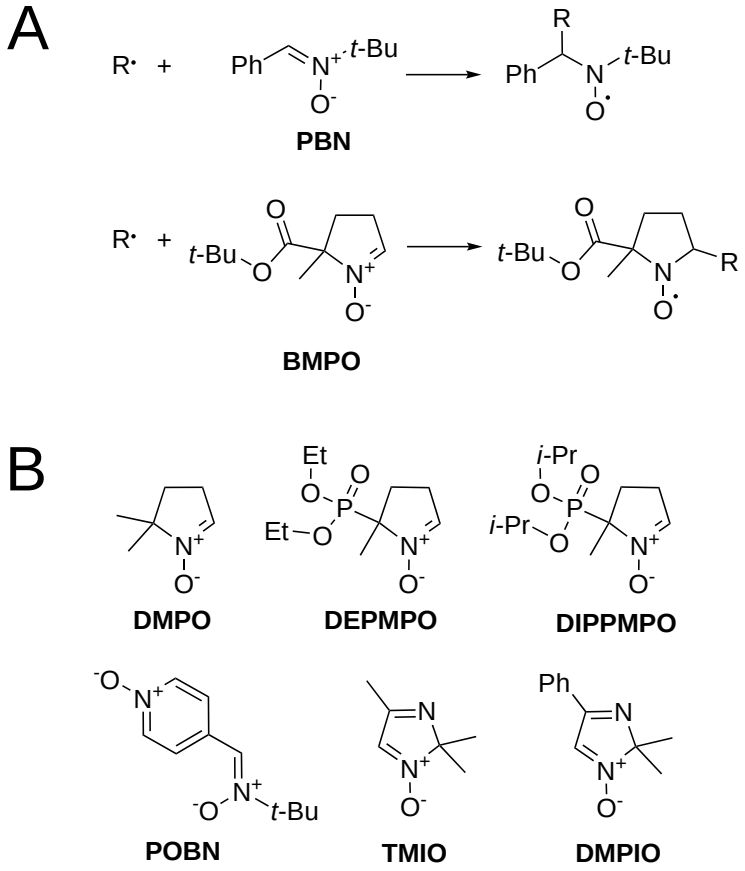

Scheme 2.2: **A**: General reaction scheme of PBN and BMPO with a radical R. **B**: Spin traps which were tested in initial experiments.

Typically, two different iron complexes are used, the hydrophilic iron-bis(*N*-methyl-*D*-glucamine-dithiocarbamate) complex (Fe^{2+}-$(MGD)_2$) and the hydrophobic iron-bis(diethyldithiocarbamate) complex (Fe^{2+}-$(DETC)_2$).[54] While the first one has been used in cigarette smoke study by Shinagawa in 1998 in an aqueous medium[36], in this work the iron-DETC complex is employed in order to trap NO in toluene. The mononitrosyl iron complex (MNIC) with DETC (MNIC-DETC) is reported to have a square-pyramidal structure with the Fe-N-O bond being almost linearly aligned along the z-axis,[35] as depicted in Scheme 2.3. As the unpaired electron is generally located in the antibonding d_{z^2} orbital, formally iron is reduced to the valence state Fe(I).[35] At room temperature the complex is characterized by a broad isotropic triplet with $g = 2.04$ and a splitting of $a_N = 12.5$ G.[35] A representative simulated spectrum can be seen in Figure 2.2.

2.3 Smoke analysis

Cigarette smoke is divided into three types of smoke: mainstream smoke (MS), sidestream smoke (SS) and environmental tobacco smoke (ETS).[1] By mainstream smoke scientists refer to the *"highly concentrated, dynamic aerosol system"*[1] which is drawn by the smoker himself from the butt end of the cigarette into the mouth and lungs. In between puffs the cigarette smolders

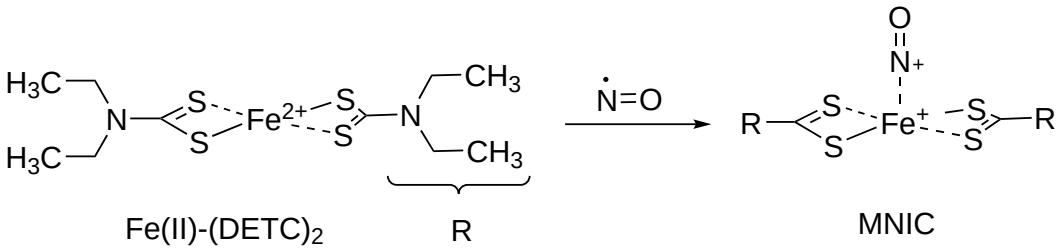

Scheme 2.3: General reaction scheme of the Fe(II)-bis(diethyldithiocarbamate) complex with an NO radical forming MNIC-DETC.

and releases sidestream smoke into the surrounding air. Environmental tobacco smoke consists of sidestream smoke and exhaled mainstream smoke greatly diluted by the ambient air.

Traditionally, for further analysis cigarette smoke is separated into a particulate phase and a gas phase by a Cambridge Filter. This glass fiber filter pad (stabilized with an organic binder) is 99% efficient at trapping smoke particulate with the size larger than 0.1μm.[1] Smoke constituents collected on the filter pad are referred to as Total Particulate Matter (TPM) while the vapor phase not held back by the filter is defined as gas phase. The latter has to be differentiated from whole smoke which is the total smoke aerosol not separated by the filter pad.

Although the separation of the gas and particulate phases is not absolute and some vapor phase is retained by the filter pad[1], it is justified since these two phases have different redox properties, for example gas phase smoke is oxidizing and the particulate phase reducing, making whole smoke slightly less oxidizing than the gas phase.[20] In research on free radicals in cigarette smoke this separation seemed to be necessary since radicals found in the two phases are significantly different: radicals in the gas phase are short-lived with expected lifetimes ranging from 30 to less than a second and thus have to be spin trapped in order to be studied.[27, 41, 56] Additionally, a combination of several different spin traps is recommended due to trapping specifity or, more generally, to variations in reaction rate constants for addition of different radicals.[26, 46] On the other hand, radicals trapped on the Cambridge Filter are long-lived and can be measured for days.[24] Based on these (and further) findings Pryor *et al.* suggested a "steady-state model" for the constant formation and destruction of radicals in cigarette smoke causing apparent lifetimes of gas phase radicals to be 5 min.[27, 41] The long-lived radicals were believed to be quinone/semiquinone type radicals which are formed from polyphenolic compounds such as catechol found in tobacco leaf.[20, 24] In modern literature TPM radicals are categorized into "primary type I", "primary type II" as well "secondary radicals", based on their respective formation temperature or process.[25] Type I radicals are assigned to tyrosyl radicals, the second type are believed to be poly- or oligomeric phenols with a delocalized unpaired electron and the last ones are found to resemble true (semi-)quinones.

However, using the Cambridge Filter pad may create artifacts and lead to wrong conclusions, as discussed in the following. The practice of phase separation by the Cambridge Filter was introduced by Tully *et al.* [57] and established in the 1970s by the group of Pryor[41] and has found wide acceptance in the scientific community for many years. This may seem contradictory to the fact that already in 1985 Borland *et al.* showed differences in reaction rates of NO in gas phase and whole smoke.[58] In 1990 Caldwell and Conner reported on artificial formation of tobacco specific *N*-nitrosamines on the CF.[59] A study by Culcasi *et al.* in 2006[60] indicated that whole smoke may be less toxic than gas phase vapor with significant implications for the overall toxicity of cigarette smoke. The publications by Bartalis *et al.* in 2007 and 2009[61, 62] which showed a decrease of trapped acyl radicals by 96% when the Cambridge Filter was used finally caused a re-evaluation of the "steady-state model" established by Pryor and his co-workers in 1984[27] and the overall usage of the CF. In his review *Gas-Phase Radicals in Cigarette Smoke: A Re-evaluation*

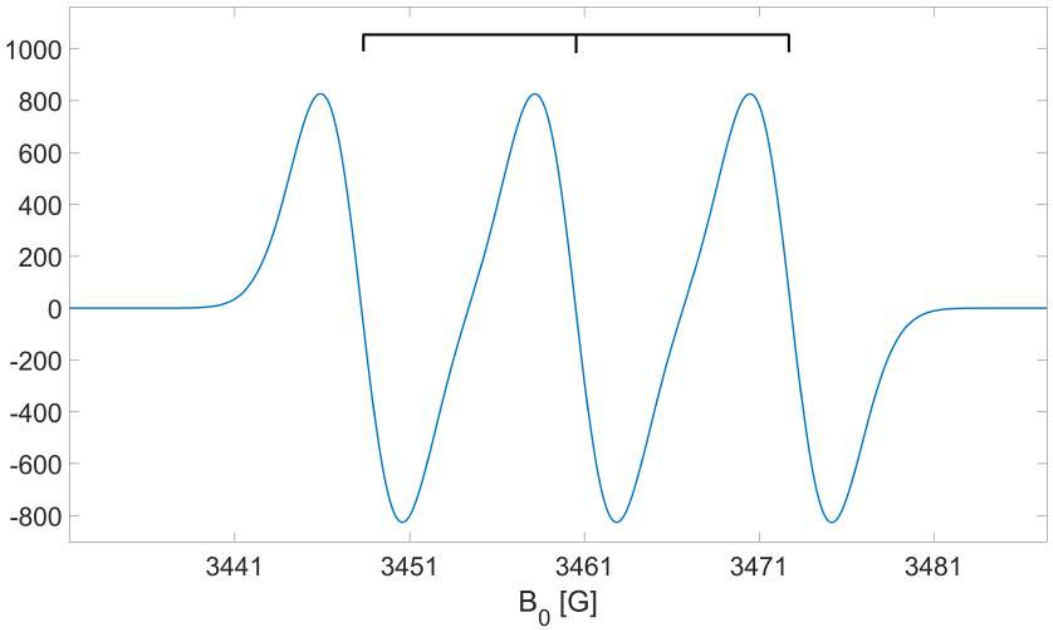

Figure 2.2: Simulated spectrum of the MNIC-DETC complex at room temperature. Simulation parameters: $g = 2.04$ and $a_N = 12.4$ G (according to [35]). The vertical bars indicates the line splitting due to coupling to nitrogen.

of the Steady-State Model and the Cambridge Filter Pad from 2011 Jan B. Wooten makes a strong argument for why the practice of phase separation by the Cambridge Filter pad is questionable and can create artifacts and lead to wrong conclusions.[7]

Analysis of cigarette smoke and overall performance requires repeatability. For quality assurance reasons cigarette manufacturers started using smoking machines as early as in the 1930s.[1] This allowed industry-wide publication of general yields for "tar", nicotine and carbon monoxide for the public to be able to differentiate levels of toxicity between different brands. While machine smoked[1] yields are often criticized for being misleading to the public, since machine smoking does not reflect actual smoking habits and may over- or underestimate the real amount of toxic substances received by the smoker[1, 6], they do help researchers to compare findings.

Early research on cigarette smoke has made it clear that comparison between different studies is flawed because the analytical methods and smoking regimes varied greatly between different publications.[1] To overcome this problem, the Cooperation Centre for Scientific Research Relative to Tobacco (CORESTA) proposed a well-defined set of recommended methods which were then adopted by the International Organization for Standardization (ISO) into standardized smoking regime parameters and instructions for smoke constituents analysis. The smoking regime parameters are commonly known as the ISO or FTC (Federal Trade Organization) testing regime. However, in modern research newer smoking regimes have been developed, specifically by the Canadian Government and the US State of Massachusetts, in order to better represent intense smoking habits.[6] Of particular importance is the requirement to block all ventilation holes in the filter since variation in filter ventilation accounts for 30% of differences in free radical levels between brands[64] and ventilation blocking reduces differences in overall yields between brands.[6] While the ranking between different cigarette brands is mostly independent of smoking regime[1, 6], in modern literature the Health Canada Intense (HCI) smoking regime is often recommended and used.[6] In Table 2.1 essential parameters of the different smoking regimes are summarized.

[1]The setup of a standard smoking machine is described in International Standard ISO 3308:2012.[63]

Table 2.1: Machine smoking parameters for different regimes.

parameters	ISO[1]	HCI[2,3]	CORESTA[4]
puff volume	35.0 ± 0.3 mL	55 mL	55.0 ± 0.3 mL
puff duration	2.00 ± 0.02 s	2 s	3 ± 0.1 s
puff frequency	60 ± 0.1 s	30 s	30 ± 0.5 s
puff profile	bell-shaped	bell-shaped	rectangular

[1] According to International Standard ISO 3308:2012.[65]

[2] According to Health Canada Official Method T-115.[66]

[3] Additional requirement: filter and tipping paper must be wrapped by single layer of tape.

[4] According to CORESTA recommended method no. 81.[67]

The same smoking regimes should not be applied to e-cigarettes. Several studies have been performed to determine vaping topography and define typical "vaping" behavior of e-cigarette consumers.[68–70] Based on these observations CORESTA proposed a recommended method no. 81 in April 2015 titled *Routine Analytical Machine for E-Cigarette Aerosol Generation and Collection — Definintions and Standard Conditions.*[67] Its essential parameters are presented in Table 2.1.

Chapter 3

Experimental procedures

3.1 Introduction of investigated products

In the course of this study four different tobacco and non-tobacco products were tested and their radical levels compared to each other. All products are presented in Figure 3.1. As a representative

Figure 3.1: Products used in this study. **1**: 3R4F research cigarette; **2**: *IQOS* (**2b**) with a *HEETS* stick (**2a**); **3**: *Solaris*, made up of a cartomizer (**3a**) and the battery (**3b**); **4**: *MESH*, made up of a cartomizer (**4a**) and the battery (**4b**).

of conventional cigarettes a 3R4F research cigarette was used (**1**). The cigarette is produced by the Center for Tobacco Reference Products (University of Kentucky, Lexington, Kentucky, USA) since

2008 and is used in the industry for quality control and brand comparison.[32] 3R4F is representative of a section of the American tobacco market with a blend consisting of flue-cured tobacco (35.41%), Burley (21.62%), Maryland (1.35%), Oriental (12.07%), reconstituted leaf (29.55%), glycerin (2.67%) and sugar (6.41%) and has a cellulose acetate filter.[32, 71]

The heat-not-burn (HNB) product *IQOS* (I Quit Ordinary Smoking) was developed by Philip Morris as a Modified-Risk Tobacco Product and is marketed as a healthier alternative to conventional smoking.[72, 73] It consists of a pen-shaped smoking device (**2b** in Figure 3.1) and an electronic charger/pen holder. Compatible tobacco sticks called *"HEETS"* (**2a**) are plugged into the pen and thus mounted on a ceramic blade which heats the stick up to 350°C.[73] Due to these relatively high temperatures the tobacco stick has to be pre-heated before drawing the first puff. The stick itself has the appearance of a short cigarette and is made up of a tobacco plug, a hollow tube, a polylactide resin filter and a final cellulose acetate filter (in this order, from plug to butt end).[74] The plug is produced from reconstituted tobacco mixed together with water, glycerol, propylene glycol, binders and flavor additives. The full list can be found in [74].

When the stick is heated, tobacco constituents evaporate and the formed aerosol is inhaled by the smoker. The important claim hereby is that the formed "aerosol" is not "smoke" since no signs of combustion are detected.[30] While traces of an incomplete combustion (pyrolysis) can still be detected, the amount of most harmful chemicals in the aerosol are reduced by 80-90% in comparison to the 3R4F cigarette.[30, 31] This can be explained by the fact that pyrolysis mostly takes place at higher temperatures as they are detected inside the combustion and pyrolysis zones of conventional cigarettes where temperatures range from 200 to 950°C.[1]

The last two products are e-cigarettes. Both of them consist of two parts, a cartomizer and a battery. Cartomizer is a portmanteau made up from "cartridge" and "atomizer" since it combines both a liquid container with the heating element and an atomizer which sprays the heated liquid (called *e-liquid*), creating the aerosol which is inhaled. The cartomizer can not be refilled and has to be disposed of after smoking.

Solaris XL, in the following called *Solaris*, is a cigarette-shaped vaping device. It was developed by Altria Group, Inc. and currently sold under this brand by PMI in Israel and Spain.[75] In the United States the product is sold as *MarkTen XL*.[76] The central element of the e-cigarette is the linear tube-shaped cartomizer (**3a**) with a "classic" wick-and-coil heating element.[77] Hereby, the wick is in contact with the liquid which is then passed onto the metallic coil. The hot coil evaporates the liquid which is then atomized. The liquid itself consists of propylene glycol, glycerol, water, tobacco derived nicotine and flavor additives (total volume: 0.8 mL). Aerosol production starts automatically when the smoker draws a puff with a diode at the end of the battery (**3b**) lighting up, mimicking conventional cigarettes.

MESH is a new product developed by Nicocigs and currently sold in United Kingdom and Ireland.[75, 78] It has a broad pen-shape but a slimmer mouth piece. *MESH* is marketed as the "next generation e-vapor product platform"[75] due to its automated assembly process and a different heating system. Although the top part is still a disposable sealed cartomizer with a pre-filled liquid called "capsules"[78] (**4a**), it does not rely on the wick-and-coil principle. Instead, it uses a metallic grid mesh to heat the liquid which is sucked in by the adjacent wick.[72] Additionally, unlike *Solaris*, *MESH* controls the level of its liquid and the battery (**4b**) refusing to power the heating element when the liquid level gets low. The composition of the liquid is very similar to that of *Solaris*: water, propylene glycol, glycerine, flavouring and nicotine (total volume: 2 mL). Aerosol is again produced on puff-by-puff bases when the e-cigarette detects a puff draw, but first the electronics have to be activated.

3.2 Materials and Products

Analytical grade spin traps were purchased from Enzo Life Sciences, Inc. (Lausen, Switzerland): *N*-*tert*-butyl-α-phenylnitrone (PBN), 5-*tert*-butoxycarbonyl-5-methyl-1-pyrroline-*N*-oxide (BMPO), sodium diethyldithiocarbamate trihydrate (DETC), 5,5-dimethyl-1-pyrroline-*N*-oxide (DMPO), 5-(diethoxyphosphoryl)-5-methyl-1-pyrroline-*N*-oxide (DEPMPO), 2,2-dimethyl-4-phenyl-2*H*-imidazole-1-oxide (DMPIO), 5-(diisopropoxyphosphoryl)-5-methyl-1-pyrroline-*N*-oxide (DIPPMPO), 2,2,4-trimethyl-2*H*-imidazole-1-oxide (TMIO) and α-(4-pyridyl 1-oxide)-*N*-tert-butylnitrone (POBN). Spin trapping agents were stored at −20°C in their original packaging and after opening under inert atmosphere. All chemicals used in this work were of analytical grade.

The following tobacco and non-tobacco products were provided by Philip Morris International R&D (Neuchâtel, Switzerland). This includes the 3R4F research cigarette, the tobacco heating system *IQOS* and complementary tobacco sticks *HEETS* (Amber label) and two e-cigarette products, namely *Solaris XL* (flavor: "Amber Bliss"; 19.3 mg/mL nicotine) and *MESH* (flavor: "Classic Tobacco High"; 19 mg/mL nicotine). These products were selected to represent a broader scale of smoking and vaping products: 3R4F as a conventional cigarette, *IQOS* as a heat-not-burn product, and the two e-cigarettes *Solaris* and *MESH* to represent different aerosol heating methods (standard wick-and-coil heating of *Solaris* and the heating by a metallic mesh of *MESH*).[72] 3R4F research cigarettes and *HEETS* tobacco sticks were stored in the original packaging or in an airtight plastic bag. For both products, a stick/cigarette pack out of ten was selected randomly and all sticks/cigarettes used. When the pack was emptied, the next was randomly selected.

Three randomly selected e-cigarette cartomizers per product were stored in the original packaging under inert atmosphere until their first usage and kept then in a constant humidity chamber (58% relative humidity, 22°C). *Solaris* does not have an indicator for liquid level and the consumers are told to "notice a reduction in flavor and vapor".[79] Although generally the liquid in one cartomizer is said to be sufficient for 2 hours of continuous use[80], in order to avoid possible dry puffing effects (low liquid level)[64] every cartomizer was used for only five experiments (equals to 60 puffs).

Finally, PMI provided 44 mm Cambridge Filter pads which were stored in an airtight plastic bag.

3.3 Spin trap solution preparation

3.3.1 Initital experiments

Due to the superiority in adduct stability and in amount of published reference studies of nitrone spin traps over nitroso compounds, only nitrone traps have been screened in this thesis. Spin trap solutions were prepared directly before performing experiments to avoid spin trap degradation and opened bottles of air sensitive chemicals were used up in no more than two days.

3.3.2 PBN and BMPO

Fresh spin trap solutions were prepared daily for a set of experiments (see chapter 4), consisting usually of four measurements (all four products). Initial experiments indicated a solution loss due to dead volume when the liquid was transferred or injected with a syringe (approx. 0.1-0.2 mL/extraction), thus spin trapping solutions were prepared with additional 10 Vol.-%. Solutions were kept at −78°C under inert atmosphere during the day and were thawed prior to usage.

For measurements with the spin trap PBN the analysis procedure of Goel *et al.* [64] was followed: approx. 273 mg (1.54 mmol) were dissolved in 30.8 mL deoxygenated toluene giving a concentration

of 0.05 M. For BMPO, the content of one whole flask (approx. 50 mg, 0.25 mmol) was dissolved in 30.8 mL deoxygenated toluene giving an approximate concentration of 8.14 mM.

3.3.3 Fe^{2+}-$(DETC)_2$

A 5 mM solution of Fe^{2+}-$(DETC)_2$ in toluene was prepared according to a modified version of the procedure described by Santos *et al.*.[81]

For the phosphate buffer, 322.33 mg (0.9 mmol) $Na_2HPO_4{\cdot}12\ H_2O$ (M = 358.14 g/mol) and 28.08 mg (0.18 mmol) $NaH_2PO_4{\cdot}2\ H_2O$ (M = 156.01 g/mol) were dissolved in 9 mL pure water. To the phosphate buffered aqueous solution (0.1 M, pH=7.4) 180.24 mg (0.8 mmol, 2 equiv) of Na-DETC$\cdot 3\ H_2O$ (M = 225.3 g/mol) were added and the solution was heated to 30°C. Under stirring 55.60 mg (0.2 mmol, 1 equiv) of $FeSO_4{\cdot}7\ H_2O$ (M = 278.0 g/mol) were slowly added. The resulting brown precipitate of Fe-$(DETC)_2$ (70.48 mg, 0.2 mmol; M = 352.4 g/mol) was extracted several times (typically 3 × 7 mL followed by 4 mL and then 3 mL) with toluene giving a clear aqueous phase and an orange residue. The combined toluene fractions of dark brown/black color were dried under reduced pressure and stored over night at +4°C. Prior to usage, the residual solid is solved in 40 mL toluene giving the desired solution of Fe^{2+}-$(DETC)_2$.

3.4 Smoke/aerosol generation

The products were smoked in a one-port smoking machine provided by PMI. This smoking machine and the smoke trapping device (Figure 3.2) consists of an electric contact-free cigarette lighter (**1**), a sidestream smoke capture apparatus called fishtail chimney based on the Health Canada normative T-212[82] (**2**), a cigarette holder and smoke trap (to hold the Cambridge Filter pad) conform with the ISO 3308 norm[63] (**3**), two consecutive impingers containing the spin trapping solutions (**4**) and a programmable electrical pump (**5**). Specifically, the electronic lighter is composed of a halogen lamp and a quartz rod which can be automatically moved to be positioned in front of the cigarette. When the lamp is lit, the quartz rod directs the infrared light to the cigarette end heating it up until it starts burning. In preliminary tests a distance of approximately 3 mm between the quartz rod and the cigarette end was found to be good to light the cigarette, although it appears that a deviation of the cigarette position from the central axis of the rod is detrimental to homogeneous lighting of the cigarette. The first puff is drawn when smoke is visible and the lighter is deactivated directly after the first draw. The advantage of the electric lighter is repeatability and that the sidestream smoke can be captured immediately after ignition. The smoke trap can be removed to perform measurements of the whole smoke. The pump can be programmed to perform according to different smoking regimes, however, only full puffs can be taken, i.e. a puff can not be stopped prematurely as it is required by the ISO 4387 norm[65].

Prior to smoking, 3R4F cigarettes were conditioned in a humidity chamber at a relative humidity of 58% and a temperature of approximately 22°C for at least 48 hours and maximum ten days.[65] Then, the cigarettes were smoked according to the Health Canada Intense regime[66] up to the standard butt length of 33 mm. This involves a puff volume of 55 mL over a duration of two seconds with a sinusoidal puffing profile. Two puffs were taken every minute with two additional immediate clearing puffs (no waiting time between them) taken after the cigarette is disposed of. Two clearing puffs are sufficient to draw several times the volume between the cigarette holder and the first impinger. Two clearing puffs were selected based on the study of Mason and Tindall.[83] Sidestream smoke wass captured by the fishtail chimney surrounding the burning cigarette and a positioned Cambridge Filter pad on top of the chimney followed by an additional soxhlet filter. The air flow rate through the fishtail chimney is set up to be 3 L/min.[82]

HEETS sticks and e-cigarettes were smoked (or vaped) according to CORESTA recommended no. 81: a rectangular puffing profile was used to draw a volume of 55 mL over a duration of

(a)

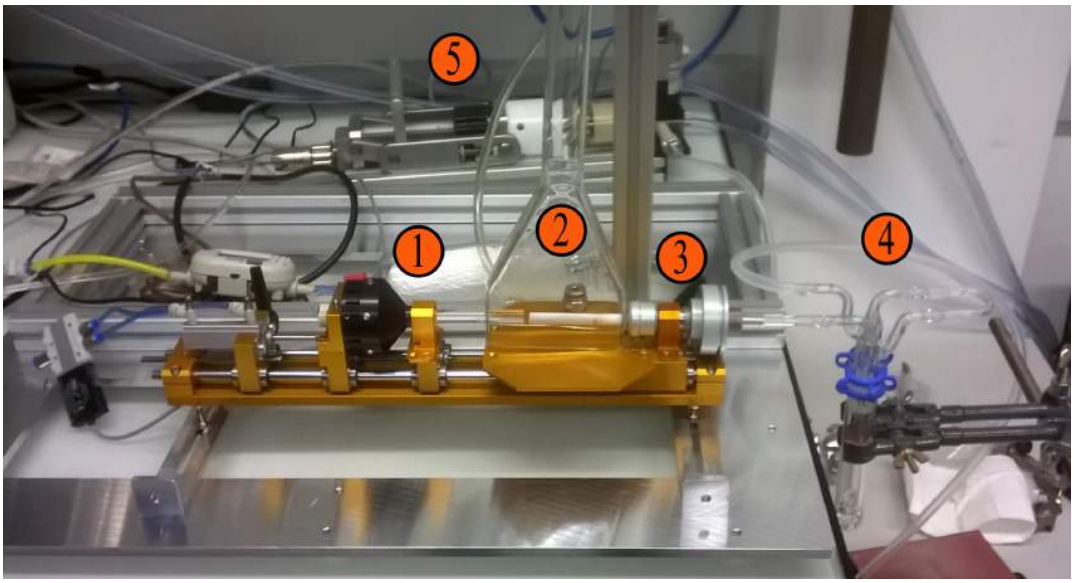

(b)

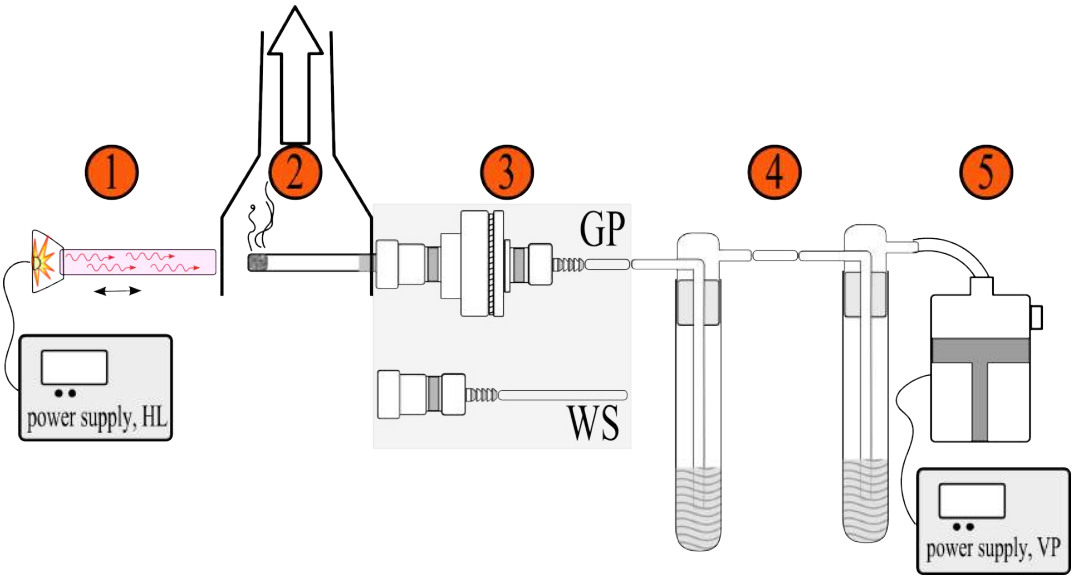

Figure 3.2: Layout of the smoking machine and the smoke trapping apparatus. **(a)**: Photo of the cigarette smoking setup. **(b)**: Sketch of the layout of the smoking machine. **1**: electric contact-free lighter, made up from a halogen lamp (HL) and a quartz rod; **2**: 3R4F research cigarette placed under the fishtail chimney, the white arrow indicates applied forced airflow; **3**: cigarette/product holder and Cambridge Filter pad holder. The gray rectangle indicates two interchangeable setups for gas phase analysis (GP) or for whole smoke analysis (WS); **4**: two impingers containing the spin trap solution; **5**: vacuum pump (VP). Same numbers refer to same parts in both figures.

3 seconds at a frequency of two draws every minute.[67] 12 puffs were drawn in total. The first

puff was taken when the product was ready (i.e. preheated) according to individual operations manuals. No sidestream smoke capturing has been performed since no smoldering in between puffs occurs. All products are preconditioned in the same fashion as the 3R4F cigarettes with the only difference that e-cigarette cartomizers are used directly after opening from the sealed packaging and are kept afterwards in the conditioning box for further experiments. Due to the flat shape of the *MESH*-mouth piece, a home-built adapter is used for inserting the e-cigarette into the cigarette holder. The adapter is built from a short glass tube which is connected to the mouth piece with a wide silicon hose.

All products were used immediately after removing from the conditioning chamber. After the last puff the products were kept in place for further 30 s for residual smoke/aerosol deposition. In order to minimize contaminations between products, each product uses its own set of labyrinth seals which are found in the cigarette holder.

3.4.1 Puff volume determination

According to ISO 4387:2000[65], puff volume has to be measured with a soap bubble flow meter and the volume accordingly adjusted. In order to do so, a bubble flow meter was designed using a graduated measuring glass (precision ± 0.5 mL) attached to a silicon hose (see Appendix; Figure D.1). A soap solution made from liquid hand soap (approx. 20 mL), water (approx. 40 mL) and a sugar cube was used to form stable bubbles. The real puff volume was determined for the apparatus setup for gas phase analysis, whole smoke analysis and for gas phase analysis with only one impinger. Measured puff volumes are presented in Table 3.1.

Table 3.1: Testing of the real puff volume for the gas phase setup (GP), whole smoke setup (WS) and the gas phase setup but only with one impinger (second impinger removed; GP, 1 imp.). Machine smoke puff volume was set to 55 mL. All values are reported as measured real puff volumes [mL].

Exp. no.	GP	WS	GP, 1 imp.
1	59	56	57.5
2	58	56.5	57
3	57	56.5	57.5
4	56	57	57
5	55	56.5	
6	57		
7	58		
8	57		
9	57		
10	57		

Independently of the apparatus setup, the smoking machine appears to be drawing more volume than it is supposed to (see Table 3.1). This comes as a surprise since the pump parameter diff. Vol. can only adjust for a decreased real puff volume. The pump is supposed to draw exactly 55 mL of air and this volume is then subsequently decreased by pressure resistance due to solutions in the two impingers and the Cambridge Filter pad. A possibility is a wrong pump calibration. It should be noted that the cigarette itself (and other tested products) add to pressure resistance. In our simple setup the puff volume can not be measured with a cigarette in place and thus the measured puff volume may be overestimated. Additionally, it should be noted that all three setups indicate similar puff volumes with 57 ± 0.5 mL.

Based on these results, vacuum pump parameters were adjusted: drawn volume is controlled by a base puff volume (PV) and a difference puff volume (diff. Vol.) which is used to adjust for discrepancies between desired and real draw volume. Since it is supposed to account for pressure resistance (and thus reduced real pressure), difference puff volume can only be positive. Results of

the input-output measurement for the gas phase setup (with two or one impinger) are presented in Table 3.2. It was found that a pump parameter setting of 53 + 0.5 mL gave a real puff volume of 55-55.5 mL for both setups. This margin of error is acceptable.

Table 3.2: Adjusting the real puff volume of the smoking machine for the gas phase setup (GP) and the gas phase setup but only with one impinger (second impinger removed; GP, 1 imp.). The smoking machine settings are reported as PV+diff. Vol. [mL].

GP		GP, 1 imp.	
settings	real volume	settings	real volume
53 + 0	54	53 + 0.5	55
54 + 0	55	53 + 0.5	55.5
54 + 0	55.5	53 + 0.5	55.5
54 + 0	55.5		
53 + 1	55.5		
53 + 0.5	55		
53 + 0.5	55		

3.5 EPR measurements

In the usual continuous-wave-EPR (CW-EPR) experiments, as used throughout this work, the microwave frequency is kept constant (by the Automatic Frequency Control, AFC) while the applied magnetic field is swept. The microwave source output is split into two arms, a sample arm and a reference arm (Figure 3.3). After passing an attenuator microwaves are sent via a circulator (from port 1 to port 2) into the resonator and thus the sample. For non-resonant frequencies all microwave power dissipates into heat and no radiation is reflected. However, for the on-resonance condition the total impedance of the resonator and the sample changes and some microwave power is reflected. These waves are directed by the circulator (port 2 to port 3) to a microwave diode for detection. Here, the reflected microwaves constructively interfere with the reference signal which is adjusted with the bias and phase regulators. This adds power to the weak signal coming from the resonator and allows sensitive measurements proportional to reflected power (operating point of the diode).[84]

To enhance sensitivity, a weak oscillating magnetic field parallel to B_0 is additionally applied which modulates the absorption signal. This signal is fed into a phase-sensitive detector (PSD) where the signal is demodulated and further amplified. Due to this modulation a first derivative spectrum instead of a typical absorption spectrum is recorded. By double integrating the derivative spectrum spin concentration can be determined. The measured paramagnetic species can be characterized by the isotropic g values and hyperfine couplings with neighboring nuclei, especially by comparison with published data.[26, 46]

The major advantage of EPR spectroscopy is its specifity. Since detection is limited to species for which the resonance conditions are fulfilled, specifically paramagnetic species (often radicals) are detected. This gives an enormous advantage for studies with complex matrices and sample mixtures, regardless of their phase of matter. In combination with a large magnetic moment of the electron and the field modulation this specifity makes the technique highly sensitive.

The price for such high sensitivity is the limit in data which can be gained from EPR measurements. Unlike the related NMR spectroscopy, EPR can only provide structural information about functional groups or atoms which are directly bound to – or at least closely neighbor (i. e. couple with) – the unpaired electron.

All quantitative measurements were performed using a Bruker AquaX (see Figure D.2). AquaX is an apparatus for quantitative EPR measurements consisting of several (in the case of this study: four) closely spaced capillaries with a single inlet and outlet, allowing continuous flow measurements.[85, 86] The use of multiple capillaries decreases off-resonant microwave power losses inside the resonator due to interactions of the electric field with the electric dipole moment of the solvent (especially relevant for polar solvents like water).[84] A major advantage is the stationary installment of the AquaX instead of a standard EPR sample tube inside the resonator which allows sample injections directly into the resonator. Baum *et al.* found 'non-satisfactory reproducibility' of the signal intensity when different sample tubes were used.[40] This source of error is eliminated by using the same apparatus. Furthermore, errors associated with repositioning of the sample tube in the resonator is avoided due to a fixed installation of the AquaX and sample solution exchange through injection.[40] These advantages lead to high reproducibility and enhanced sensitivity.

The EPR measurement setup is shown in Figure 3.3b. AquaX is vertically installed inside the resonator (**2**; red dashed line). New sample solutions are injected with a 10 mL syringe from the bottom and the syringe was kept in place as a sealing device (**1**). Teflon tubing coming from the top directed the samples into a waste container (**3**) and both (tubing and container) were kept open throughout the work.

The spectra were taken using an X-band spectrometer with the following parameters: microwave frequency, 9.88 GHz; modulation frequency, 100 kHz, microwave power, 2.01 mW; scan range, 100 G; modulation amplitude, 2 G; sweep time, 10.49 s; time constant, 1.28 ms; conversion time, 5.12 ms, receiver gain 50 dB, 2048 points.

Prior to each smoking experiment, a background measurement of the spin trap solution is taken by injecting 3 mL of the spin trap solution into the AquaX. Measurements are performed at room temperature (21°C). Spin concentrations are determined by double integration of the derivative signal and comparison with calibration based on standardized 4-hydroxy-2,2,6,6-tetramethylpiperidinyloxyl (TEMPOL) solutions (see Appendix C). The spectra simulation and fitting is performed using the MATLAB toolbox EasySpin.[87, 88]

3.6 Preparation of Mainstream smoke radicals

Mainstream smoke (gas phase or whole smoke) is passed into two sequential impingers (25 mL volume), each filled with 4 mL of the spin trap solutions. When the second impinger is not analyzed, the spin trap solution is replaced by pure toluene. The connections between the smoke machine and the first impinger as well as between the first and the second impinger are made of glassware and kept as short as possible in order to trap radicals as fast as possible (without aging). In total, the distance between cigarette butt end (or product mouth piece) and the surface of the solution in the first liquid is approximately 32.5 cm. Inside the tubing the gas flow rate r is $r_{HCI} = 218$ cm/s for the HCI smoking regime and $r_{COR} = 146$ cm/s for the CORESTA regime. Based on these flow rates radicals are expected to reach the surface of the spin trap solution in $t_{HCI} = 0.149$ s or $t_{COR} = 0.223$ s, respectively.

After machine smoking the toluene volume is adjusted if necessary. For immediate measurements without additional deoxygenation 3 mL of the spin trap solution are taken out and injected into the AquaX. The time between the last puff and the start of the EPR measurement is 5 min.

For deoxygenated measurements approximately 4 mL of the solution is transferred into a Schlenk flask and three cycles of freeze-pump-thaw are performed. Briefly, the solution is frozen using liquid nitrogen and a vacuum is subsequently applied. The solution is then thawed and dissolved gases leave the liquid. Afterwards, gaseous nitrogen is introduced into the flask and the procedure is repeated two more times. Then, 3 mL of the deoxygenated solution are injected into the AquaX. The time between the last puff and the start of the first EPR measurement is 20 min.

3.7 Preparation of Particulate Phase Radicals and Total Particulate Matter

Particulate phase of the mainstream smoke is trapped by a conditioned (58% relative humidity, 22°C, at least 12 h in the conditioning box[89]) Cambridge Filter pad which is inserted into the smoke trap. Immediately after smoking the smoke trap is removed and sealed from both sides, as required by [89] and [82]. The filter is weighted together with the seals and the smoke trap and the Total Particulate Matter is determined by subtracting the weight of the apparatus prior to smoking.

The filter is then removed from the smoke trap with tweezers and folded two times, with the tar side being on the inside. The two clean quarters are used to collect residual tar in the smoke trap (front side and back side). The filter is then extracted with 10 mL of pure toluene for 20 min by gently shaking the Erlenmeyer flask. Afterwards, approximately 4 mL of the extract are transferred into a Schlenk flask and three cycles of freeze-pump-thaw are performed. Then, 3 mL of the deoxygenated solution are inserted into the AquaX.

(a)

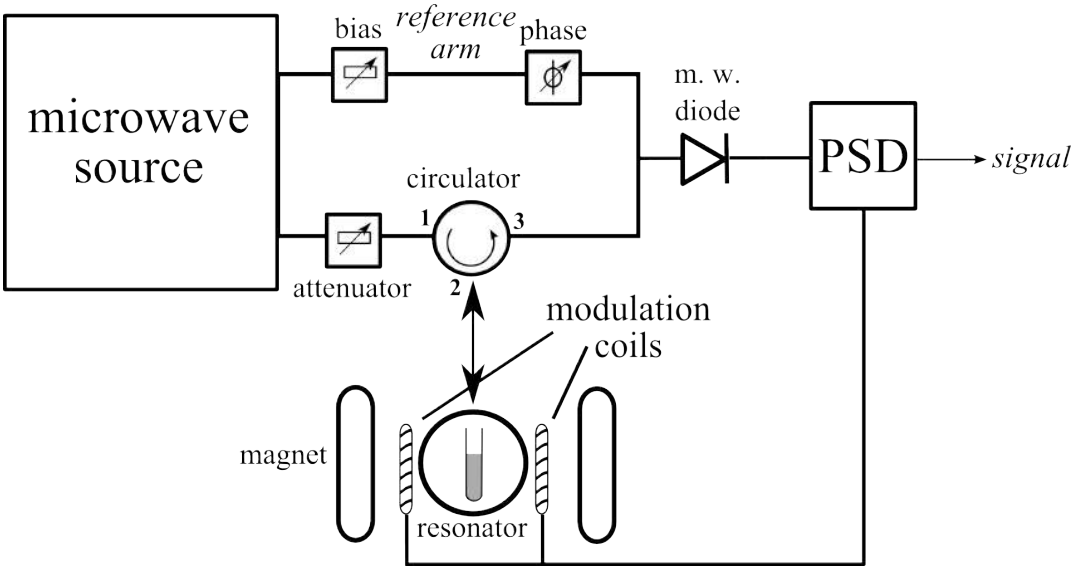

(b)

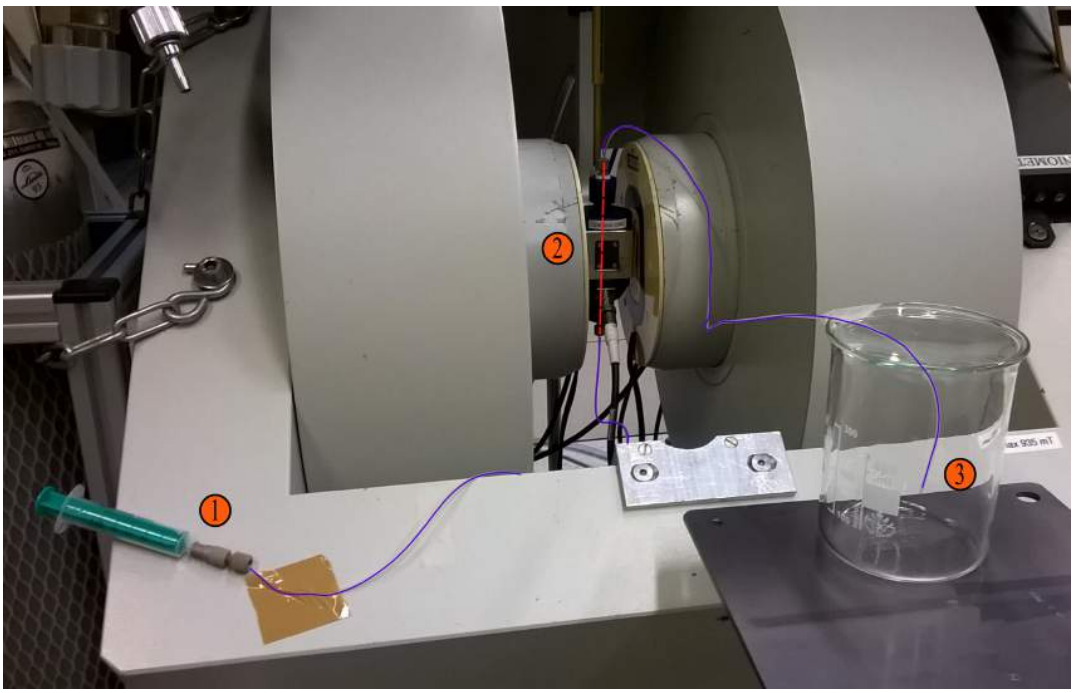

Figure 3.3: **(a)**: General scheme of a CW spectrometer. Microwaves exiting the source are divided into two arms, a sample arm and a reference arm. The sample arm passes an attenuator and enters the resonator where the electromagnetic radiation is partially reflected. The reflected radiation constructively interferes with the reference arm (bias and phase adjusted) and hits the detector (microwave, m. w., diode). The signal is demodulated in the phase-sensitive detector (PSD) with respect to field modulation by the additional coils. Presented scheme was drawn following [84]. **(b)**: Installed AquaX inside of the resonator. **1**: Sample inlet. Solution injection with a 10 mL syringe from the bottom teflon capillary. **2**: Resonator with the AquaX inside. Installed capillary bundle is indicated with the red dashed line. **3**: Sample outlet. Solution exits the AquaX (and thus the resonator) on top and is directed into a waste container with a further teflon capillary. Both teflon capillaries are highlighted with a blue line.

Chapter 4

Results

In this study, levels of free radicals in smoke of conventional cigarettes were compared to aerosols generated by a heat-not-burn (HNB) product and by e-cigarettes. Direct EPR measurements were performed with extracts of Total Particulate Matter collected on Cambridge Filter pads while spin trapping experiments were carried out with smoke/aerosol gas phase. Two spin traps, PBN and BMPO, were selected based on their performance in the initial experiments. Additionally, experimental conditions were optimized prior to quantitative measurements using 3R4F research cigarettes. Finally, levels and dynamics of NO production in different products were compared in spin trapping experiments.

4.1 Initial experiments

Standardization in cigarette smoke analysis greatly facilitates comparison of results between different cigarette brands, products and laboratories. However, while detection of many chemical compounds has been standardized or a standard procedure proposed by CORESTA, no standardized experimental setup and detection method for free radicals in smoke have been established. The reason for this is likely that currently the FDA list of 93 *Harmful and Potentially Harmful Constituents in Tobacco Products and Tobacco Smoke* does not include radicals.[4] However, radicals are known to induce oxidative stress and thus levels of radicals in smoke or aerosol should be considered and determined.[19, 90, 91]

Prior to performing quantitative measurements experimental methodology had to be established. In the often cited study by Baum *et al.* [40] the authors addressed standardization issues and tried to optimize the experimental procedure. However, their work is limited by the number of tested spin traps and no explicit comment was made concerning spin trap solution concentrations.

For this reason, a series of initial experiments has been performed to determine optimal measurement conditions. In the first set of experiments a large library of spin traps was screened in different solvents (toluene, water and/or ethanol) and solutions from both impingers were measured. Afterwards, reproducibility of AquaX with toluene and water as well as that of a home-built AquaX analogue dubbed "ToluX" was tested. ToluX is built with the same principle of continuous flow as AquaX from a standard EPR sample tube instead of a combination of several capillaries. Its purpose was to overcome a major limitation of the AquaX: the small capillary volume. Radical adducts dissolved in toluene produced a stronger signal when a simple 3 mm EPR sample tube was used in comparison to signals measured with AquaX.

Several experiments with PBN as spin trap were performed: trapping with different concentrations of the spin trap, stability of the spin trap solution, comparison of two deoxygenation methods, measurement of gas phase and whole smoke. The last three experiments were also tested on the

NO spin trap Fe(II)-$(DETC)_2$. It should be mentioned that in many of these experiments no standardized procedure was employed and thus parameters may vary.

In this section initial experiments and theirs results are discussed and consequences for quantitative measurement are drawn.

4.1.1 Spin trap library screening

Trapping capabilities of different spin traps were tested on gas phase smoke of the 3R4F research cigarette: immediately after smoking, the solution from the first impinger was transferred by syringe into the cavity. Toluene measurements were performed using standard 3 mm EPR sample tubes while for measurements in water as solvent the AquaX was used. All spectra are presented in Figure 4.1.

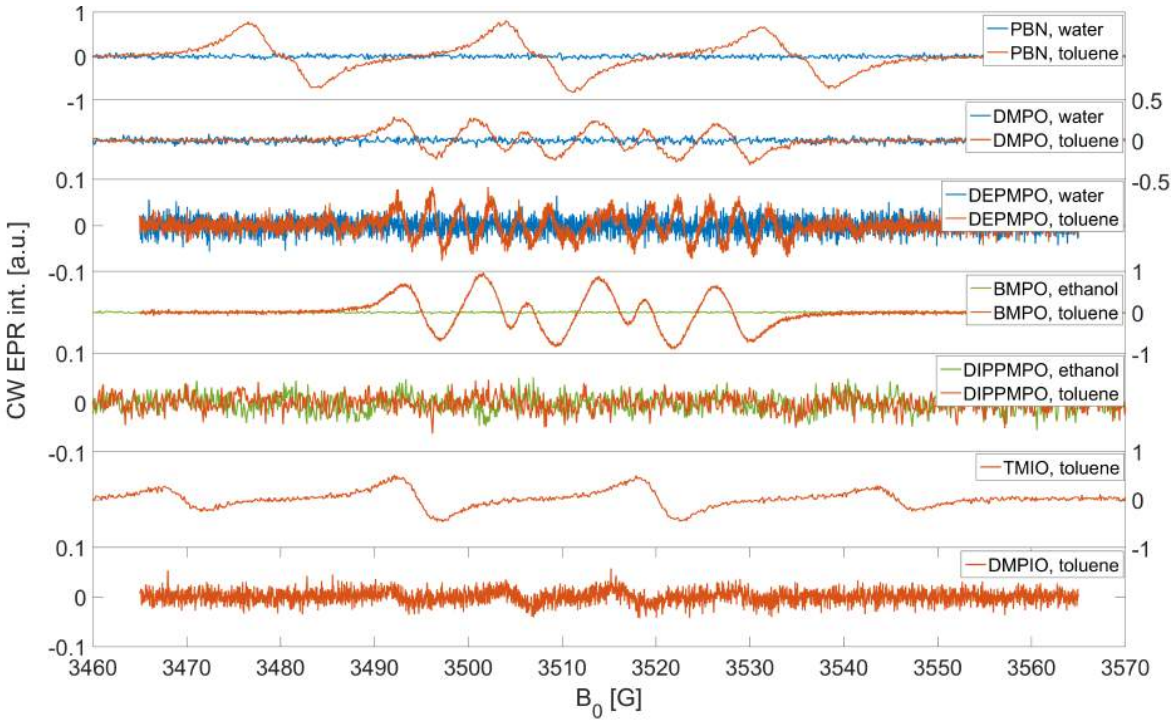

Figure 4.1: Spectra of gas phase radicals of 3R4F smoke trapped by different spin traps. Solvents are indicated by color: water = blue, toluene = red, ethanol = green. From top to bottom (concentration of spin traps in brackets): PBN in water (20 mM) and in toluene (20 mM); DMPO in water (20 mM) and in toluene (40 mM); DEPMPO in water (2.2 mM) and in toluene (0.87 mM, recorded 30 min after smoking); BMPO in ethanol (7.3 mM, recorded using an EPR sample tube) and in toluene (10 mM); DIPPMPO in ethanol (6.3 mM, recorded using the AquaX) and in toluene (8 mM); TMIO in toluene (5.7 mM); DMPIO in toluene (10 mM). For clarity the y-axis labels of every second spectrum is located on the right hand side.

For the first experiments all available spin traps were screened in toluene and water or ethanol. Solution concentrations vary due to differences in available amount of substance between different spin traps. After smoking of the 3R4F cigarette, solutions of both impingers were measured subsequently but approximately 30 min apart since in all cases kinetic series were taken as well.

Although the concentrations of the spin traps strongly differ (0.87 mM of DEPMPO vs. 40 mM of DMPO in toluene), the general trend is visible nonetheless. The strongest signals were recorded in measurements of PBN, DMPO, BMPO, DEPMPO and TMIO in toluene. Differences in signal intensity for the most part arise from differences in adduct formation rates. In contrast, when water or ethanol were used as solvent no signal could be detected.

A majority of reported solution spin trapping experiments of the gas phase have been performed in organic solvents.[11, 17, 19, 27, 40, 41, 50, 56, 64, 92–97] Successful spin trapping of smoke gas phase radicals in an aqueous medium (usually phosphate-buffered) has been reported but the concentration of spin trapping agents used was 2–3 orders of magnitude higher with 1 M of DEPMPO[60] and 4 M of DMPO[98]. Baum *et al.* tested polar and apolar solvents and did not find any radicals in polar solvents neither with PBN (methanol, isopropanol, water) nor with DMPO (isopropanol, water) nor with POBN (isopropanol).[40] These findings agree with our observations. Trapping difficulties in polar solvents could stem from insufficient partition coefficients and diffusion limitations of organic apolar radicals from the smoke into the water/ethanol.

A further spin trap, POBN was tested in water along the spin traps whose spectra are presented in Figure 4.1. Once again, no clear signal was detected. Nonetheless, POBN showed surprising properties since it was completely insoluble in toluene. This is contradictory to published articles indicating solubility in apolar solvents such as benzene.[47] An NMR spectrum of the substance did not clarify its identity (data not shown) and it was decided to not use POBN in further experiments.

Furthermore, solutions both from the first and second impinger were measured and additional kinetic measurements taken. In Figure 4.2 subsequent measurements of the two impingers with PBN as spin trap are shown. The measurement were taken 30 min apart; solution from impinger 1 was measured first. The double integral ratio between the two impingers $R = A(\text{imp2})/A(\text{imp1})$ in

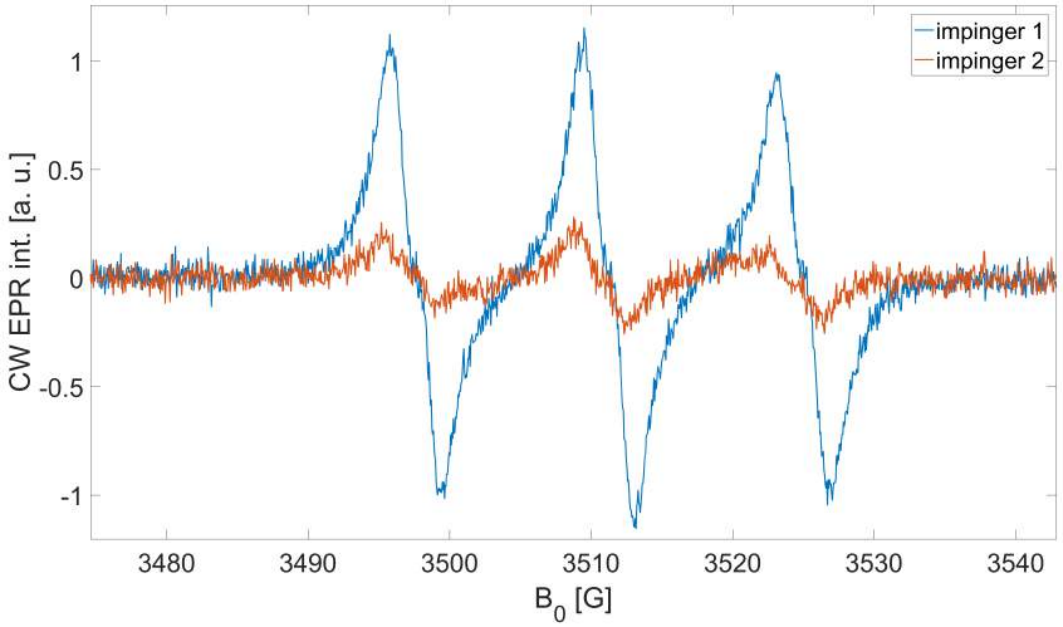

Figure 4.2: Spectra of solutions of PBN in toluene (20 mM) from the first and second impinger. Gas phase radicals of 3R4F cigarette smoke were trapped and solutions from the two impingers measured subsequently (time difference 30 min). The first measured spectrum is that of impinger 1.

Figure 4.2 is $R_{1\to2}^{\text{PBN}} \approx 0.28$, i.e. the signal from the second impinger is approximately 70% weaker

than that from the first impinger. Comparison of the two impingers with PBN as spin trap clearly shows that not all gas phase radicals are trapped. Not only are trapping reactions competing with side reactions, especially with oxygen[99], radicals partially leave the impinger solution before being absorbed by the solution and reacting due to short dwelling time. For this reason the double integral of the second impinger was approximately 28% of that of the first impinger. When the decay of the adducts from the second impinger is taken into account (spectrum of the second impinger was taken approximately 30 min after smoking), this number increases to approximately 40%.

A brief estimation based on previous reports makes clear that the spin trap concentration is sufficient to theoretically trap all radicals: Goel *et al.* reported trapping 7.72 nmol of gas phase radicals from the 3R4F research cigarette with PBN.[64] A 20 mM solution in 4 mL toluene contains 0.08 mmol of PBN. Even when a generous estimation by Flicker and Green[99] is taken into account, that the real number of radicals is 100 fold higher, it still leaves approximately 0.77 μmol of radicals to a 1000 fold greater amount of spin trapping molecules (80 μmol).

While radicals are known to be constantly produced in the gas phase of the cigarette smoke[27] it is unlikely that all existing radicals are trapped in the first impinger and the radicals detected in the second one result from radicals being generated in the gas phase between the two impingers. Ghosh *et al.* trapped radicals on a puff-by-puff basis and found radicals in the first puff right away.[50] This proves that the radicals do not have to be formed during smoke aging to be trapped. Menzel *et al.* reported a spin trapping efficiency of 47% for PBN in benzene based on comparison of spectra from two subsequent impingers.[56] Additionally, in the same study radicals were trapped in the second impinger even when no spin trapping agents were added to the solution of the first. Signal intensity was found to be 67% of the signal from the usual measurement of the first impinger. While Menzel's experimental conditions differ from those employed in this work, this does make clear that a signal in the spectrum of the second impinger is expected. In contrast to that, Baum *et al.* reported to trap more than 95% of all radicals in the first impinger, although the PBN concentration and solution volume were much smaller than that of Menzel and co-workers (10 mM in comparison to 200 mM, 4 mL in comparison to 15 mL) while the gas flow rate, estimated on puff parameters, is expected to be similar (35 mL/2 s = 17.5 ml/s; 23 mL/1.5 s = 15.3 s). Unfortunately, since in the present thesis no control experiments were performed to determine the percentage of radicals lost in the gas phase between the first and second impinger solutions, the trapping efficiency can not be determined.[56] If this loss is neglected, the trapping efficiency is estimated to be 74%.

Measurements of kinetic decay in most cases showed a steady intensity loss without changing spectral properties. This is expected since Baum *et al.* [40] reported very similar decay rates for DMPO in toluene, although Pryor *et al.* observed lineshape changes over time that hint to differences in decay rates for PBN in benzene.[27] It should be pointed out that the measurement of DEPMPO in toluene took place approximately 30 min later than measurements with other spin traps, however, no visible decay was then observed in a subsequent measurement (data not shown). Out of all spin traps BMPO indicated the greatest variability in decay rates.

In Figure 4.3 spectra of the two impingers with BMPO in toluene are presented. Since both impingers can only be measured subsequently (time difference 30 min), **A** shows spectra from the experiment with impinger 1 measured first and impinger 2 second while **B** presents spectra from the next experiment with a reversed measurement order. The double integral ratio between the two impingers in **A** is $R_{1\rightarrow2}^{\mathrm{BMPO}} \approx 0.23$ and in **B** $R_{2\rightarrow1}^{\mathrm{BMPO}} \approx 0.33$. This increase in signal ratio is clearly attributed to decay of radical adduct in both impingers. The six broad lines identified in the first impinger are reduced to four in the second. It was proven by an experiment with a reverse measurement order (Figure 4.3 **B**) that this difference stems from diverse adduct decay rates and not from different trapping efficiencies for different radicals. In this case, spectrum of impinger 2 shows six lines and impinger 1 (measured 30 min later) only four.

Based on these observations it was decided to use PBN and BMPO in quantitative measurements. The reasoning involves strong signal-to-noise ratios and difference in observed coupling constants:

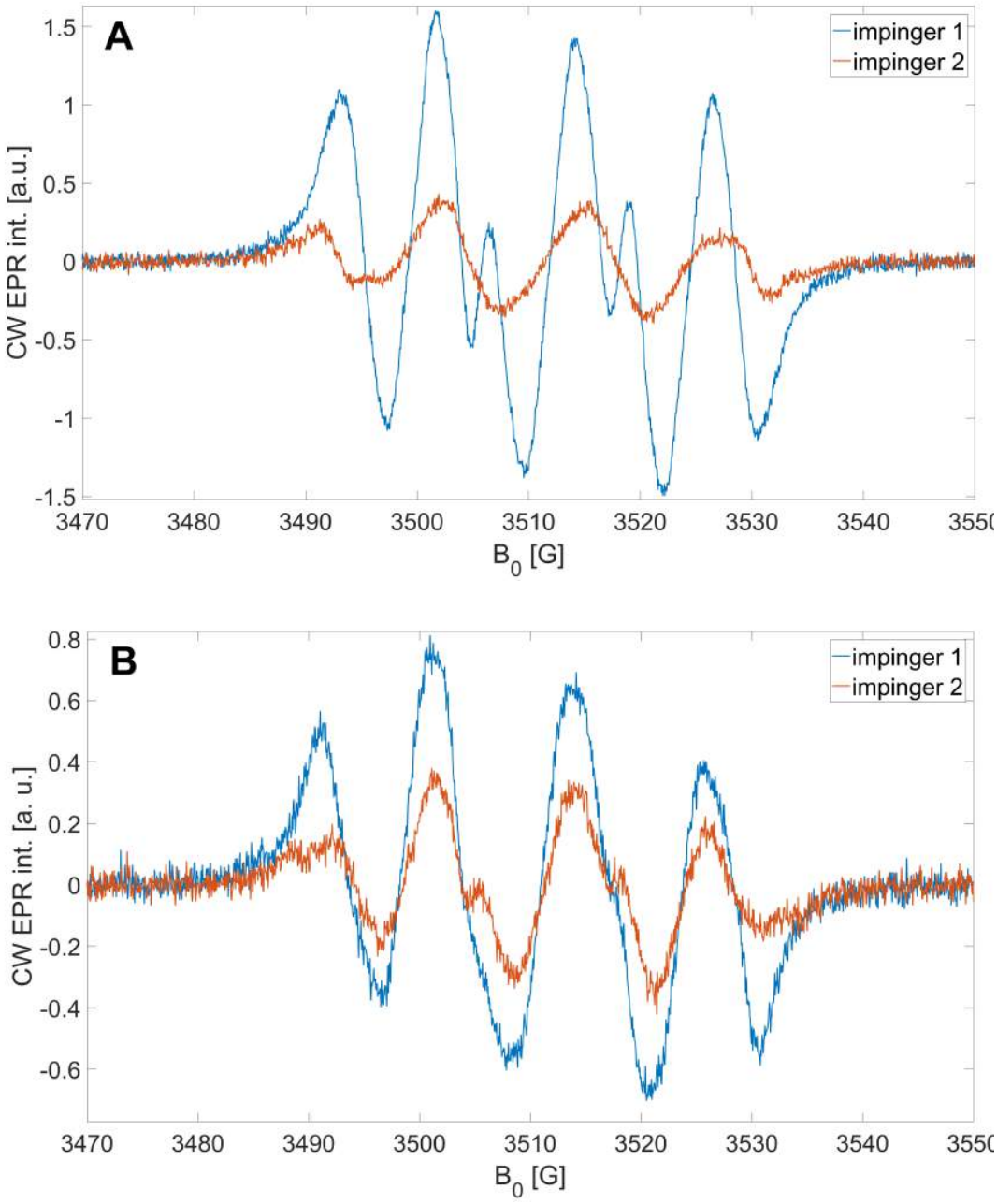

Figure 4.3: Spectra of solutions of BMPO in toluene from the first and second impinger. Gas phase radicals of 3R4F cigarette smoke were trapped and solutions from the two impingers measured subsequently (time difference 30 min). **A**: Solution of impinger 1 measured first. **B**: Solution of impinger 2 measured first.

the linear PBN is a well-studied spin trap which has been used in many smoke radical related studies (e.g. [41, 50, 64, 96]) but it lacks variability in hyperfine structure. In contrast to that, cyclic nitrone trap DMPO and its analogues exhibit greater variation in the magnitude of the

β-hydrogen coupling constants.[46] Although reported data on BMPO is scarce, however, its decay properties appeared promising.

In the following sections all measured solutions were taken from the first impinger.

4.1.2 Residue and error estimation

Although the AquaX insert is designed to be used in quantitative continuous-flow measurements, it seemed important to estimate the error in double integration of two subsequent measurements. A series of experiments was performed on an injected 50 μM solution of TEMPOL alternating with injections of pure toluene, varying the volumes of injected solutions. Experimental parameters and relative double integrals are presented in Table 4.1. As reference intensity, the integral of the last experiment was chosen. Similar series of measurements were performed with water as solvent with AquaX and with toluene with ToluX. Respective experimental parameters and relative double integrals are presented in the Appendix in Table A.1.

Table 4.1: Testing of AquaX with toluene. Solutions: A = toluene, B = TEMPOL in water (50 μM). Parameters: power attenuation 20 dB, modulation amplitude 0.5 G, receiver gain 50 dB, 10 scans. For sensitive measurements, parameters were changed to: modulation amplitude 2 G, receiver gain 60 dB, 60 scans.

Exp. no.	sample	volume [mL]	rel. integral[a]
0	A	full[b]	-[c]
1	B	2	0.968
2	A	2	0.0148
3	B	2	1.0014
4	A	4	0.0079
5	B	2	1.0026
6	A	6	0.0093
7	B	2	1.0250
8	A	8	0.0082
9	B	1.5	0.9991
10	A	8	0[d]
11	B	3	1

[a] in comparison to the integral of exp. no. 11
[b] AquaX completely filled with toluene
[c] no spectrum saved
[d] below detection limit, relative intensity is set to 0; sensitive measurement, however, shows weak signals

From the results in Table 4.1 it becomes clear that TEMPOL is carried over to the toluene measurement. In experiment no. 2 a double integral of approximately 1.5% intensity of that of TEMPOL was measured. This integral decreased to 0.8% when the toluene volume was increased. Only when the toluene volume was increased to 8 mL and the volume of TEMPOL reduced to 1.5 mL, no more residual TEMPOL could be found in the toluene measurement. On the other hand, the TEMPOL integral increased over the course of the experiment, possibly due to residue being carried over to the next measurement. The integral peaked at the seventh measurement when 2 mL of TEMPOL solution was added after 6 mL of toluene.

Similar results were found for experiments with ToluX with toluene and AquaX with water (Appendix Table A.1). The difference here is that with ToluX it took at least 16 mL of pure toluene to flush all residual TEMPOL out of the device. This can be attributed to the design of the device: the diameter of the inject capillary is the same as for AquaX but the body of ToluX is much broader (3 mm EPR sample tube). Thus, solvent flow is not optimal. On the other hand, AquaX seemed

to perform better with water as solvent as it took only 2 mL to fully exchange the solution inside the capillaries. It is probable that the difference here is the viscosity of the solvent in comparison to that of toluene.

In summary, based on these observations it was decided to flush the AquaX with 10 mL of pure toluene in between measurements and inject 3 mL of spin trap solution for quantitative measurements. The error due to residue from former experiments and due to dilution then seems to be negligible.

4.1.3 Deoxygenation method

Deoxygenation of the sample is important to suppress oxygen broadening of the spectral lines. A comparison is drawn in Figure 4.4 between a non-deoxygenated sample, a sample through which dry nitrogen gas has been passed through for 5 min and a sample which was deoxygenated with two cycles of freeze-pump-thaw. Results show a strong decrease in line broadening and the equivalent increase in sensitivity when the sample is deoxygenated prior to measurement. Both deoxygenation methods reduce line width to a similar extent.

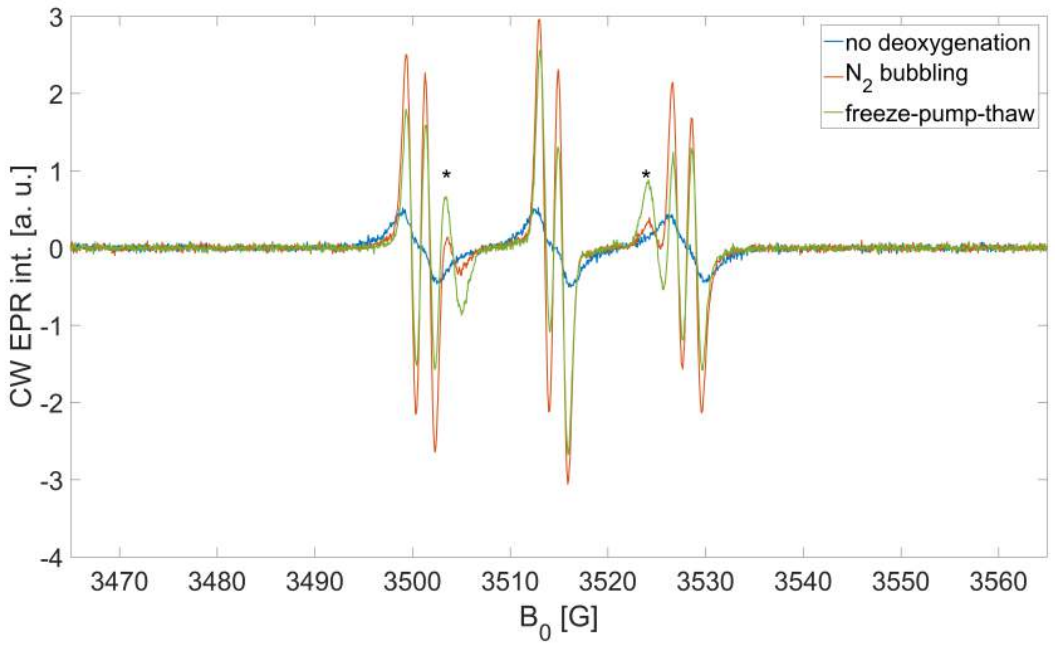

Figure 4.4: Spectra of solutions of PBN in toluene (20 mM) using various deoxygenation methods: blue = no deoxygenation; red = bubbling with nitrogen gas for 5 min; green = freeze-pump-thaw, two cycles. Lines marked with an asterisk indicate oxygenated PBN (PBNOx).

Although in recent studies deoxygenation of the sample is often performed using the freeze-pump-thaw technique[50, 64, 92, 93, 96], this method has the disadvantage of taking more time than simple nitrogen bubbling. In one study argon was used instead of nitrogen bubbling.[94] Baum *et al.* reported that freeze-pump-thaw was more efficient at oxygen removal than deoxygenation with dry nitrogen gas.[40]

The advantages of deoxygenation are clearly seen in Figure 4.4. Not only is the oxygen-rich sample lacking well resolved hyperfine-structure, the overall signal intensity (and thus signal-to-noise ratio) is much worse than with the deoxygenated samples due to the oxygen induced broadening of lines.

Additionally, it has to be taken into account that the oxygen-rich sample was measured immediately after smoking while the deoxygenated samples only after 5 min (in case of nitrogen bubbling) or 15 min (in case of freeze-pump-thaw), respectively. It is expected that the intensity of PBN adducts will decrease over time as the species decay. This is probably the reason for a weaker intensity of the PBN-adducts in the freeze-pump-thaw spectrum. Additional measurements with a smaller modulation amplitude showed the efficiency of the freeze-pump-thaw deoxygenation method and slight superiority over nitrogen bubbling, although overall the differences in oxygen removal are negligible.

In both spectra of the deoxygenated samples an additional radical species is seen (marked with an asterisk). This stems from the oxidation product of PBN (PBNOx). The difference in intensity is significant in this sample. However, while also found in quantitative measurements, such a strong signal of the oxidation products was never observed again.

As mentioned, fast measurements are essential to increase the signal of radical adducts. While freeze-pump-thaw has the disadvantage to take more time, its repeatability was found to be superior. Nitrogen bubbling suffered from toluene evaporation, even when nitrogen gas was presaturated with the solvent. This may be a result of a mechanical drag of the solvent with the uprising gas and the general evaporation of the liquid. Furthermore, since no flow meter was used, nitrogen flow rate was found to be difficult to control and repeat. For these reasons it was decided to use three cycles of freeze-pump-thaw for deoxygenation.

4.1.4 Spin trap concentration determination

Although Baum *et al.* [40] determined that for a 10 mM spin trap solution the optimal solution volume is 4–5 mL, concentration has not been optimized. In this work a short set of experiments was performed to study effects of spin trap concentration.

With PBN as a spin trap different concentrations of the solution were tested in the presence and absence of oxygen. For a set of four concentrations, 2 mM, 20 mM, 100 mM and 200 mM, were chosen in order to test the influence of spin trap concentration over two orders of magnitude. In the second experimental set, concentrations were kept closer together: 2 mM, 10 mM, 20 mM and 50 mM. This time, however, solutions were deoxygenated by bubbling nitrogen gas for 5 min prior to EPR measurement. All spectra are presented in Figure 4.5.

As expected, the signal intensity increases in **A** from the lowest concentration to the highest. Since spin trapping competes with other free radical side reactions[99], it can be assumed that by increasing spin trap concentration more radicals can be trapped. This increase in signal intensity should indicate saturation for very high concentrations when the trapping rate is apparently no longer dependent on the concentration and the reaction order changes to a pseudo-order.

Surprisingly, the increase in intensity is not linear and the spectra of solutions with 20 mM concentration and 100 mM are generally very similar. The slight intensity rise of the higher concentrated solution can not be rationalized with the significantly higher concentration. Since the signal intensity further increases for a 200 mM solution, it is clear that the saturation point is not achieved and not all radicals trapped. The likely explanation is that these two measurements were taken several days apart with different PBN solutions. It is possible that one of the solutions was prepared with a wrong concentration.

Measurements of deoxygenated solutions further support the need for the freeze-pump-thaw method (Figure 4.5 **B**): generally a steady increase from 2 mM to 20 mM to 50 mM is seen. However, the most intense signal is reached with a 10 mM spin trap solution. All measurements were taken on one day but for each experiment a new solution was prepared. Since solutions with 20 mM and 50 mM concentrations were bubbled with toluene saturated nitrogen (instead of dry gas), it is possible that the two solutions with the lowest concentrations lost toluene to evaporation and thus became higher concentrated. This seems plausible but unlikely since – based on the difference

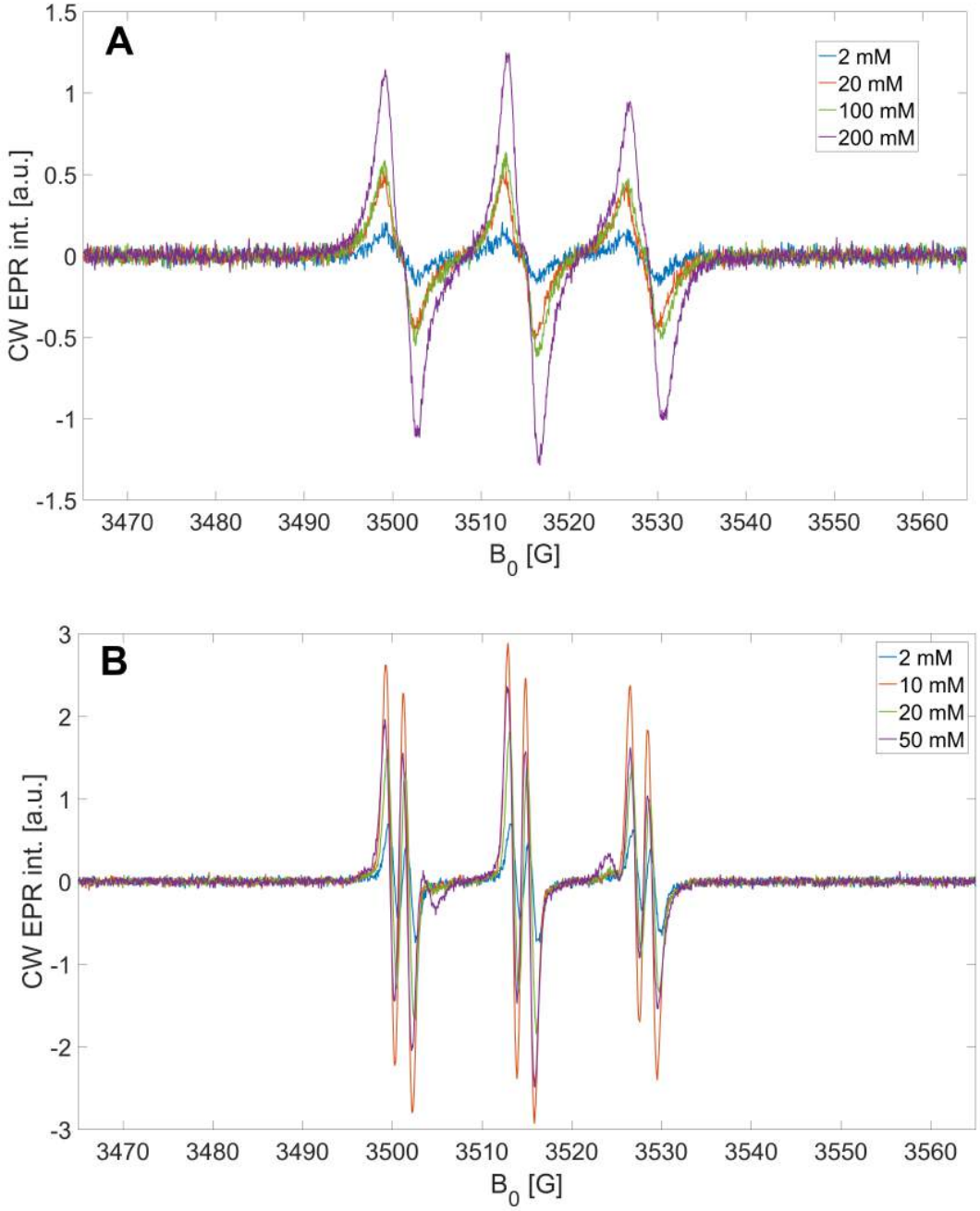

Figure 4.5: Spectra of solutions of PBN in toluene with different concentrations of the spin trap. **A**: Solutions were measured immediately after smoking. **B**: Solutions were deoxygenated prior to the measurement. Solutions of 20 mM and 50 mM were deoxygenated with saturated toluene.

between 20 mM and 50 mM – the "real" concentration of the 10 mM solution would have to be approximately 70–75 mM, i.e. a 7-fold decrease in solvent volume.

These observations made clear that no saturation in regards to radical trapping will be reached. Since for a concentration of 50 mM an additional radical species was clearly observed and the overall signal intensity is sufficient for integration, it was decided to perform quantitative measurements with this concentration. The same spin trap concentration was used by Yu *et al.* [93], Goel *et al.* [64] and Pryor *et al.* [41].

4.1.5 Measurements of whole smoke radicals

An experiment was performed to test the capability of this setup to trap radicals from whole smoke. 20 mM solution of PBN in toluene was used. In Figure 4.6 a comparison is drawn between a whole smoke and gas phase measurement. No radicals were trapped in the whole smoke measurement.

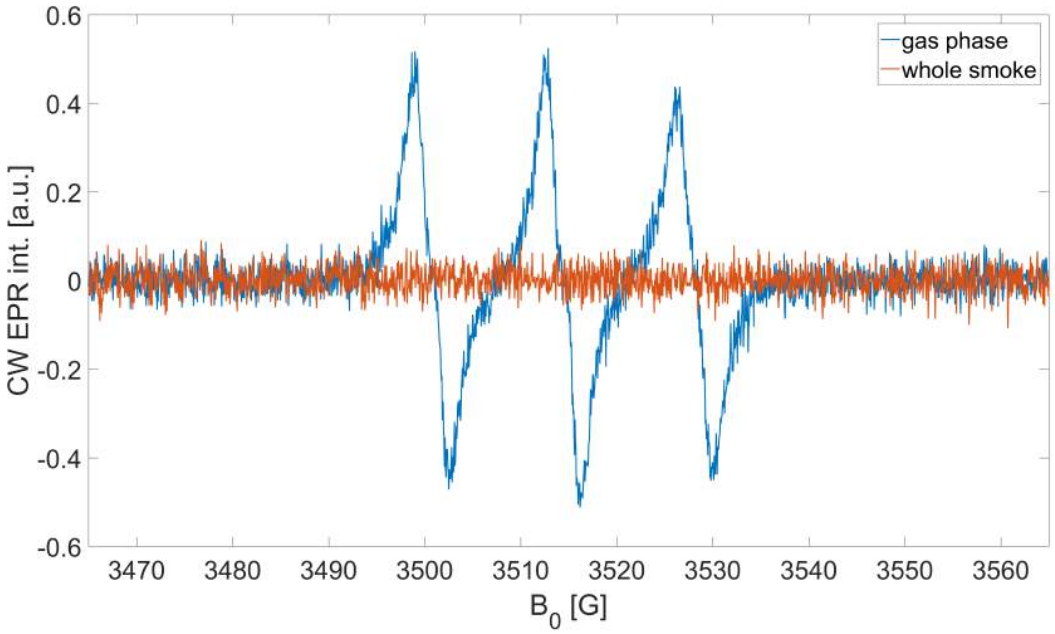

Figure 4.6: Comparison of spin trapping with PBN (20 mM in toluene) of whole smoke radicals and gas phase radicals.

The fact that no radicals were spin trapped when whole smoke passed through the impingers comes at no surprise. As previously discussed, whole smoke radicals (mostly superoxide and hydroxyl radicals) were found in highly concentrated aqueous solutions.[60, 98] The fact that no study - to the best of the author's knowledge - has published results of radical trapping with nitrones in organic solvents from whole smoke suggests that previous attempts were as unsuccessful as the one of this work. Pryor *et al.* explicitly stated that whole smoke trapping in benzene did not yield any signal in the EPR measurements.[41] Particulate phase and gas phase have very different properties.[1] It has been speculated that in whole smoke the particulate phase or radical-containing "tar", which is deposited along the glass tube, quenches the short lived radicals.[41, 58] Bartalis *et al.* successfully trapped radicals from whole smoke, however, they used a nitroxide probe 3-amino-2,2,5,5-tetramethyl-1-pyrrolidinyloxy (3AP).[62] Nitroxides are reported to react readily with carbon-centered radicals[100] and the faster kinetics for these compounds could explain why Bartalis and co-workers were successful at radical trapping when we did not.

Based on this observation only gas phase spin trapping with PBN and BMPO was performed throughout the quantitative measurements.

4.1.6 NO trapping

Two different methods of preparation of the NO spin trap were tested. The first procedure simply required the mixing of Na-DETC with $FeSO_4$ in an aqueous phosphate-buffered solution (pH = 7.4) followed by extraction into the organic phase with toluene (*extract*). For the second synthesis method both reagents are again mixed in a aqueous buffered solution, but then filtered and the solid recrystallized in acetonitrile (*crystallization*). Both methods follow an adapted synthesis protocol by Santos *et al.* [81], where Cu-$(DETC)_2$ complex was formed from $CuSO_4$ and Na-DETC. Additionally, whole smoke was passed through an extract-based spin trap solution. The three spectra are compared in Figure 4.7.

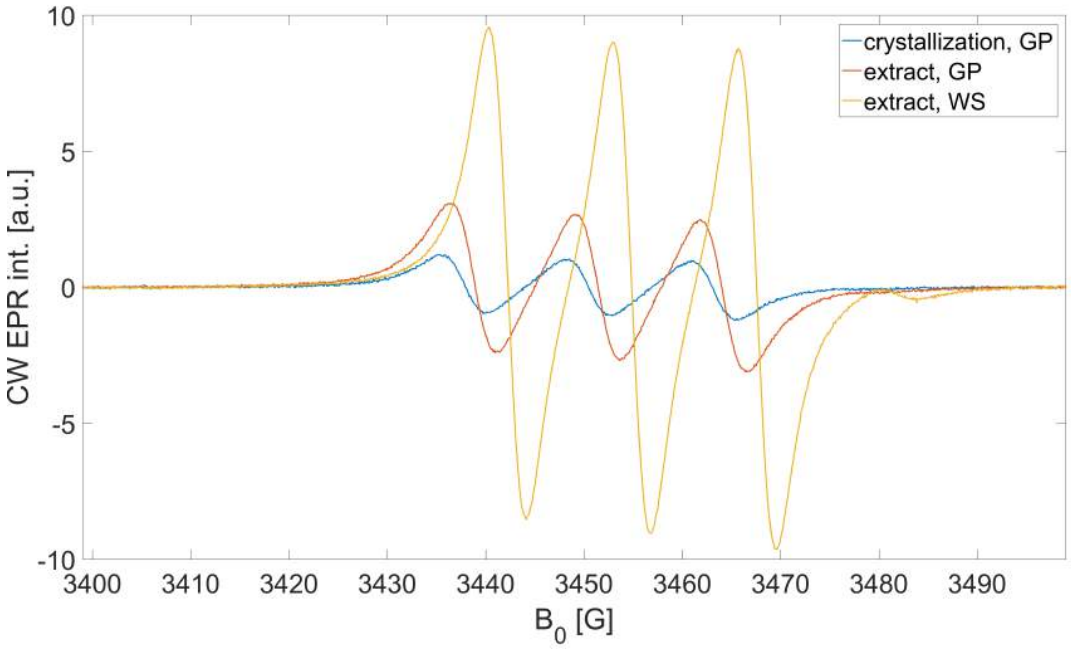

Figure 4.7: Comparison of gas phase NO trapping with the Fe(II)-$(DETC)_2$ spin trap gained from the extract (extract, GP) or from crystallization (crystallization, GP). Additionally, NO from the whole smoke was trapped using a spin trap gained from another extract (extract, WS). In the case of the WS measurement the sample was deoxygenated using the freeze-pump-thaw method.

A broad triplet of MNIC-DETC was observed in all three measurements in testing experiments of the NO spin trap Fe(II)-$(DETC)_2$. Both gas phase studies performed similarly in terms of signal intensity. Less NO was spin trapped when the crystallization synthesis method was used in comparison to the extraction method. This can be attributed to the loss of substance while filtering and on the filter itself. Additionally, re-crystallization resulted in some product loss. Since both methods yielded a functioning NO trapping product, it was decided to rely on the extraction method since it was simple and relatively fast. For this reason the whole smoke measurement was performed with a fresh spin trap extract.

Although it does seem that the whole smoke gives rise to a stronger NO signal, this preliminary result has to be considered carefully. While results of previous studies suggest that NO could react on the Cambridge Filter pad (i.e. during gas phase measurement)[33, 58] and thus decreasing the overall NO yield, several points should be noticed with regards to the present measurement. First of all, it should be mentioned that the extraction procedure slightly varied between the two measurements so that the exact spin trap concentrations may differ. Secondly, for the whole smoke measurement the sample was deoxygenated, slightly decreasing the line width and increasing

the sensitivity. Generally, no additional splitting was found when the modulation amplitude was decreased so that all quantitative measurements were performed without deoxygenation. Finally, as is discussed below, the NO signal increases over time. Since freeze-pump-thaw deoxygenation takes approximately 20 min, differences in intensity may result from different timing. A quantitative comparison between GP and WS measurements drawn in section 4.2.3 suggests that the amount of NO trapped from the gas phase is only 75% of the amount trapped from whole smoke. The reasons for this are discussed in 5.1.4.

Finally, the gas phase measurements appear to have a triplet that is slightly shifted to higher g-values by approximately 0.0075. However, this shift disappears if the spectrum is resonance frequency corrected.

4.1.7 Spin trap stability

In addition to the instability of spin adducts, it is known that the spin trap compounds are relatively unstable and spin trap solutions have to be prepared freshly before usage. Even analytical grade spin traps often contain impurities which give rise to weak signals in the EPR spectrum.

Stability of the spin trap solution was examined over the course of a day. In Figure 4.8 a series of measurements of the same PBN stock solution (50 mM) is shown. The measurements were taken approximately two hours apart and the main solution is kept frozen in liquid nitrogen in between. A broad weak triplet was observed already in the first spectrum, however, its intensity did not increase over the course of the day.

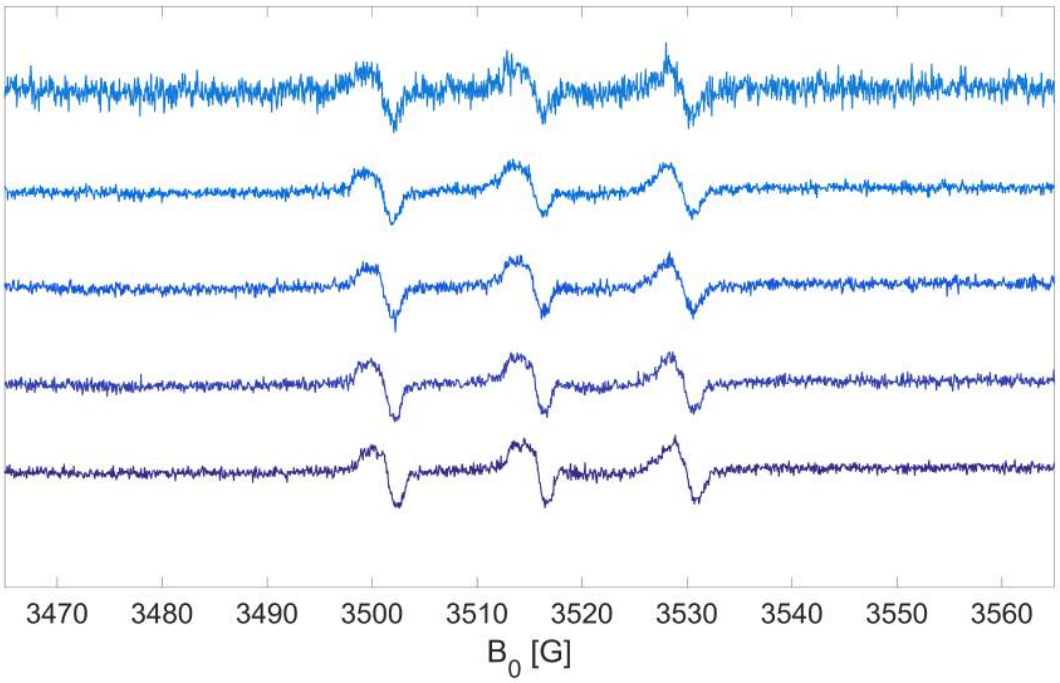

Figure 4.8: Measurements of a stock PBN solution in toluene (50 mM) over the course of a day. The bottom spectrum was taken in the morning, all subsequent spectra with an approximate time difference of 2 h. The last spectrum (top) was measured with a reduced number of scans.

While it is clear that some impurities exist in the solution, they do not increase the background signal over the course of a day, when the stock solution is kept frozen. This emphasizes the importance

of keeping exposure of the compound to the surrounding atmosphere as minimal as possible and to record a background daily. It can be assumed that similar rules apply to other spin traps. Neither PBN nor BMPO are required to be kept in an inert atmosphere (BMPO has to be protected from moisture), however, both spin traps have to be kept at -20°C for long term storage.[101, 102] In further experiments in was confirmed that the NO spin trap Fe(II)-$(DETC)_2$ remained stable over two days when kept at +4°C.

4.2 Quantitative measurements

Based on results of the preliminary experiments, a procedure was established to perform quantitative measurements. The exact experimental procedure is described in chapter 3. Briefly, spin trapping experiments using PBN, BMPO and Fe(II)-$(DETC)_2$ have been performed with all four products. Spin trap solutions have been prepared daily and, when possible, smoke/aerosols of all four products was trapped using the same solution. In order to minimize contaminations of samples from products with a low level of radicals by residual radicals in the apparatus from products with higher radical level, the usual experimental order over a day would be: "smoking" of the two e-cigarettes (in random order), then measurement of *IQOS* and then the 3R4F research cigarette. All spin trapping experiments have been performed in triplicate. Whenever the signal-to-noise ratio was sufficient, based on the three measurements results are presented as a mean and a standard deviation.

Measurements of the particulate phase radicals turned out to be challenging and therefore, no mean value can be reported except for 3R4F cigarettes. In the respective section, the details and problems as well as results are shown and discussed further below.

4.2.1 Spin trapping with PBN

Spin trapping experiments with PBN yielded detectable nitroxide signals in all four products. Figure 4.9 presents typical spectra and their best fits of the deoxygenated PBN solutions of all products. In all four cases a mixture of two radical adducts is found that we tentatively assign to oxygen-centered radicals ($a_N = 13.8 - 13.9$ G, $a_H = 1.8 - 1.9$ G) and the oxidation product of PBN, PBNOx ($a_N = 10.0 - 10.6$ G). The best fit of 3R4F spectrum taken with a reduced modulation amplitude can be found in Appendix Figure B.1. Comparison of relative integrals and the amount of substance of radicals between the products and air blanks are reported in Table 4.2. Air blanks were taken using the standard HCI puff protocol by either drawing laboratory air directly into the first impinger (air background) or by drawing the air through the whole smoking machine setup (incl. cigarette holder and Cambridge Filter pad) but without any product attached (machine background).

Additionally, kinetic measurements have been performed, repeating measurements of the same solution over a period of time. The decay of spin adducts for one 3R4F cigarette is clearly seen in Figure 4.10. A comparison between three kinetic measurements is found in Figure 4.11 **A**, where the logarithm of the signal intensity (instead of the integral in order to not include increase of PBNOx) is plotted against time. Assuming an exponential decay of the form

$$[R] = [R_0] \cdot e^{-kt} \tag{4.1}$$

with $[R]$ being the radical concentration and $[R_0]$ the value at the beginning of the kinetic measurements (time $t = 0$), a decay rate of $(2.09 \pm 0.23) \cdot 10^{-4}$ 1/s, equivalent to a half-life time $t_{1/2} = 3350 \pm 357$ s, is found.

Similar plots are found for *IQOS* and *Solaris* in Figures **B** and **C**. In both cases no decay can be found and in the case of *IQOS* even the opposite seems to be the case. In two out of three measurements with *MESH* the signal was found to be below the limit of detection or quantification

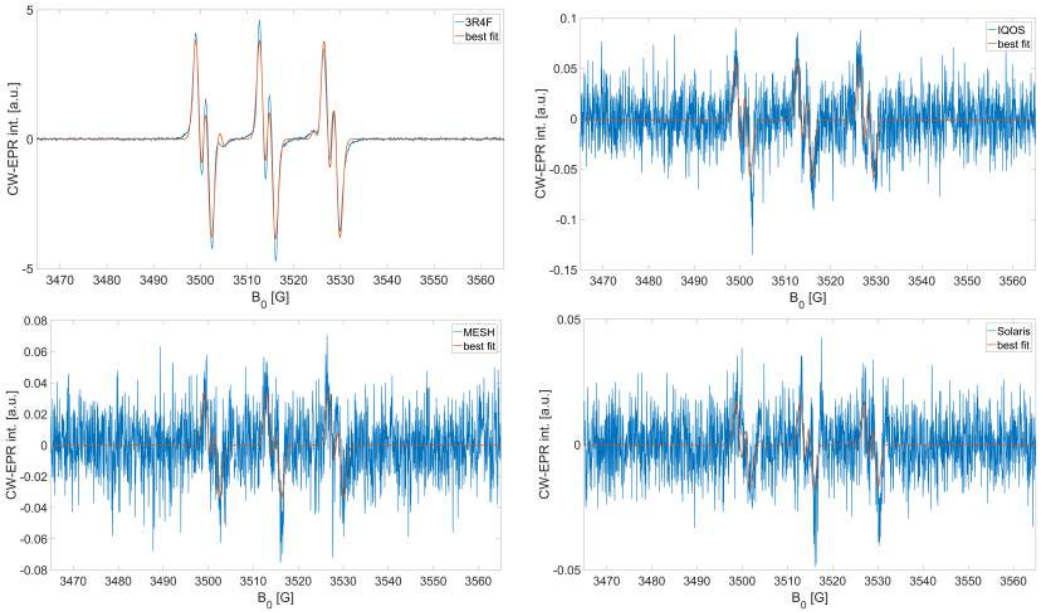

Figure 4.9: Spectra of solutions of PBN in toluene of different products. **A**: 3R4F research cigarette; **B**: *IQOS*; **C**: *MESH*; **D**: *Solaris*. In red, best fits of the spectra are shown.

(30 scans taken). For this reason, no attempt has been made to examine adduct decay for this e-cigarette.

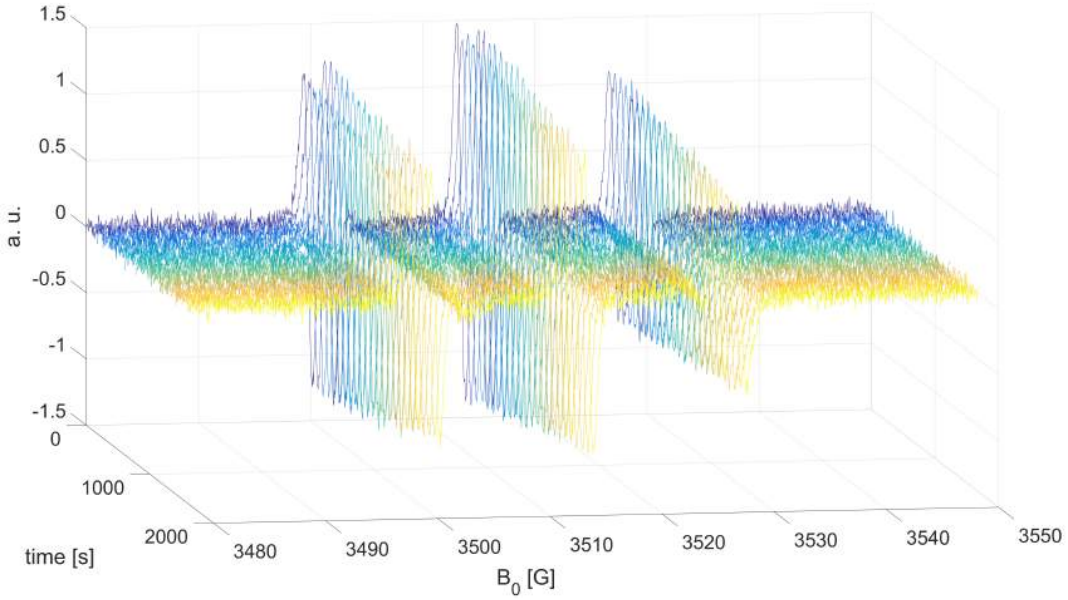

Figure 4.10: Kinetic measurement of the PBN solution from a 3R4F sample indicating a decay of spin adducts. Deviation from standard EPR parameters: modulation amplitude 0.3 G.

Table 4.2: Summary of results from PBN measurements. Shown is the relative integral in comparison to the signal from the 3R4F research cigarette (rel. int.) and amount of radicals.

Exp.	rel. int.	n [nmol]
3R4F	1	25.9 ± 0.6
IQOS	0.016	0.394 ± 0.055
MESH [a]	0.010	0.251
Solaris	0.0077	0.193 ± 0.056
machine bg	0.010	0.252
air bg	0.015	0.390
air bg[b]	0.0049	0.125

[a] No mean or standard deviation given, since in two out of three measurements signal intensity was below the limit of detection.
[b] repetition

4.2.2 Spin trapping with BMPO

Spin trapping experiments with BMPO yielded detectable nitroxide signals in all four products. Figure 4.12 presents typical spectra of the deoxygenated BMPO spin adducts of all products and their best fits. An example of an oxygen-rich sample with trapped gas phase radicals from the 3R4F cigarette was already shown in Figure 4.3 **A**. Highly complex spectra were recorded and the reproducibility was poor. In all four cases a mixture of three radical adducts is found: OH-radical ($a_N = 12.83 - 12.87$ G, $a_{H1} = 11.39 - 11.42$ G, $a_{H2} = 1.4 - 1.7$ G), OOH-radical ($a_N = 12.81 - 12.85$ G, $a_H = 11.37 - 11.48$ G) and an unidentified radical ($a_N = 12.42 - 12.54$ G, $a_{H1} = 7.04 - 7.16$ G, $a_{H2} = 1.3 - 1.7$ G). Additionally, all products beside the 3R4F cigarette indicated a presence of a carbon-centered radical ($a_N = 12.62 - 12.67$ G, $a_H = 21.4 - 21.8$ G). Neither exact components nor the hyperfine structure could be determined precisely, thus the fits do not fit measured spectra well. Comparison of relative integrals and amount of substance of radicals between the products are reported in Table 4.3. No air blanks (as described for PBN) were measured. Since PBN measurements indicate a faster decay of radical adducts from the 3R4F samples, BMPO measurements were carried out twice in the absence of oxygen and once solutions were not deoxygenated and instead immediately measured.

Additionally, kinetic measurements have been performed, repeating measurements of the same solution over a period of time. Due to poor repeatability and for better comparison between products the spin concentrations (i.e. double integrals) are plotted as ratios between integral at time t and integral of at time $t = 0$ min (int_0) in Figure 4.13. Products behave differently with some obvious decay observed for 3R4F cigarettes and a slight decrease in intensity for *IQOS* but a possible increase for *Solaris* and *MESH*.

Kinetic measurements of 3R4F cigarettes showed a fast decay of the unidentified radicals and a slow decay of the superoxide radicals (OOH) and an even slower of hydroxyl radicals (OH). In Figure 4.14 **A**, for comparison, spectra at time $t = 0$ min and at time $t = 73$ min are presented. Their respective fits are shown in Figure **B** and **C**.

4.2.3 Spin trapping with Fe(II)-$(DETC)_2$

Nitric oxide (NO) whole smoke trapping experiments with Fe(II)-$(DETC)_2$ yielded detectable signals only in measurements of 3R4F cigarettes and of *IQOS*. Figure 4.15 compares spectra of the cigarette smoke solution (both from gas phase and whole smoke) and of *IQOS*. In these cases, a broad triplet characteristic of NO with a nitrogen hyperfine coupling of ($a_N = 12.67 - 12.82$ G) is observed. These values are higher than 12.5 G reported by Vanin *et al.* in DMSO but pair well

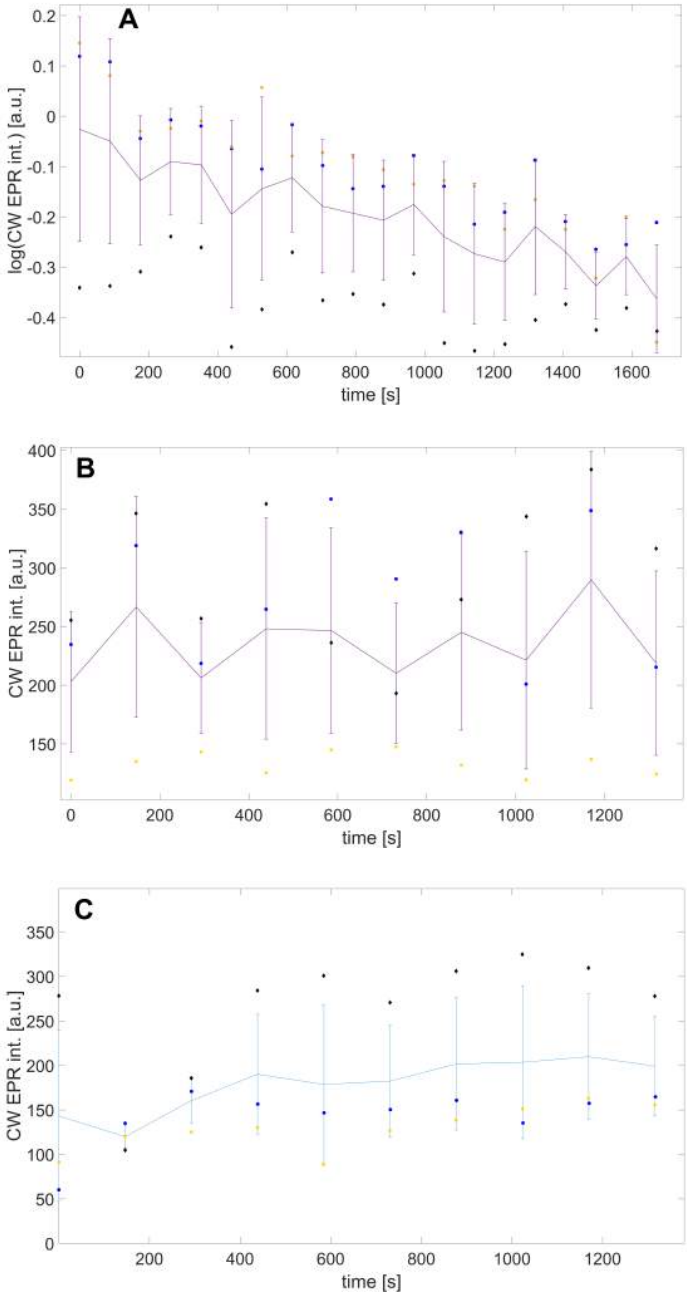

Figure 4.11: Decay of spin adducts of PBN from 3R4F, *IQOS* and *Solaris* samples over time. In case of the 3R4F research cigarettes (**A**), logarithm of the signal intensity (arbitrary units) is plotted against time. In the case of *IQOS* (**B**) and *Solaris* (**C**) the total double integral is plotted against time. Deviation from standard EPR parameters for 3R4F samples: modulation amplitude 0.3 G.

with results of Shinagawa *et al.* who measured 12.7 G in water.[35, 36] Best fits of the presented spectra can be found in Appendix Figure B.2. Comparison of fitting parameters, double integrals,

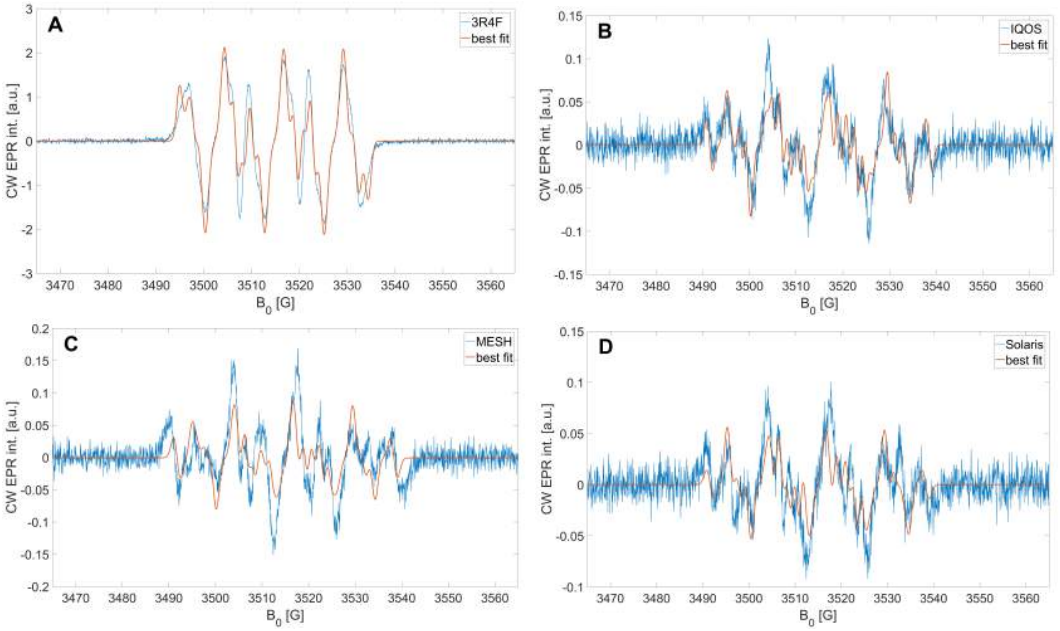

Figure 4.12: Spectra of solutions of BMPO in toluene of different products. **A**: 3R4F research cigarette; **B**: *IQOS*; **C**: *MESH*; **D**: *Solaris*.

relative intensities and mass of NO between the products are reported in Table 4.4. No air blanks (as described for PBN) were measured. An additional line was observed (marked with and asterisk in Figure 4.15). Its identity remains unclear since the MNIC-DETC triplet is very broad, but the signal has a much lower intensity than the main signal.

Additionally, kinetic measurements have been performed, repeating measurements of the same solution over a period of time. For better comparison between products and setups the spin concentrations (i.e. double integrals) are plotted as ratios between integral at time t and integral of the first measurement of the experiment (int_0) in Figure 4.16. While the MNIC-DETC signal of the *IQOS* measurement stays constant over a long period of time, the signal from the 3R4F measurements increases (**A**). The gas phase measurement shows an even stronger increase with a higher saturation value of approximately 2.9 in comparison to the saturation value of 1.3 from whole smoke (**B**). Furthermore, the saturation value of the whole smoke measurement is reached approximately after 450–550 min and then the signal slowly decreases. In contrast to that, the signal from the gas phase measurement did not reach a final saturation value even after 780 min, although the intensity increase points to a plateau. Based on reasoning by Shinagawa *et al.* [36], the increase in concentration (C) of NO should occur following

$$\frac{\mathrm{d}C}{\mathrm{d}t} = kC_0 \exp(-kt) \tag{4.2}$$

with k as the rate constant and C_0 as the initial concentration. Shinagawa's approach with a term

$$C(t) = C_0 \cdot (1 - \exp(-kt)) \tag{4.3}$$

was modified in order to account for the plotting of integral ratios R:

$$R(t) = C_0 \cdot (1 - \exp(-kt)) + 1 \tag{4.4}$$

Although in the work of Shinagawa *et al.* only values of first 25 min of measurement time were fitted, we used this approach to fit the whole kinetic series. The gas phase measurements can be fitted with $R_{GP}(t) = 1.9 \cdot (1 - e^{-0.006732 \cdot t}) + 1$ and the whole smoke measurements with $R_{WS}(t) = 0.2924 \cdot (1 - e^{-0.01591 \cdot t}) + 1$.

Table 4.3: Summary of results from BMPO measurements. Relative integral in comparison to the signal from the respective 3R4F research cigarette measurements (rel. int.), amount of radicals and measurement procedure. The samples were either measured immediately after smoking without deoxygenation (ox.) or the solutions were deoxygenated and measured 20 min after smoking (deox.).

Exp. nr.	Product	rel. int.	n [nmol]	procedure
1[a]	3R4F		1.32	deox.
2[b]	3R4F	1	42.0	deox.
3[b]	3R4F	1	82.0	ox.
1	*IQOS*		2.70	deox.
2	*IQOS*	0.0647	2.67	deox.
3	*IQOS*	0.0205	1.64	ox.
1	*MESH*		0.920	deox.
2	*MESH*	0.0612	2.52	deox.
3	*MESH*	0.00381	0.301	ox.
1	*Solaris*		0.858	deox.
2	*Solaris*	0.0476	1.96	deox.
3	*Solaris*	0.0110	0.878	ox.

[a] 20 puffs in total. The integral is unusually low, so no relative intensity was calculated.
[b] 14 puffs

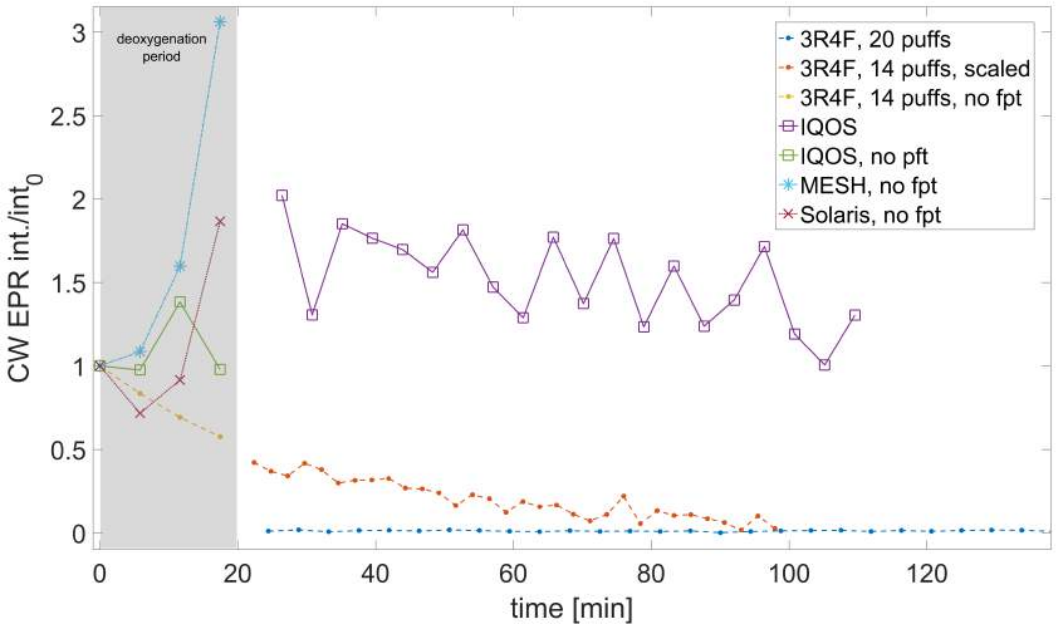

Figure 4.13: Decay of spin adducts of BMPO from 3R4F (·), *IQOS* (▫), *MESH* (∗) and *Solaris* (x) samples over time. For experiments, where no deoxygenation (freeze-pump-thaw) has been done prior to the measurement, "no fpt" is added in the legend. In case of the 3R4F research cigarettes the puff number is shown in the legend. Furthermore, one kinetic series has been measured with a reduced modulation amplitude and scaled up to 2 G ("scaled"). The deoxygenation period is indicated by a grey background.

Table 4.4: Summary of results from NO measurements. Relative integral in comparison to the signal from the 3R4F research cigarette (rel. int.), mass of NO and the coupling constants from the fit. No standard deviation for the 3R4F gas phase experiment is given since only two measurements were performed; the given value is a mean between the two values.

Exp.	rel. int.	m [μg]	a_N [G]
3R4F (WS)[a]	1	16.4 ± 4.7	12.75 ± 0.05
3R4F (GP)	0.75	12.3	12.77
IQOS	0.073	1.17 ± 0.14	12.73 ± 0.04
MESH	-[b]		
Solaris	-[b]		

[a] Higher standard deviation and lower mean value results from the contribution of one measurement, where a cigarette was burnt in 17 puffs instead of 10-13 puffs.
[b] not detected

4.2.4 Measurement of the Total Particulate Matter

Total Particulate Matter (TPM) was weighted after smoking and its extracts of toluene measured with EPR. Additionally, air was passed through the Cambridge Filter pad to measure the background water uptake of smoking but the results were inconclusive. EPR background spectra were recorded by measuring toluene extracts of clean Cambridge Filter pads. Due to extremely weak signal intensities the final experiments were performed after accumulating TPM of two or three cigarettes, sticks etc. on one pad. Longer extraction (2.5 h instead of 20 min) did not yield a significant increase in signal. The spectrum from the extract of three 3R4F cigarettes is shown in Figure 4.17. The broad signal with a total width of approximately 30 G and a peak-to-peak width of 7 G is very similar to the TPM signals reported by Pryor *et al.* [20, 24] and referred to as "Primary type II" radicals[26]. Results concerning TPM weight and radical yield are presented in Table 4.5. Photos of the filters after smoking are presented in Figure D.3.

4.2.5 Repeatability and measurement significance

Generally, repeatability of PBN experiments was found to be sufficient. A comparison between integrals of three 3R4F measurements as seen in Figure 4.11 **A** shows good agreement between two measurements. It is unclear, why the third sample indicates a lower radical level and an overall slower decay. All three cigarettes have been smoked with 11 puffs. The differences in radical level could possibly be explained by slight differences in PBN concentration between the three solutions or solvent evaporation during smoking. Radical levels varied strongly in other products, especially in *MESH* for which in two out of three measurements the signal was found to be below the limit of detection. Stronger variability is expected since errors of integration become larger when operating near the detection limit.

In this work the reproducibility of BMPO measurements was poor due to different factors. The first measurement of the 3R4F cigarette suffered from slow burning. It took 20 puffs in total for the cigarette to be consumed. Generally, the cigarette appeared to be smoldering rather than burning and the Cambridge Filter pad was significantly cleaner than usual. The amount of spin trapped radicals is greater than that of most measurements of the e-cigarettes (see Table 4.3), but drastically lower than the levels of the other two measurements. Further, the spin adducts do not show a clear decay over a measurement time of 900 min (Figure 4.13); the time axis is cut after 140 min), so this measurement was ignored for comparison with the other products.

Unfortunately, only *IQOS* measurements were successfully reproduced, as indicated by the similar radical levels in measurement one and two (2.70 nmol and 2.67 nmol). *MESH* and *Solaris* indicate in experiment nr. 2 a similar radical level as *IQOS* (2.52 nmol and 1.96 nmol, respectively), but show

Table 4.5: Results of the TPM measurements. Number of accumulations on the filter pad (nr. of cigs.), relative integrals in comparison to 3R4F cigarettes, amount of substance and TPM weight per accumulation for each product. Means do not include measurements with signal below detection or quantification limit. Standard deviation is not given when the number of measurement points is lower than two.

Exp. nr.	Product	nr. of cigs.	rel. int.	n [nmol]	TPM/cig [mg]
1	3R4F	1		1.07	35.9
2[a]	3R4F	1		1.39	33.8
3	3R4F	1		0.74[b]	38.4
4	3R4F	3		2.30	22.4
Mean	3R4F	6	1	0.95 ± 0.25	32.6 ± 6.1
1	*IQOS*	1		-[c]	27
2	*IQOS*	3		0.177	27.0
3	*IQOS*	3		-[c]	24.3
Mean	*IQOS*	6	0.062	0.0590	26.1 ± 1.3
1	*Solaris*	1		-[c]	23.6
2	*Solaris*	3		0.0580	25.5
3	*Solaris*	3		-[c]	22.5
Mean	*Solaris*	7	0.020	0.0193	23.8 ± 1.2
1	*MESH*	1		0.0852	56.7
2[d]	*MESH*	2		0.0687	48.1
Mean	*MESH*	3	0.054	0.0513	52.4

[a] extraction for 2.5 h
[b] Measured with a modulation amplitude of 0.3 G and scaled to 2 G. Not included in mean calculation.
[c] not detected
[d] Only 2 instead of 3 times smoked in order to accumulate less than 150 mg TPM in total.

a significant decrease in experiment nr. 1 and resemble those values of non-deoxygenated samples (experiment nr. 3). A possible explanation is an error in the deoxygenation procedure: possibly, the nitrogen gas supply was sealed during the freeze-pump-thaw cycles. This explanation is supported by the fact that *IQOS* was the first product to be measured during that day and could have been supplied with residual nitrogen gas inside the Schlenk line. Based on this reasoning, experiment nr. 2 is expected to yield more reliable results, followed by experiment nr. 3.

NO trapping experiments were successfully repeated and the error for *IQOS* measurements (standard deviation of 12%) is acceptable. One cigarette showed again an increased puff number resulting in decreased emission.

Measurements of particulate phase radicals turned out to be challenging and repeatability poor. In this study it was decided to measure TPM extracts instead of the filters themselves in order to be able to use the AquaX and avoid reproducibility issues due to questionable positioning of the filters in the cavity or a sample tube. However, this sample dilution is the source of sensitivity issues. In many studies, either the filters (or equivalent collection matter, e. g. glass wool) are measured directly by placing them in the spectrometer[24, 64, 103–105] or by measuring TPM extracts which were dried completely or at least the extraction volume reduced by evaporation.[11, 19] Evaporating the extraction solvent completely and subsequently dissolving the particulate in a reduced volume of toluene (e.g. 3 mL) for the measurement of particulate phase radicals should increase sensitivity.

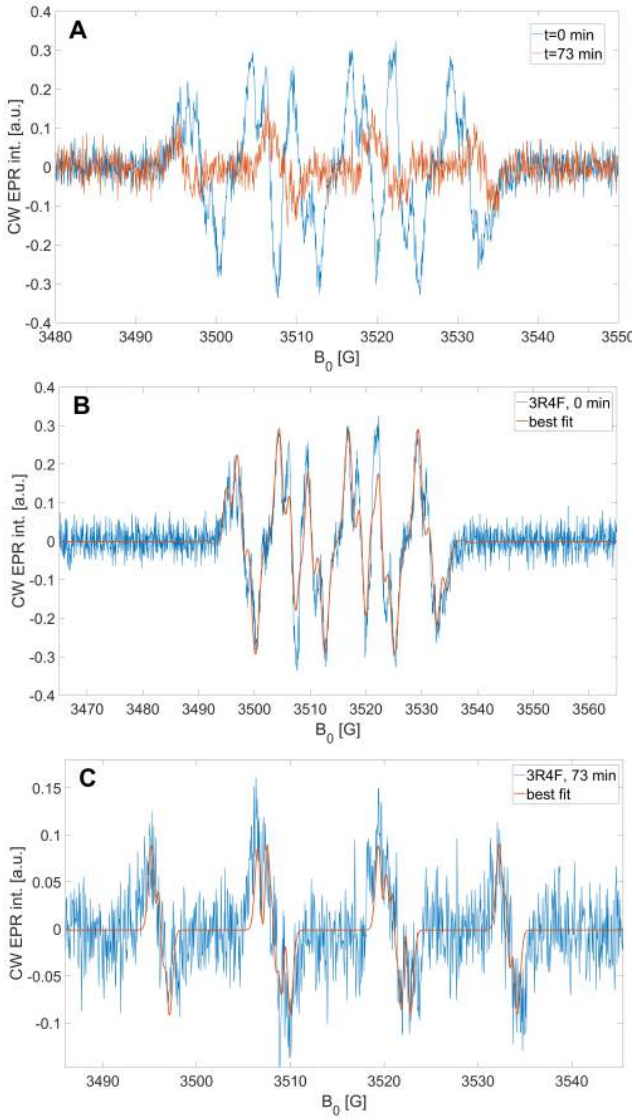

Figure 4.14: **A**: A comparison between BMPO spectra of 3R4F at 0 and 73 min. **B**: Best fit of the spectrum at 0 min. **C**: Best fit of the spectrum at 73 min.

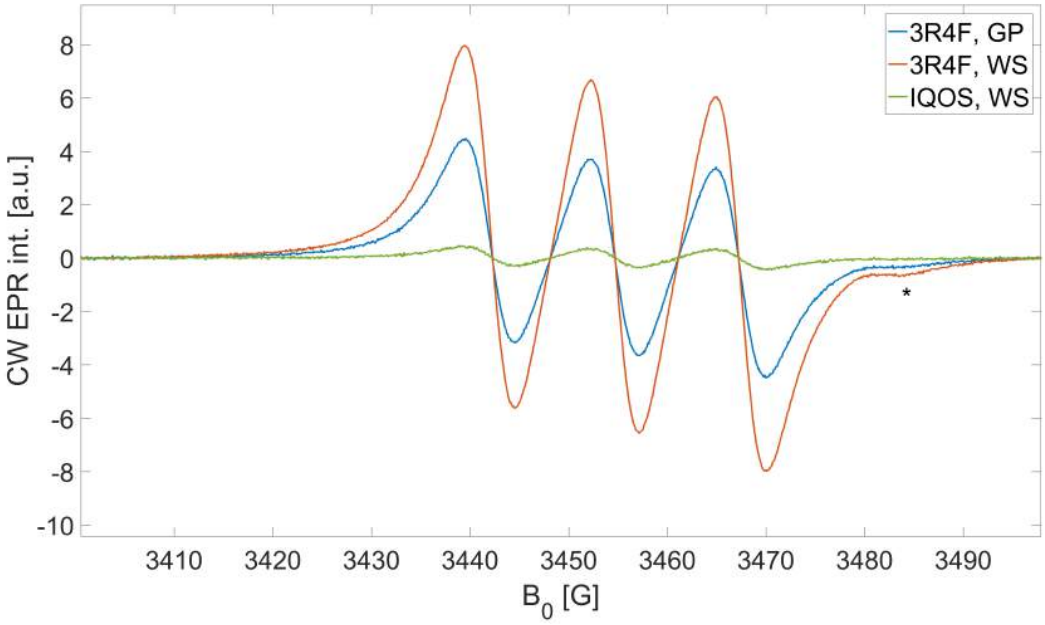

Figure 4.15: Typical MNIC-DETC spectra of the 3R4F research cigarette and of *IQOS*. Additionally, a spectrum of NO captured from the gas phase (GP) is shown for comparison with the whole smoke capturing (WS). The identity of the signal marked with an asterisk is unknown.

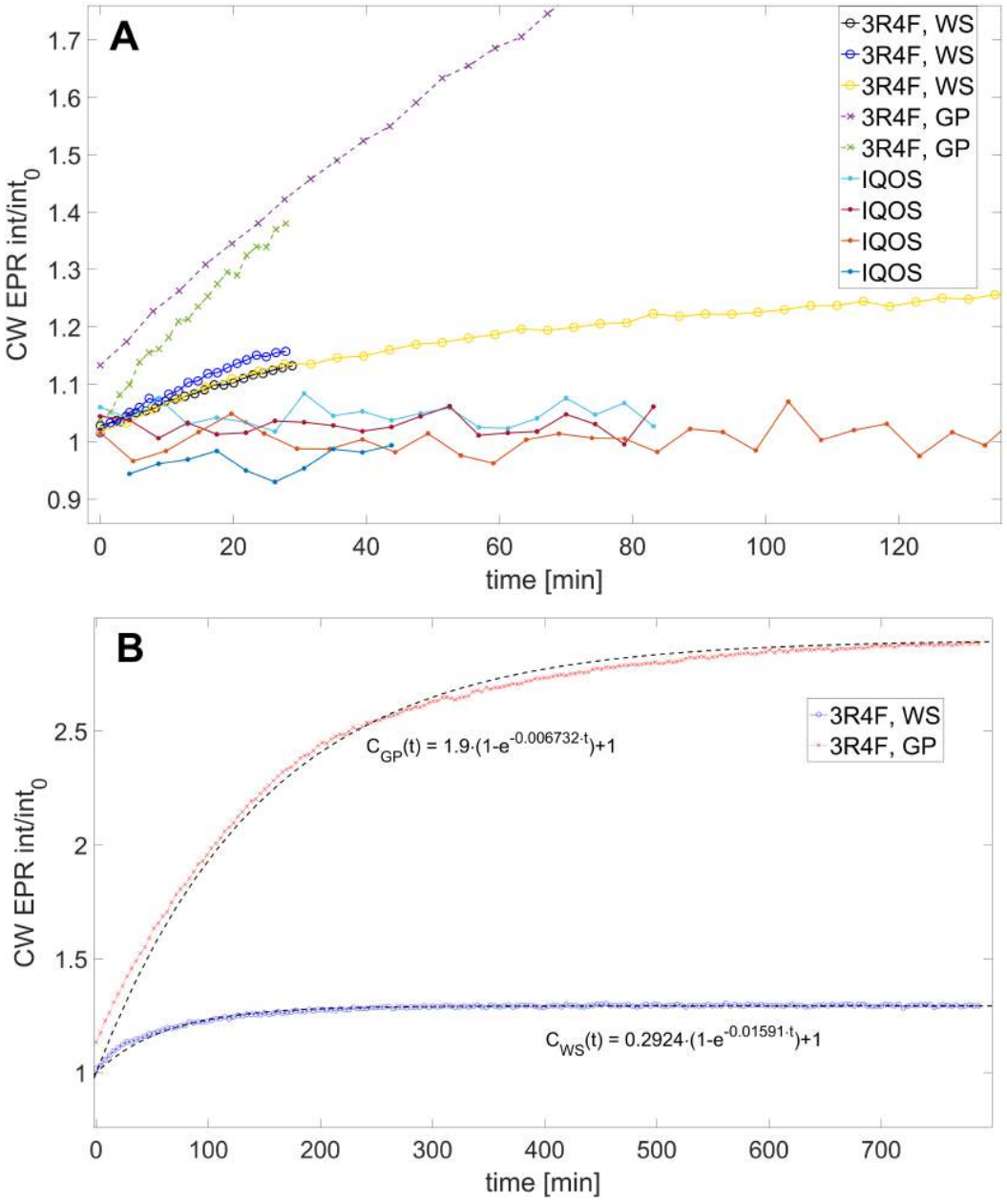

Figure 4.16: Integral ratios of MNIC-DETC spectra between the measurement at time t and time $t = 0$ min for the whole smoke (WS) measurement of 3R4F and *IQOS*. Additionally, gas phase (GP) measurements of 3R4F are presented. **A**: NO spin trapping kinetics over a short period of time. **B**: A comparison between long measurements of GP and WS from NO spin trapping. The fits of the measurements are added.

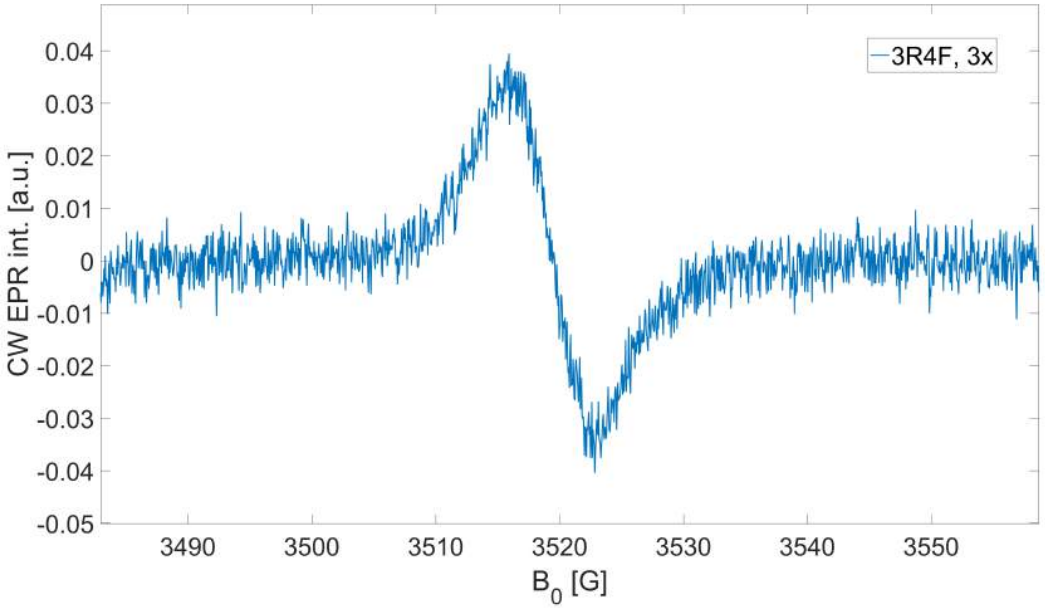

Figure 4.17: Measurement of the toluene extract of TPM from three 3R4F cigarettes showing a "Primary type II" radical with a total width of 30 G.

Chapter 5

Discussion

5.1 Quantitative measurements

The major goal of quantitative measurements is to directly compare levels of radicals and NO between conventional cigarettes and other products (HNB, e-cigarettes) in the gas and particulate phases. Radical levels are compared based on signal double integrals of the spin trapping (gas phase) and TPM extraction experiments (particulate phase). Additionally, types of radicals found in different products are compared and their buildup and decay kinetics discussed.

5.1.1 Identity of radicals

In general, the PBN spectra of the four products look very similar in terms structural properties (see Table 5.1). Three radical adducts were identified in all four products: an alkoxy radical ($a_N = 13.7-13.8$ G, $a_H = 1.8-1.9$ G) and the oxidation product of PBN, PBNOx ($a_N = 10.0-10.6$ G). A similar hyperfine structure was found in the air samples. These radicals have been previously trapped in cigarette smoke.[41, 45, 93] Although the coupling constants of the radicals significantly differ between different products (e.g. $a_N^{OR} = 13.69$ G for *IQOS* and $a_N^{OR} = 13.84$ G for *Solaris*), the implications of these findings are unclear; it could indicate the presence of different radicals. The signal-to-noise ratios for all measurements except of 3R4F cigarettes are low and many lines are not clearly resolved. For this reason, the coupling constants derived from 3R4F spectra are more reliable than those from other measurements. The difference in the nitrogen coupling constant of the oxidation product is significant: Pryor *et al.* measured a coupling of $a_N = 10.4$ G while Church *et al.* reported $a_N = 8.0$ G, a value similar to the $a_N = 8.4$ G reported by Ghosh *et al.*.[41, 45, 50] These differences do not result from different solvents (all measured in benzene). In this work, we found a PBNOx coupling constant of $a_N = 10.3-10.5$ G which is similar to the results by Pryor *et al.* [41] Pryor also found a different oxidation product with a nitrogen coupling of $a_N = 7.9-8.1$ G. This value is similar to the ones reported by the two previously mentioned studies and also similar to the value for the decomposition product found by Ghosh. This could imply that differences in these values result from different oxidation products.

In Figure 4.12 the spectra of the second measurement of BMPO adducts are presented. These spectra indicate the presence of several trapped species. In order to identify the radicals, a kinetic measurement was performed. In Figure 4.14 **A** a comparison is shown between the first kinetic measurement of the deoxygenated 3R4F sample and the last. The spectrum has lost many lines, indicating a difference in decay rates between radical adducts or even an increase in the concentration of other radicals over time. The simple structure of the measurement at $t = 73$ min can be fitted with a mixture of hydroxyl and peroxyl radicals (see Table 5.2). Additional comparison with spectra acquired around the 73$^{\text{rd}}$ minute show a structural change from four lines with same intensity

Table 5.1: Coupling constants reported for PBN adducts and found in this work.

Study	Radical type	a_N [G]	a_H [G]
3R4F	OR	13.80 ± 0.002	1.88 ± 0.02
	PBNOx	10.25 ± 0.29	-
IQOS	OR	13.69 ± 0.08	1.83 ± 0.02
	PBNOx	10.65 ± 0.28	-
MESH	OR	13.8	1.82
	PBNOx	10.6	-
Solaris	OR	13.84 ± 0.27	1.84 ± 0.10
	PBNOx	9.98 ± 0.37	-
air	OR	13.87 ± 0.08	1.73 ± 0.28
	PBNOx	10.37 ± 0.45	-
Pryor *et al.*, 1976[41]	OR	13.9 ± 0.3	1.9 ± 0.2
	PBNOx	10.4	-
Church *et al.*, 1994[45]	OR	13.6	1.9
	C-R	14.4	2.0
	PBNOx	8.0	-
Ghosh *et al.*, 2008[50]	C-R	14.2	2.05
	PBNOx	8.4	-
	D[a]	7.6	-
Goel *et al.*, 2015[92]	R1[b]	14.05	2.21
	R2[b]	14.17	2.47

[a] D = decomposition product
[b] Measurement of e-cigarette aerosols. Radical identities not specified.

(OOH) to the quartet of OH.[51] The adduct BMPO-OOH could have been reduced to BMPO-OH by other smoke constituents over time[51], although the gas phase is considered to be oxidizing.[1] Unlike DMPO, BMPO adducts with superoxide radicals do not decompose to hydroxyl adducts on their own, but can be enzymatically reduced to these species.[51] It is unknown whether the hydroxyl adducts of BMPO can be formed in a Forrester-Hepburn reaction, but it seems unlikely since the solvent is not water.[28] To the best of our knowledge, BMPO has not been used with an organic solvent before. In an aqueous solution Khan *et al.* found a half-life time for BMPO adducts to be 8.4 min for methyl radicals and 19.3 min for hydroxyl radicals.[106] Both values support our findings of fast decay of the major radicals and a slow decay of the hydroxyl radicals. The appearance of both OOH and OH radicals in cigarette smoke is not surprising and their correlation has been often studied in aqueous media (e. g. by Culcasi *et al.* [60], Takanami *et al.* and Tanigawa *et al.* [98]). In his review, Wooten summarized previous findings and explains that trace metal ions such as Fe(II) or Cu(I) can catalyze the formation of hydroxyl radicals from hydrogen peroxide via Fenton chemistry.[7] This is the likely source of the trapped hydroxyl radicals.

For the fit of the first kinetic measurement an additional radical was considered. However, the small coupling constant $a_{H1} = 7.1$ does not compare well with known constants for oxygen- or carbon-centered radicals (Table 5.2). Zhao *et al.* assigned two sets of coupling constants to diastereomeres of the same radical. Hyperfine structure data referenced in Table 5.2 has been identified in an aqueous solutions and the coupling constants are generally higher than the ones we observe. We performed short DFT calculations to estimate coupling constants of different diastereomeres of peroxyl and hydroxyl adducts in toluene. However, our findings were inconclusive. It is possible that we assigned coupling constants incorrectly and the unknown radical is just a diastereomere

of OH or OOH adducts. Without reference studies for BMPO in toluene or other apolar solvents further assignments are unsafe.

Interestingly, no alkoxy or carbon-centered radicals were detected in 3R4F cigarette smoke by spin trapping with BMPO, but the carbon-centered radicals have been trapped from aerosol of other products. It is possible that the carbon-centered radicals originate from polypropylene glycol or glycerol.[92] On the other hand, reaction of BMPO with hydroxyl radicals is one to two orders of magnitude faster than the reaction with carbon-centered radicals (in water).[46] It seems likely that the reaction rate of BMPO with the alkoxy and carbon-centered radicals specifically found in cigarette smoke is too slow and the radicals decay before being trapped.

Moreover, neither hydroxyl nor peroxyl radicals have been trapped by PBN, while BMPO did not trap any alkoxy and carbon-centered radicals in cigarette smoke. This emphasizes the importance of the use of several spin traps.

Table 5.2: Coupling constants reported for BMPO adducts and found in this work.

Study	Radical type	a_N [G]	a_{H1} [G]	a_{H2} [G]
3R4F	OH	12.85 ± 0.02	11.4 ± 0.004	1.65 ± 0.04
	OOH	12.8 ± 0.02	11.4 ± 0.03	-
	unknown	12.5 ± 0.02	7.17 ± 0.13	1.58 ± 0.07
IQOS	OH	12.8	11.4	1.47
	OOH	12.8	11.5	-
	unknown	12.5	7.15	1.37
	C-R	12.7	21.8	-
MESH	OH	12.8	11.4	1.63
	OOH	12.8	11.5	-
	unknown	12.5	7.15	1.51
	C-R	12.7	21.5	-
Solaris	OH	12.8	11.4	1.7
	OOH	12.8	11.5	-
	unknown	12.4	7.07	1.52
	C-R	12.6	21.4	-
Arangio *et al.*,[a] 2016[107]	OR	14.5	16.6	-
	OOH	14.3	8.1	-
	OH	14.3	12.7	0.61
	R	15.2	21.6	-
Zhao *et al.*,[b] 2001[51]	OOH	13.37-13.4	9.42-12.1	-
	OH	13.47-13.56	12.30-15.31	0.62-0.66
	GS[c]	14.3-14.36	14.7-16.6	1.3-1.8
Huang *et al.*,[b] 2013[108]	t-BuO	14.09	14.02	-
	CH3	15.61	22.24	-
	CBQ-OH[d]	16.28	26.5	-

[a] System: aqueous extract of aerosol particles.
[b] System: phosphate buffer, pH=7.4.
[c] GS = glutatiyl radical.
[d] CBQ-OH = carbon-centered quinone ketoxy radical

5.1.2 Radical levels in the gas phase

The major difference between products in measurements of PBN spin trapping is the radical level. Aerosol of *IQOS* and the two e-cigarettes show a relative intensity of approximately 1-1.6% of that of the research cigarette. The amount of radicals found in the 3R4F cigarette with 25.9 ± 0.6 nmol is four times higher than that reported by Goel *et al.* with 8 ± 2 nmol. However, Goel *et al.* followed the ISO norm for smoke generation and not the HCI norm used in this work. For a filter ventilation of 38% (as found for the 3R4F cigarette by Goel *et al.*) or a 29% ventilation found by Roemer[32], Counts *et al.* [109] and Purkis *et al.* [110] predict 2-4 times higher emissions from HCI regime than from ISO. Considering a difference in measurement timing - in the work of Goel *et al.* 6 min passed in total for deoxygenation - and the decay rate determined from our kinetic measurements, the initial radical concentration produced by the 3R4F cigarette is approx. $[R_0] \approx 33.3$ nmol. This number is within the fourfold range of 8 ± 2 nmol reported by Goel *et al.* [64] Reported amount of radicals varies greatly: Yu *et al.* found only 2.5 nmol ($1.5 \cdot 10^{15}$ spins)[93], Ghosh *et al.* accumulated 2.0 nmol ($12 \cdot 10^{14}$ spins) from a measurement on a puff-by-puff basis[50]. In the latter work, PBN indicated a loss in trapping efficiency at the last ($9^{\mathbf{th}}$) puff. The authors speculated prolonged exposure to cigarette smoke to be the source of this error. Another explanation is the quenching of new gas phase radicals by the particulate phase deposited on the Cambridge Filter.[26] This further indicates that increased puff numbers make comparison between individual measurements difficult and decrease precision by reducing the apparent radical levels.

The radical level of $[R_0] \approx 33.3$ nmol is still an order of magnitude lower than the 225 nmol from whole smoke solid-phase trapping by Bartalis *et al.* and still lower than the approximate 70 nmol trapped from whole smoke in toluene.[61, 62] While Bartalis *et al.* used the ISO smoking regime which leads to lower emissions, they used a nitroxide probe which traps alkyl radicals five times more efficiently than PBN.[62] This could explain the major differences in radical levels between their results and ours. Furthermore, it points out that solid-phase spin trapping could be more efficient than solution spin trapping and additionally, solvent-free trapping prevents radicals from forming secondary radicals by reacting with solvent molecules.[26, 62] However, in both studies, radical adducts were quantified using fluorescence detection after a separation by HPLC. Thus, radical levels between the two different quantification techniques may not be directly comparable.

Margham *et al.* pointed out the importance of air background measurements when determining emissions from e-cigarettes in order to avoid false positive findings.[111] Our measurements support these observations. While a general difference between the HNB-product and the e-cigarettes appears to be present (a radical amount of 0.394 ± 0.055 nmol was measured for *IQOS* in comparison to 0.193–0.251 nmol measured for the e-cigarettes), the values lie below the air or machine background of 0.0125–0.390 nmol. Radical levels of the machine background lie between the levels of the two air measurements. This indicates that residual chemicals in the smoking machine from previous experiments do not noticeably increase the background noise. Nevertheless, this raises the questions regarding limits of quantification. Furthermore, fitting parameters of the air samples are similar to those of the four products and could indicate contribution of Environmentally Persistent Free Radicals (EPFRs) to the integrals of the aerosols. Radical levels for *IQOS* are very similar to the highest air background. The present data suggests a higher radical level in the heat-not-burn product in comparison to the e-cigarettes, however, this difference could stem from false positive findings. It cannot be excluded that the aerosol of e-cigarettes quenches EPFRs. In general, due to high level of noise in the spectra integration is difficult and may be solely responsible for differences in radical levels in these products and air samples. The usage of multiple port smoking machines to accumulate gas phase radicals without time loss for subsequent smoking should increase the signal intensity.

Pryor *et al.* found that gas phase radical levels of a heat-not-burn product are less than 1% of the levels of a conventional cigarette.[11] This generally corresponds to the ratio between 3R4F and *IQOS* radical levels as found in this work (1.6%). Goel *et al.* reported $2.5 - 10.3 \cdot 10^{13}$ radicals per puff of an e-cigarette (based on 40 accumulated puffs).[92] This corresponds to 0.50–2.05 nmol

per 12 puffs (as were used in this work). These values are two to eleven times higher than the 0.19–0.25 nmol found in this thesis and lie above air and machine background levels. This could indicate a high variability in emissions of different e-cigarettes. It should be stressed, nonetheless, that in our case two out of three *MESH* measurements resulted in a signal below the limit of detection or quantification.

BMPO spin trapping measurements indicate a higher relative intensity of radicals in aerosols in comparison to the 3R4F cigarette smoke than found in PBN measurement. Spectra of 3R4F cigarettes show a signal several times stronger than the other products which produce spectra generally similar to each other. For the deoxygenated samples 42.0 nmol of radicals were found in the sample of the conventional cigarette. This number increased to 82.0 nmol when the sample was measured without deoxygenation immediately after smoking. At the same time, relative intensity of the other products decreased from 4.8–6.5% of the 3R4F signal for the oxygen-free measurement to 0.4–2.1% for the immediate, oxygen-rich measurement. The implications of this finding are discussed below in 5.1.4.

It should be stressed that no air background measurements have been performed. Almost all aerosol experiments find a higher radical level (0.88–2.67 nmol) than the machine background measured with PBN (0.39 nmol); only the oxygen-rich sample of *MESH* shows a lower amount of radicals. However, it is unclear, whether the background radical levels found with PBN can be directly translated to BMPO measurements. BMPO is often used as a superoxide scavenger[51, 112] and could react differently with oxygen than PBN. Finally, non-deoxygenated measurements of aerosols suffer from very low signal-to-noise ratios which makes integration difficult and can further add to interpretation errors.

Significant differences in radical emissions from different products were found when Fe(II) complexes of dithiocarbamates were used for NO trapping. From Figure 4.15 a general trend can be estimated: more NO can be trapped from whole smoke than from the gas phase and the cigarette produces several times more NO than *IQOS*. No nitric oxide has been detected in either of the e-cigarettes. This is consistent with the findings of Margham *et al.* [111] who compared emissions from the e-cigarette *Vype ePen* to those from the 3R4F. This comes at no surprise since the main source of the NO is cigarette smoke are nitrates and tobacco proteins.[1] The main ingredients of the e-liquids are, however, glycerol, propylene glycol, water and nicotine. The oxidation of nitrogen gas from the surrounding air to NO (which occurs during cigarette combustion[1]) is unlikely due to low heating temperatures of the e-cigarettes. Thus, the absence of NO is e-cigarette aerosols is expected.

In general, total NO mass from whole smoke (16.4 ± 4.7 μg) of the 3R4F cigarette is larger than the mass from gas phase (12.3 μg). The large standard deviation results from one experiment with a lower NO mass. In that experiment, the cigarette burnt in 17 puffs. Following the reasoning from the BMPO experiments, it is expected that the overall yields are lower when the cigarette burns slowly. Slow burning could decrease combustion temperatures and thus oxidation of proteins to NO. When the result from the 17-puff experiment is ignored, the average NO-mass from whole smoke is 19.5 μg. The lower mass of NO in the gas phase comes at no surprise. NO is reported to have a faster oxidation rate in gas phase than in whole smoke.[58] Additionally, NO_2, the main oxidation product of NO in air, is only present in the first puff when whole smoke is measured, presumable from cigarette lighting.[33] In contrast to that, NO_2 is present in every puff when the gas phase is measured.[33] This implies oxidation of NO to NO_2 on the Cambridge Filter pad itself.[7] This explains the lower yields of nitric oxide in gas phase smoke in comparison to whole smoke.

IQOS produced low levels of nitric oxide, approximately 7.3% of the amount from cigarette whole smoke. However, if the value of 19.5 μg for NO trapped in the 3R4F smoke is considered to be more accurate, then the relative NO productions by *IQOS* decreases to 6.0%. This percentage is higher than 2-3% as reported by Schaller *et al.* and Gonzalez-Suarez *et al.* [30, 31] In both studies *IQOS* was smoked using the HCI regime (as was the 3R4F cigarette) and the comparison is more

direct. In the case of this study, *IQOS* was smoked following the CORESTA recommendation for electronic devices. Both regimes use the same puff volume and frequency and differ only in puff duration and profile (see Table 2.1). Further, in both studies NO was measured in gas phase and not in whole smoke, as in this thesis. This could account for the differences in our and previously reported results.

The absolute values are more than an order of magnitude lower than previously reported values. For *IQOS*, 13.0 and 16.8 μg have been measured with a NO meter[31] or following a Health Canada Official method[30]. The same goes for results of the cigarette smoke. Schaller *et al.* reported 510 μg[30], Gonzales-Suarez *et al.* 491 $\pm$ 12 μg[31] and Margham *et al.* 503 $\pm$ 23 μg[111] of NO in cigarette smoke. The reason for such discrepancies could be that some NO leaves the impinger before being trapped if the trapping kinetics are not sufficiently high, despite NO being an apolar gas.[36] This is not an issue for detection methods when the smoke is collected in a gas collection bag.

Shinagawa *et al.* trapped smoke of Japanese cigarette with Fe(II)-$(MGD)_2$, a water soluble analogue of the spin trap used in ths work.[36] The smoking procedure was non-standard (continuous air flow, 600 ml/min) and based on calibrations with an NO donor *S*-nitroso-*N*-acetylpenicillamine they found $1.52 \cdot 10^{17}$ spins, i.e. 252 nmol or 7.57 μg. It is unclear, whether the trapping method or the non-standard smoking procedure results in this low NO yield.

5.1.3 Analysis of the particulate phase

3R4F research cigarettes yielded 32.6 $\pm$ 6.1 mg TPM. This compares well to the 37.7 $\pm$ 0.3 mg reported by Roemer *et al.* [32], but is significantly less than 49 $\pm$ 1.5 mg or 44.7 mg reported in [31] and [30]. It is unclear, why these values differ this much, considering that in all cases the HCI smoking regime was used. Experimental results reported in table 4.5 suggest that smoking of several cigarettes on one Cambridge Filter decreases the yield per cigarette. Only *Solaris* does not follow this trend. While TPM loss due to continuous smoking is known, it should not occur for two and three smoked cigarettes.[83] The 44 mm Cambridge Filter pad is designed to uptake 150 mg of TPM[65] which is much more than was collected in a single experiment of this study.

Similarly, significant differences are found for *IQOS* with 26.1 $\pm$ 1.3 mg of collected TPM in comparison to 48.2 $\pm$ 0.8 mg[31] and 54.7 $\pm$ 3.2 mg[30]. Here, partially the difference could be explained with differences in the smoking regimes. For *Solaris* and *MESH* no TPM data has been published so far. Interestingly, we found similar levels of TPM for *IQOS* and *Solaris*. Since *IQOS* plugs have similar ingredients as usual e-cigarettes (water, glycerol, propylene glycol, nicotine), it is not surprising for both products to yield similar TPM levels. The fact that *MESH* produces more TPM than the cigarette or the other products is surprising and has to be attributed to a different liquid heating method. Sussan *et al.* collected 30.4 mg of TPM from 50 puffs (equals to 7.3 mg for 12 puffs) of another e-cigarette employing a modified ISO regime.[104]

The spectrum of the toluene extract of 3R4F TPM indicates the presence of long-lived radicals (Figure 4.17). Interestingly, the amount of radicals found in the tar extract (0.95 $\pm$ 0.25 nmol) is more than one order of magnitude larger than values reported by Goel with 64 $\pm$ 13 pmol.[64]

In most cases, signal intensity of the TPM extract of *IQOS* and of the e-cigarettes was below detection limit. While it is not surprising per se since already the detection of gas phase radicals appeared to be problematic due to low radical levels, it does create ambiguity in regards to the signals eventually detected. Goel *et al.* reported a linear correlation between signal intensity and the number of cigarettes smoked.[64] The integrals in our measurements do not follow this trend; three 3R4F cigarettes yield only 2.30 nmol of radicals instead of 3.21–4.17 nmol, as would be expected from a linear correlation. This further questions the sensitivity of our measurements.

Sussan *et al.* found $7 \cdot 10^{11}$ long-lived spins in TPM collected after 50 puffs. This corresponds to 0.3 pmol for 12 puffs.[104] However, in that study no blank measurements have been performed

so a false positive finding is possible. On the other hand, Lerner *et al.* reported findings of 4.8 and 7.7 μmol from 20 4-5 s puffs.[103] Unfortunately, the authors did not comment on the large differences in radical levels between their results and those of previously published studies. Pryor *et al.* did not detect any particulate phase radicals from a HNB product.[11] These findings may indicate limits of EPR detection for aerosol samples or they may describe a great variability in e-cigarette products. Gehling *et al.* [113] measured EPFR levels in ambient particulate matter ($PM_{2.5}$) and detected long-lived stable organic radicals, very similar to those found by Sussan *et al.* and Lerner *et al.* On average, the initial radical concentration was $2.02 \cdot 10^{16}$–$3.48 \cdot 10^{18}$ 1/g. This equals to $4.81 \cdot 10^{14}$–$1.82 \cdot 10^{17}$ radicals or 0.80–302.2 nmol if the TPM weight from our results is used (23.8–52.4 mg). This is more than the radical levels detected in this work and further emphasizes the importance of background measurements.

5.1.4 Radical kinetics

The decay of the main radical adducts found in PBN solutions of 3R4F cigarette gas phase smoke (Figure 4.11 **A**), as seen in Figure 4.10, is steady and is accompanied by a slow increase of the oxidation product of PBN, PBNOx.

Kinetic measurements of *IQOS* do not indicate any clear decay (Figure 4.11 **B**). This additionally hints at the possibility that these radical adducts are distinctively different from the smoke based. Surprisingly, the adducts from *Solaris* even show an initial increase in intensity (**C**) but it is difficult to interpret this result considering the possibility of a false positive finding. Furthermore, it is possible that a decay could have been observed, if the samples were measured immediately after smoking. Smoke composition can influence the stability and formation of spin adducts: for instance, in an organic solvent, the presence of water drawn from the air could facilitate adduct formation via Forrester-Hepburn mechanism.[28] On the other hand, nitroxides with an β-hydrogen are prone to bimolecular disproportionation, forming a nitrone and a hydroxylamine.[45] Finally, smoke constituents can deactivate newly formed PBN adducts of carbon-centered radicals.[62]

Kinetic measurements of BMPO samples support the findings of a fast adduct decay, explaining the difference between the immediate (not deoxygenated) and deoxygenated measurements (Figure 4.13). In contrast ot that, radical levels of the other products decreased when the samples were measured immediately after smoking (Table 4.3). The increase in amount of radicals for the aerosols of the e-cigarettes is supported by the kinetic measurements which indicate a fast radical build-up, explaining the increase from 0.301 nmol (t = 0 min) to 2.52 nmol (t = 20 min) for *MESH* or from 0.878 nmol (t = 0 min) to 1.96 nmol (t = 20 min) for *Solaris*. Kinetic measurements of *IQOS* contradict this trend since the spin adducts show a slow long decay (Figure 4.13) and thus a higher initial concentration is expected. The increase from 1.64 nmol (t = 0 min) to 2.67 nmol (t = 20 min) is a direct contrast to the kinetic measurement. However, for one measurement point the integral seams to be increasing. The same was found for kinetic measurements of PBN, but the error and time difference between single measurements is too great to be relied upon. Without a thorough investigation to bridge the gap in the between the two *IQOS* experiments of BMPO the kinetics can not be determined. Possible is an initial increase in radical levels followed by a slow decay, as observed for spin adducts in aged cigarette smoke (adduct intensity increases for a short period as the smoke ages before entering the spin trap solution) and for NO_2 in gas phase of cigarette smoke.[34, 41] This could imply a continuous production of radicals in the aerosols, similar to the "steady-state mechanism".

Since the increase in adduct intensity was found in BMPO as well as PBN measurements for e-cigarette aerosols, this could indicate a different mechanism of radical production. Further, this poses the question of toxicity assessment, as immediately inhaled aerosols could initially contain less radicals and the radical level could increase over time. If the steady-state hypothesis is more accurate, than the radical level should reach a steady level over time. Kinetic measurement of PBN adducts of the *Solaris* aerosol (Figure 4.11 **C**) supports this idea as the intensity does not vary significantly between 450 and 1250 min.

In the same study kinetics of NO trapping were examined. Following the example of Shinagawa *et al.* [36], the authors used equation 4.3 to fit the results of the first 25 min. We decided to prolong the fit to the whole data set and found sufficient agreement between the data and the fit (Figure 4.16 **B**). Shinagawa *et al.* reported a rate constant of 0.018 1/s. Surprisingly, this corresponds to the rate constant found in whole smoke. However, Shinagawa *et al.* passed the smoke through a Milipore AP 200 filter, so it is expected for them to measure gas phase NO. In our study, MNIC-DETC concentration from whole smoke reaches a maximum concentration of 1.3 times the initial concentration and then slowly decays. Gas phase measurements show a much faster increase in concentration which has not reached its maximum (approx. 2.9 times the initial concentration) after 800 min. This is unexpected: Fe(II) can easily be oxidized to the EPR silent Fe(III) by the heated air, halogens and NO_2 bubbled through the spin trap solutions.[35, 36] NO does not react with Fe(III) complexes.[55] This would suggest that in a setup with strongly oxidizing gas phase, NO trapping would be limited by availability of the spin trapping reagent. On the other hand, whole smoke is less oxidizing and the uptake of NO should be higher. Oxidized spin trap could be eventually reduced (e.g. by NO itself with a resulting yield of 50%[28]), however, this reaction should rather occur in whole smoke than in gas phase. Instead, the final mass of gas phase NO ($m_{max} \approx 35.7\ \mu g$) is even higher than that of the whole smoke ($m_{max} \approx 27.7\ \mu g$). No additional NO sources are expected to exist in the spin trap solution injected into the AquaX and NO should slowly react with dissolved oxygen to NO_2.[27, 28] Thus, nitric oxide which is already dissolved in toluene must slowly react with spin trapping reagent. However, is possible that new NO is formed from nitrite. The reaction of Fe(II)-$(MGD)_2$ with nitrite has been demonstrated at different pH-levels.[116] Interestingly, increase in NO concentration follows a very similar curve as measured in this work. Further, NO formation rate and concentration increases with lower pH-values. Nicotine (dibasic) is found predominantly in particulate phase.[1] Hence, it is plausible that whole smoke could have a higher pH-value than the gas phase, although the concept of a pH-value poorly applies to a toluene solution.

NO concentration produced from *IQOS* stays constant over a period of 450 min. This supports the findings of kinetic measurements of with PBN adducts where no change in radical intensity was observed. Considering the importance of NO in radical production in smoke it seems likely that the stable adduct concentration observed with PBN is related to the stable NO concentration.

Chapter 6

Conclusion

Free radical and NO levels and kinetics in mainstream smoke or aerosols created by different tobacco products have been studied by EPR spectroscopy. Short-lived radicals from the gas phase have been spin trapped with PBN and BMPO, while toluene extracts of Total Particulate Matter were analyzed for long-lived radicals. NO was trapped from whole smoke by Fe(II)-$(DETC)_2$ complexes.

The tobacco products were chosen to represent a broad variety of "smoking" products, including a conventional cigarette (3R4F research cigarette), a heat-not-burn product (*IQOS*) and two e-cigarettes with different liquid heating mechanisms (*Solaris* and *MESH*).

PBN spin trapping experiments revealed a hundredfold reduction in gas phase radical levels of the aerosols generated by *IQOS* and e-cigarettes in comparison to 25.9 nmol found in 3R4F smoke. *IQOS* showed a slightly higher radical production than the two e-cigarettes, however, for both *IQOS* and the e-cigarettes the intensity of the radical adduct signals was close to the background levels. For all four products fitting parameters suggest a presence of alkoxy radicals and an oxidation product of PBN.

Spin trapping experiments with BMPO suffered from poor reproducibility, but indicated significantly higher concentrations of trapped radicals than found with PBN. While the main radicals trapped from 3R4F smoke by PBN were alkoxy radicals, BMPO trapped mostly superoxide and hydroxyl radicals. Spin adducts decayed fast, such that 82 nmol of radicals found in 3R4F samples immediately after smoking decreased to 42 nmol after 20 min. This emphasizes the importance of fast measurements immediately after smoking and of a constant time lag between smoking and the measurement, especially when adduct decay kinetics are fast, in order not to underestimate the amount of radicals truly inhaled by the smoker. Radical levels of aerosols varied from 1.1% to 6.5% of the 3R4F signal, depending on the product and measurement time. For *IQOS* a slightly higher amount of radicals (2.7 nmol after 20 min) than produced by the e-cigarettes (2–2.5 nmol after 20 min) was found. Since no air blanks have been measured the error margin of these findings remains uncertain.

Absolute levels of NO were found by more than one order of magnitude lower than those found in previous publications by different analysis methods for both 3R4F smoke and *IQOS* aerosol. This could be a result of incomplete trapping due to limited contact time in the solution. However, the relative amount of NO between the two products appear rather well between different analysis methods. No nitric oxide has been trapped from aerosols of either e-cigarette. Immediately after smoking, in the gas phase of the cigarette smoke only 75% of NO from the whole smoke were found. Kinetic measurements, nonetheless, showed a faster increase in NO mass over time in gas phase in comparison to the whole smoke measurement which lead ultimately to a higher end-value.

A significant amount of particulate phase radicals was only found in 3R4F smoke. Most measurements of the particulate phase suffered from low sensitivity due to dilution. *MESH* produced most

particulate (52.4 mg), followed by the 3R4F cigarette (32.6 mg) and followed by *IQOS* and *Solaris* with similar TPM masses (26.1 mg and 23.8 mg, respectively).

In conclusion, radical levels produced by the HNB-product *IQOS* and by the e-cigarettes *MESH* and *Solaris* were 94-99% lower than those of the research cigarette 3R4F and generally similar to background levels. No nitric oxide was found in aerosols of the e-cigarettes and only 6-7% of the 3R4F level was found in the aerosol of *IQOS*.

Chapter 7

Outlook

The general findings of this thesis prove a significant reduction in NO and radical levels of tobacco product aerosols in comparison to smoke of conventional cigarettes. However, some questions remain unanswered and several results are uncertain.

First and foremost, BMPO measurements have to be repeated, since the reproducibility of these experiments was insufficient. Additionally, it is important to measure machine background with BMPO to verify whether the small amounts of radicals trapped for *IQOS* and the e-cigarettes are significant. Furthermore, coupling constants of model compounds with BMPO in organic solvents have to be studied to better understand the identity of trapped radical from cigarette smoke. Radical evaluation with different spin traps might be helpful as well.

Measurements of particulate phase radicals were inconclusive for *IQOS*, *MESH* and *Solaris*. The main reason for this is the low spin adduct concentration of the toluene extracts. Solvent evaporation and extraction of several filters may improve sensitivity.

Puffing numbers of 3R4F cigarettes varied greatly and were sometimes unusually high. Results of experiments with extraordinarily high puff count numbers (17, 20) should be dismissed and such experiments repeated.

Our results hint at somewhat higher radical levels in the HNB product in comparison to the e-cigarettes. These differences in amount of radicals should be studied more carefully, perhaps with multiport smoking machines to allow simultaneous accumulation of puffs for higher sensitivity.

The overall toxicity of radicals in smoke and aerosols of various tobacco products remains unclear and should be studied further.

Chapter 8

Acknowledgment

First and foremost I want to express my gratitude to Prof. Dr. Gunnar Jeschke for giving me the opportunity to work on this exciting project and being a supportive and involved supervisor while at the same time leaving room for me to make my own mistakes. Special thanks go to Dr. Daniel Klose for his review of the thesis and for helpful discussions along the way. I want to thank Oliver Oberhänsli and his co-workers in the mechanical workshop for technical support especially in the first weeks and the design of ToluX. I am grateful to Rene Tschaggelar for his assistence with the cleaning of the resonator, for his help with the glassware (even if it didn't work out) and his advices over the course of this thesis. I thank Christoph Gmeiner for taking the workload off me by purchasing my chemicals. Moreover, my thanks go to Luis I. Fábregas for having an open ear and for his assistance with data evaluation.

I wish to thank Philip Morris International for covering the expenses of this study and providing me with the necessary equipment. I would like to specifically thank Arno Knorr in his role as the communicator for the project, Falk Radtke and Andrée Stoop for the introduction to cigarette machine smoking and Mark Bentley as the head of group.

Finally, my gratitude goes to all the unnamed members of the EPR group for a warm welcome and constant support over the course of these months. I really enjoyed my stay with you!

Appendix A

Residue and error estimation

Table A.1: Testing of ToluX with toluene and AquaX with water. Solutions: A = toluene, B = TEMPOL in water (50μM). Parameters: power attenuation 20 dB, modulation amplitude 0.5 G, receiver gain 50 dB, 10 scans. For sensitive measurements, parameters were changed to: modulation amplitude 2 G, receiver gain 60 dB, 30 scans.

		ToluX, toluene		AquaX, water	
Exp. no.	sample	volume [mL]	rel. integral[a]	volume [mL]	rel. integral[b]
0	A	full[c]	-[d]	full[c]	0
1	B	2	0.977	1	-[d]
2	A	2	0.064	1	0.0652
3	B	2	1.0378	1	0.888
4	A	4	0.0139	1	0.106
5	B	2	1.0139	1	0.931
6	A	6	0.0067	2	0[e]
7	B	2	1.0060	2	1
8	A	8	0.0060	2	0[e]
9	B	2	1.0056	3	0.997
10	A	16	0[e]	2	0[e]
11	B	2	1	1.5	0.988
12	A	20	0[e]	1.5	0[e]
13	B	1.5	0.970		
13	A	20	0[e]		

[a] in comparison to the integral of exp. no. 11
[b] in comparison to the integral of exp. no. 7
[c] device completely filled with toluene/water
[d] no spectrum saved
[e] below detection or quantification limit, relative intensity is set to 0

Appendix B

Best fits

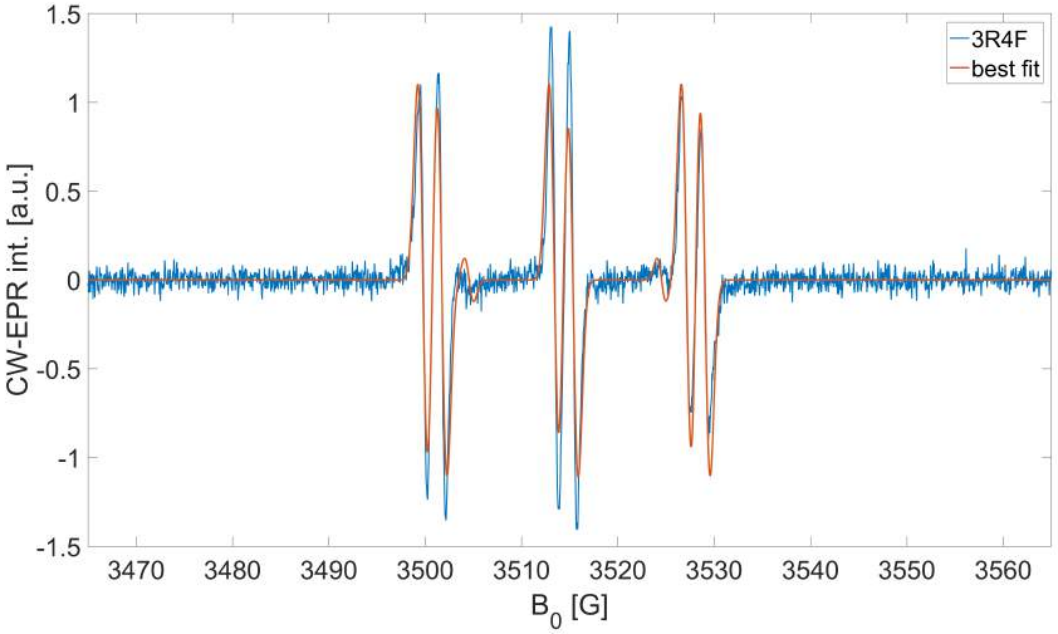

Figure B.1: Best fit of the PBN spectrum of 3R4F cigarettes measured with a modulation amplitude of 0.3 G.

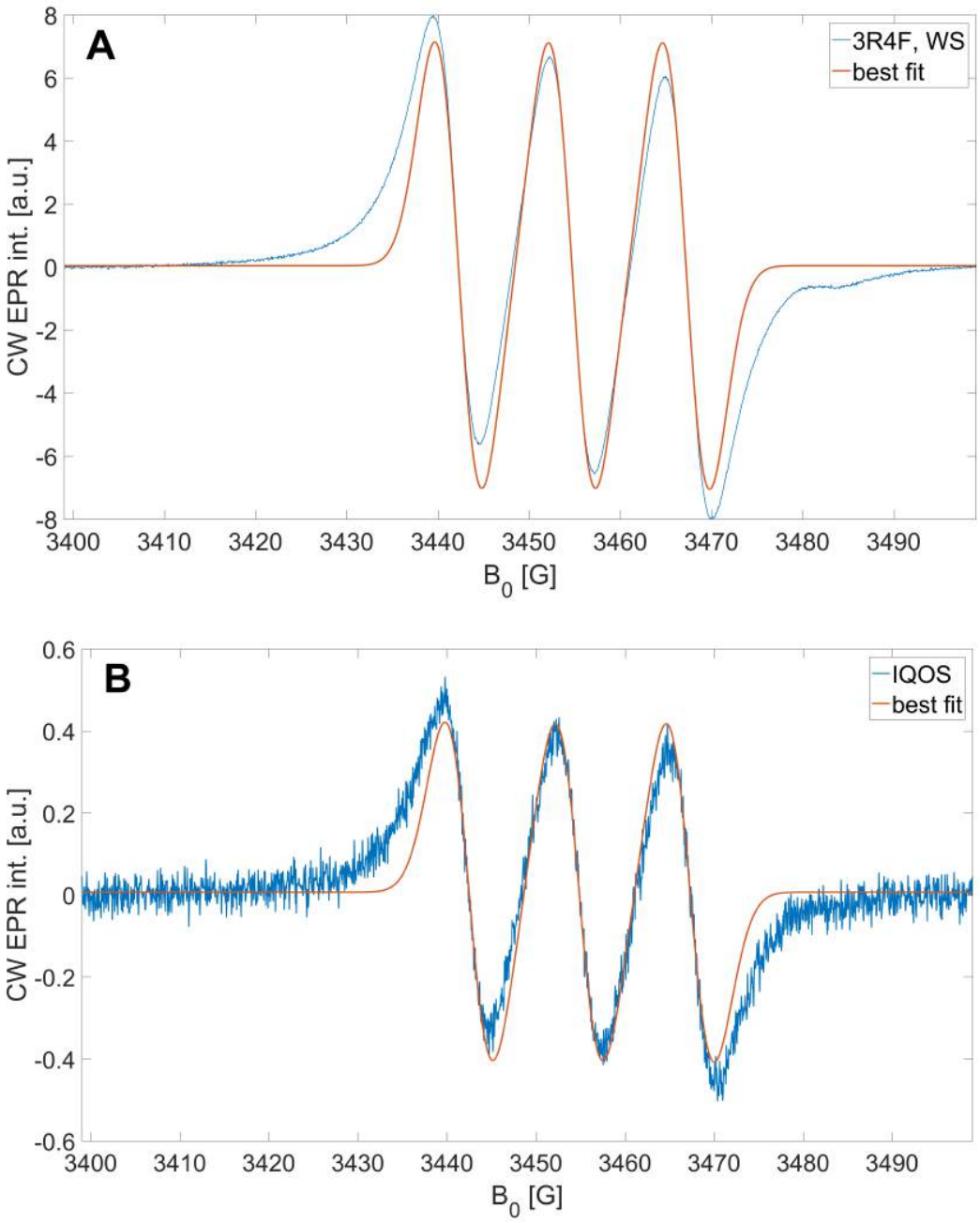

Figure B.2: Best fits of MNIC-DETC spectra of 3R4F (**A**) and *IQOS* (**B**).

Appendix C

Spin concentration calibration with TEMPOL

For concentration calibrations, TEMPOL was used as a stable nitroxide. Four 4 mL toluene solutions with respective concentrations of 0.05 μM, 0.5 μM, 5 μM and 50 μM were prepared by diluting a TEMPOL stock solution of 522.5 μM. For EPR measurements the spin trap radical analysis procedure was imitated:

- All TEMPOL solutions were deoxygenated using three cycles of freeze-pump-thaw.
- Prior to the first measurement AquaX was filled with toluene.
- Measurement order was from the lowest concentration to the highest.
- Between measurements the AquaX was flushed with 10 mL pure toluene.

A double logarithmic plot of double integral against concentration (c, in nmol/L) is shown in figure C.1. The linear calibration fit has form $y = 0.9938c + 0.6533$.

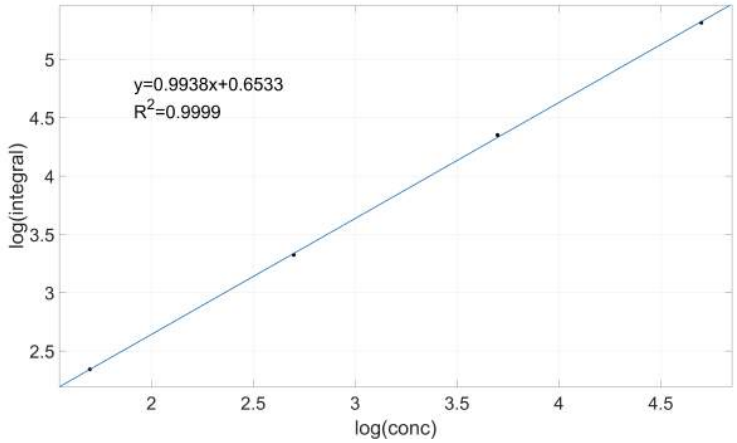

Figure C.1: Spin concentration calibration curve based on TEMPOL measurement. The logarithm of the double integral is plotted against the logarithm of TEMPOL concentration (in nM).

Appendix D

Miscellaneous

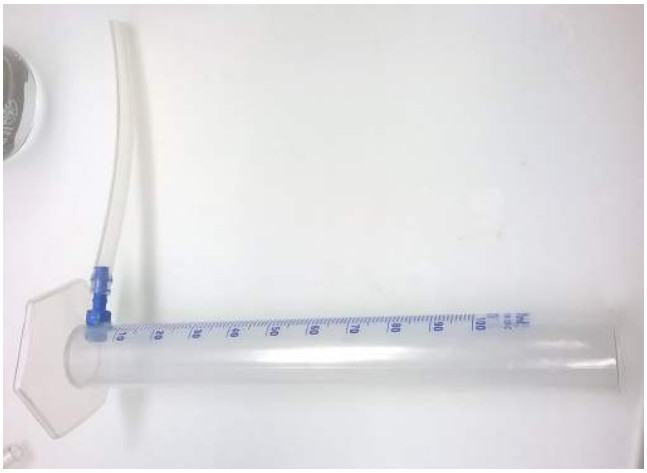

Figure D.1: Soap bubble flow meter. The bubble surface level is adjusted with a syringe to 100 mL and then the silicon tube is inserted into the cigarette holder of the smoking machine. During the puff, the soap bubble moves down towards the silicon tube. The difference in bubble level before and after the puff indicates the real puff volume.

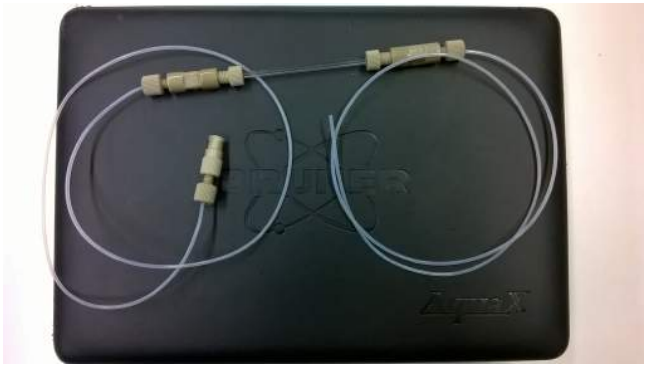

Figure D.2: AquaX system outside of the resonator. Two tubing adapters are provided but only one used in this study. The attached adapter is necessary for sample injection while the loose tubing is placed inside a waster container.

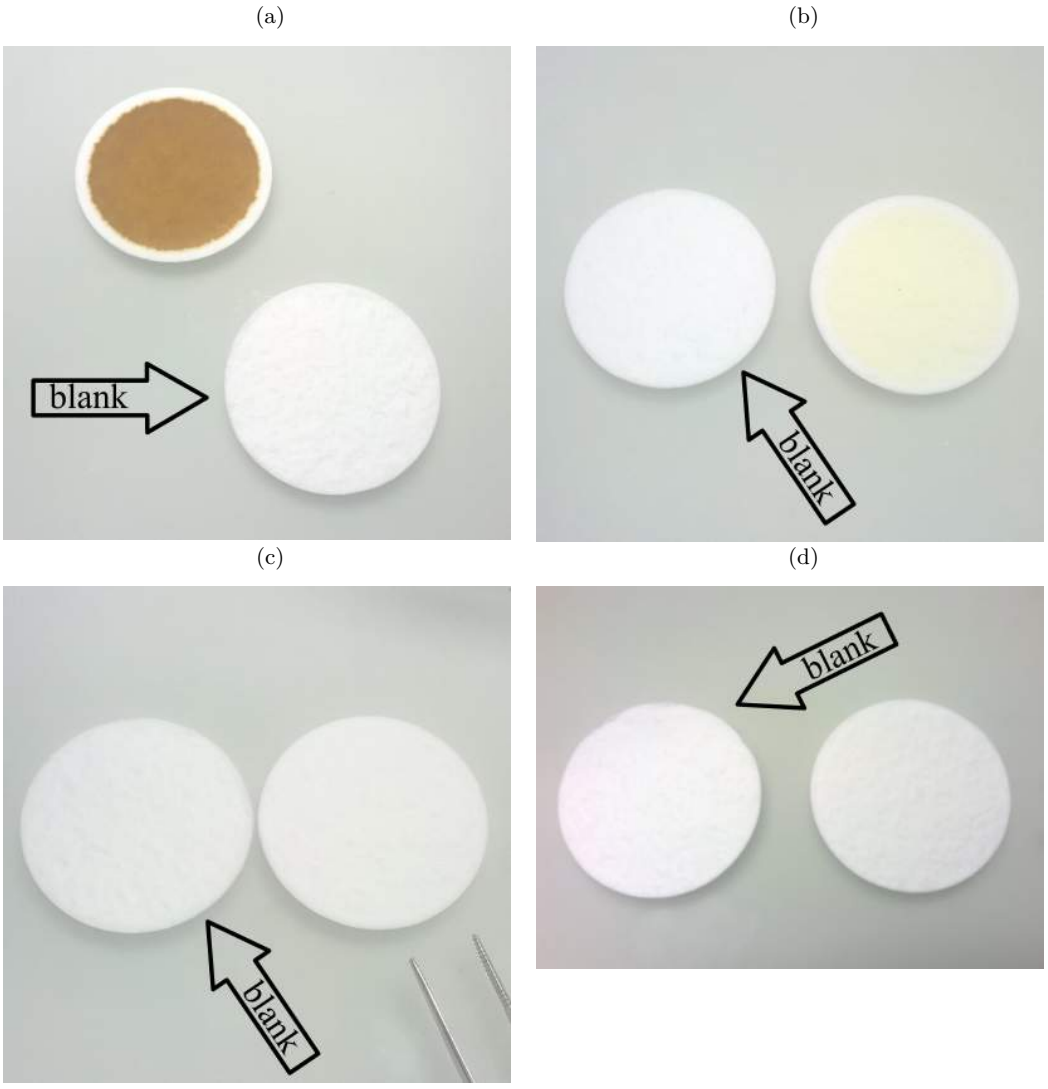

Figure D.3: Photos of Cambridge Filters after smoking of three cigarettes/sticks etc. In case of *MESH*, only two smoking experiments were accumulated. For comparison, a clean Cambridge Filter is placed beside the filter with the particulate. The arrow points at the clean reference filters. **(a)**: Filter from the 3R4F cigarette experiment. **(b)**: Filter from the *IQOS* experiment. **(c)**: Filter from the *MESH* experiment. **(d)**: Filter from the *Solaris* cigarette experiment.

Bibliography

(1) Baker, R. R. In *Tobacco. Production, Chemistry and Technology*, Davis, L., Nielsen, M. T., Eds.; Blackwell Science Ltd.: Oxford, 1999, pp 398–439.
(2) Baker, R. R. *Progress in Energy and Combustion Science* **2006**, *32*, 373–385.
(3) Rodgman, A.; Perfetti, T. A., *The Chemical Components of Tobacco and Tobacco Smoke, Second Edition*, 2nd ed.; CRC Press: Boca Raton, 2013.
(4) Harmful and Potentially Harmful Constituents in Tobacco Products and Tobacco Smoke: Established List. US Food and Drug Administration, `https://www.fda.gov/TobaccoProducts/Labeling/RulesRegulationsGuidance/ucm297786.htm` (accessed 02/01/2018).
(5) *The Health Consequences of Smoking—50 Years of Progress: A Report of the Surgeon General*; National Center for Chronic Disease Prevention, Health Promotion (US). U.S. Department of Health, and Human Services, 2014.
(6) Burns, D. M.; Dybing, E.; Gray, N.; Hecht, S.; Anderson, C.; Sanner, T.; O'Connor, R.; Djordjevic, M.; Dresler, C.; Hainaut, P.; Jarvis, M.; Opperhuizen, A.; Straif, K. *Tob. Control* **2008**, *17*, 132–141.
(7) Wooten, J. B. *Mini-Rev. Org. Chem.* **2011**, *8*, 412–426.
(8) Gilbert, H. A. Smokeless non-tobacco cigarette., US Patent 3,200,819, 1965.
(9) Hon, L. An aerosol electronic cigarette., WO Patent App. PCT/CN2005/000,337, 2005.
(10) Dawkins, L.; Turner, J.; Roberts, A.; Soar, K. *Addiction* **2013**, *108*, 1115–1125.
(11) Pryor, W. A.; Church, D. F.; Evans, M. D.; Rice, W. Y.; Hayes, J. R. *Free Radic. Biol. Med.* **1990**, *8*, 275–279.
(12) Caputi, T. L. *Tobacco Control* **2017**, *26*, 609–610.
(13) *Public Health Consequences of E-Cigarettes*; Washington, DC: National Academies of Sciences, Engineering, and Medicine, 2018.
(14) Belluz, J. *Philip Morris wanted to market a new tobacco device as safer than cigarettes. An FDA panel said no.* `https://www.vox.com/science-and-health/2018/1/26/16935950/safer-cigarette-iqos-heat-not-burn-fda` (accessed 02/10/2018).
(15) Drummond, M. B.; Upson, D. *Ann. Am. Thorac. Soc.* **2014**, *11*, 236–242.
(16) Lyons, M. J.; Gibson, J. F.; Ingram, D. J. E. *Nature* **1958**, *181*, 1003–1004.
(17) Bluhm, A. L.; Weinstein, J.; Sousa, J. A. *Nature* **1971**, *229*, 500.
(18) Borish, E. T.; Cosgrove, J. P.; Church, D. F.; Deutsch, W. A.; Pryor, W. A. *Biochem. Biophys. Res. Commun.* **1985**, *133*, 780–786.
(19) Valavanidis, A.; Vlachogianni, T.; Fiotakis, K. *Int. J. Environ. Res. Public Health* **2009**, *6*, 445–462.
(20) Church, D. F.; Pryor, W. A. *Environ. Health Perspect.* **1985**, *64*, 111–126.
(21) Messner, B.; Bernhard, D. *Arterioscler. Thromb. Vasc. Biol.* **2014**, *34*, 509–515.
(22) Domej, W.; Oettl, K.; Renner, W. *Int. J. Chron. Obstruct. Pulmon. Dis.* **2014**, *9*, 1207–1224.
(23) Andersen, J. K.; Davies, K. J. A.; Forman, H. J. *Free Radic. Biol. Med.* **2013**, *62*, 1–3.
(24) Pryor, W. A.; Prier, D. G.; Church, D. F. *Environ. Health Perspect.* **1983**, *47*, 345–355.
(25) Dellinger, B.; Khachatryan, L.; Maskos, Z.; Lomnicki, S. *Mini-Rev. Org. Chem.* **2011**, *8*, 427–433.
(26) Robinson, E. A.; Johnson, J. D. *Mini Rev Org Chem* **2011**, *8*, 401–411.

(27) Pryor, W. A.; Tamura, M.; Church, D. F. *J. Am. Chem. Soc.* **1984**, *106*, 5073–5079.
(28) Villamena, F. A.; Zweier, J. L. *Antioxid. Redox Signal.* **2004**, *6*, 619–629.
(29) Wei, T.; Chen, C.; Hou, J.; Xin, W.; Mori, A. *Biochim Biophys Acta.* **2000**, *1498*, 72–79.
(30) Schaller, J.-P.; Pijnenburg, J. P. M.; Ajithkumar, A.; Tricker, A. R. *Regul. Toxicol. Pharmacol.* **2016**, *81*, S48–S58.
(31) Gonzalez-Suarez, I.; Martin, F.; Marescotti, D.; Guedj, E.; Acali, S.; Johne, S.; Dulize, R.; Baumer, K.; Peric, D.; Goedertier, D.; Frentzel, S.; Ivanov, N. V.; Mathis, C.; Hoeng, J.; Peitsch, M. C. *Chem. Res. Toxicol.* **2016**, *29*, 3–18.
(32) Roemer, E.; Schramke, H.; Weiler, H.; Buettner, A.; Kausche, S.; Weber, S.; Berges, A.; Stueber, M.; Muench, M.; Trelles-Sticken, E.; Pype, J.; Kohlgrueber, K.; Voelkel, H.; Wittke, S. *Beitr. Tabakforsch. Int.* **2012**, *25*, 316–335.
(33) Shorter, J. H.; Nelson, D. D.; Zahniser, M. S.; Parrish, M. E.; Crawford, D. R.; Gee, D. L. *Spectrochim. Acta A, Mol. Biomol. Spectrosc.* **2006**, *63*, 994 –1001.
(34) Cueto, R.; Pryor, W. A. *Vibrational Spectroscopy* **1994**, *7*, 97–111.
(35) Vanin, A. F. In *Nitric Oxide Part C: Biological and Antioxidant Activities*; Methods Enzymol. Vol. 301; Academic Press: 1999, pp 269–279.
(36) Shinagawa, K.; Tokimoto, T.; Shirane, K. *Biochem. Biophys. Res. Commun.* **1998**, *253*, 99–103.
(37) Cheng, T. *Tob. Control* **2014**, *23*, ii11–ii17.
(38) Geiss, O.; Bianchi, I.; Barahona, F.; Barrero-Moreno, J. *Int. J. Hyg. Environ. Health* **2015**, *218*, 169–180.
(39) Corvaja, C. In *Electron Paramagnetic Resonance: A Practitioner's Toolkit*, Brustolon, M., Giamello, E., Eds.; John Wiley & Sons, Inc.: Hoboken, New Jersey, 2008, pp 1–36.
(40) Baum, S. L.; Anderson, I. G. M.; Baker, R. R.; Murphy, D. M.; Rowlands, C. C. *Anal. Chim. Acta* **2003**, *481*, 1–13.
(41) Pryor, W. A.; Terauchi, K.-i.; Davis, W. H. J. *Environ. Health Perspect.* **1976**, *16*, 161–175.
(42) Povich, M. J. *J. Phys. Chem.* **1975**, *79*, 1106–1109.
(43) Janzen, E. G. *Acc. Chem. Res.* **1971**, *4*, 31–40.
(44) Janzen, E. G. In *Bioradicals Detected by ESR Spectroscopy*, Ohya-Nishiguchi, H., Packer, L., Eds.; Birkhäuser Basel: Basel, 1995, pp 113–142.
(45) Church, D. F. *Anal. Chem.* **1994**, *66*, 419A–427A.
(46) Hawkins, C. L.; Davies, M. J. *Biochim. Biophys. Acta — Gen. Subj.,* **2014**, *1840*, 708–721.
(47) Buettner, G. R. *Free Radic. Biol. Med.* **1987**, *3*, 259–303.
(48) Spin Trap database. National Institute of Environmental Health Sciences, `https://tools.niehs.nih.gov/stdb/` (accessed 01/25/2018).
(49) Finkelstein, E; Rosen, G. M.; Rauckman, E. J. *Mol. Pharmacol.* **1982**, *21*, 262–265.
(50) Ghosh, M.; Liu, C.; Ionita, P. *ARKIVOC*, *2008*, 318–327.
(51) Zhao, H.; Joseph, J.; Zhang, H.; Karoui, H.; Kalyanaraman, B. *Free Radic. Biol. Med.* **2001**, *31*, 599–606.
(52) Krainev, A. G.; Williams, T. D.; Bigelow, D. J. *J. Magn. Reson. B* **1996**, *11*, 272–280.
(53) Chalier, F.; Tordo, P. *J. Chem. Soc., Perkin Trans. 2* **2002**, 2110–2117.
(54) Nedeianu, S.; Páli, T. *Cell Mol. Biol. Lett.* **2002**, *7*, 142–143.
(55) Paschenko, S. V.; Khramtsov, V. V.; Skatchkov, M. P.; Plyusnin, V. F.; Bassenge, E. *Biochem. Biophys. Res. Commun.* **1996**, *225*, 577–584.
(56) Menzel, E. R.; Vincent, W. R.; Wasson, J. R. *J. Magn. Reson.* **1976**, *21*, 321 –330.
(57) Tully, G. W.; Briggs, C. D.; Horsfield, A. *Chem. Ind. (London)* **1969**, *7*, 201–203.
(58) Borland, C. D. R.; Chamberlain, A. T.; Higenbottam, T. W.; Barber, R. W.; Thrush, B. A. *Beitr. Tabakforsch. Int.* **1985**, *13*, 67–73.
(59) Caldwell, W. S.; Conner, J. M. *J. Assoc. Off. Anal. Chem.* **1990**, *73*, 783–789.
(60) Culcasi, M.; Muller, A.; Mercier, A.; Clément, J.-L.; Payet, O.; Rockenbauer, A.; Marchand, V.; Pietri, S. *Chem. Biol. Interact.* **2006**, *164*, 215–231.
(61) Bartalis, J.; Chan, W. G.; Wooten, J. B. *Anal. Chem.* **2007**, *79*, 5103–5106.
(62) Bartalis, J.; Zhao, Y.-L.; Flora, J. W.; Paine, J. B.; Wooten, J. B. *Anal. Chem.* **2009**, *81*, 631–641.

(63) ISO 3308:2012. *Routine analytical cigarette-smoking machine — Definitions and standard conditions.*
(64) Goel, R.; Bitzer, Z.; Reilly, S. M.; Trushin, N.; Foulds, J.; Muscat, J.; Liao, J.; Elias, R. J.; Richie, J. P. *Chem. Res. Toxicol.* **2017**, *30*, 1038–1045.
(65) ISO 4387:2000. *Cigarettes — Determination of total and nicotine-free dry particulate matter using a routine analytical smoking machine.*
(66) Health Canada Official Method T-115:1999. *Determination of "Tar", Nicotine and Carbon Monoxide in Mainstream Tobacco Smoke.*
(67) CORESTA recommended method no. 81. *Routine Analytical Machine for E-Cigarette Aerosol Generation and Collection — Definitions and Standard Conditions*, 2015.
(68) Farsalinos, K. E.; Romagna, G.; Tsiapras, D.; Kyrzopoulos, S.; Voudris, V. *Int. J. Environ. Res. Public Health* **2013**, *10*, 2500–2514.
(69) Spindle, T. R.; Breland, A. B.; Karaoghlanian, N. V.; Shihadeh, A. L.; Eissenberg, T. *Nicotine Tob. Res.* **2014**, *17*, 142–149.
(70) Talih, S.; Balhas, Z.; Eissenberg, T.; Salman, R.; Karaoghlanian, N.; El Hellani, A.; Baalbaki, R.; Saliba, N.; Shihadeh, A. *Nicotine Tob. Res.* **2015**, *17*, 150–157.
(71) 3R4F Preliminary Analysis. Center for Tobacco Reference Products, University of Kentucky, `https://ctrp.uky.edu/resources/pdf/webdocs/3R4F%20Preliminary%20Analysis.pdf` (accessed 01/29/2018).
(72) PMI R&D. Philip Morris International, Inc. *Scientific update for smoke-free products. Issue 02*, 2017.
(73) Our Tobacco heating System *IQOS*. Tobacco meets technology. Philip Morris International, `https://www.pmi.com/smoke-free-products/iqos-our-tobacco-heating-system` (accessed 01/30/2018).
(74) Making Heated Tobacco Products. What's in our Heated Tobacco Products? Philip Morris International, Inc., `https://www.pmi.com/our-business/about-us/products/making-heated-tobacco-products` (accessed 01/30/2018).
(75) Taking E-cigarettes further. E-Vapor Products. Philip Morris International, Inc., `https://www.pmi.com/smoke-free-products/mesh-taking-e-cigarettes-further` (accessed 01/23/2018).
(76) Homepage of MarkTen. `https://www.markten.com/` (accessed 01/30/2018).
(77) Tucker, C.; Jordan, G. Electronic smoking article and improved heater element., US Patent App. 13/774,609, 2013.
(78) Homepage of Nicocigs. `https://www.nicocig.co.uk/` (accessed 01/23/2018).
(79) Product information guide. MarkTen, `https://www.markten.com/skin/frontend/markten/default/uploads/product-info-guide.pdf?c75d89f18215d65f9f8fdf53487dbb18` (accessed 01/31/2018).
(80) How long does a single Mark Ten XL cartridge last? `https://help.electrictobacconist.com/support/solutions/articles/9000132143-how-long-does-a-single-mark-ten-xl-cartridge-last` (accessed 01/31/2018).
(81) Santos, J. H.; Bond, A. M.; Mocak, J.; Cardwell, T. J. *Anal. Chem.* **1994**, *66*, 1925–1930.
(82) Health Canada Official Method T-212:1999. *Determination of "Tar" and Nicotine in Sidestream Tobacco Smoke.*
(83) Mason, T.; Tindall, I. *TSRC, Tob. Sci. Res. Conf.* **2011**, *65*, abstr. 25.
(84) Jeschke, G., *Kurze Einführung in die elektronenparamagnetische Resonanzspektroskopie*; Lehrstuhl PC: Struktur und Dynamik der Materie, Universität Konstanz: 2008.
(85) Hofmann, M. Apparatus for analyzing a liquid sample using a multiple-lumen capillary., US Patent App. 11/798,345, 2007.
(86) EPR Accessories. The Solutions for Multiple-Choice EPR Experiments. Bruker BioSpin, `https://www.bruker.com/fileadmin/user_upload/8-PDF-Docs/MagneticResonance/EPR_brochures/EPR_accessories.pdf` (accessed 01/31/2018).
(87) Stoll, S.; Schweiger, A. *J. Magn. Reson.* **2006**, *178*, 42–55.
(88) Stoll, S. In *Multifrequency Electron Paramagnetic Resonance*; Wiley-VCH Verlag GmbH & Co. KGaA: 2014, pp 69–138.

(89) CORESTA recommended method no. 23. *Determination of Total and Nicotine-Free Dry Particulate Matter Using a Routine Analytical Cigarette-Smoking Machine — Determination of Total Particulate Matter and Preparation of Water and Nicotine Measurements*, 1991.
(90) Huang, M. F.; Lin, W. L.; Ma, Y. C. *Indoor Air* **2005**, *15*, 135–140.
(91) Zhao, J.; Hopke, P. K. *Aerosol Sci. Technol.* **2012**, *46*, 191–197.
(92) Goel, R.; Durand, E.; Trushin, N.; Prokopczyk, B.; Foulds, J.; Elias, R. J.; Richie, J. P. *Chem. Res. Toxicol.* **2015**, *28*, 1675–1677.
(93) Yu, L. X.; Dzikovski, B. G.; Freed, J. H. *J. Vis. Exp.* **2012**, *59*, e3406.
(94) Ariciu, A.-M; Ionita, G.; Ionita, P. *Rev. Roum. Chim.* **2014**, *59*, 781–787.
(95) Wang, Y.; Liu, M.; Zhu, Y.; Cheng, K.; Wu, D.; Liu, B.; Li, F. *Talanta* **2016**, *160*, 106–112.
(96) Ghosh, M.; Ionita, P.; McAughey, J.; Cunningham, F. *ARKIVOC*, *2008*, 74–84.
(97) Halpern, A.; Knieper, J. *Z. Naturforsch* **1985**, *40b*, 850–852.
(98) Tanigawa, T.; Yoshikawa, T.; Takahashi, S.; Naito, Y.; Kondo, M. *Free Radic. Biol. Med.* **1994**, *17*, 361–365.
(99) Flicker, T. M.; Green, S. A. *Environ. Health Perspect.* **2001**, *109*, 765–771.
(100) Flicker, T. M.; Green, S. A. *Anal. Chem.* **1998**, *70*, 2008–2012.
(101) BMPO. Spin trapping reagent. Enzo Life Sciences, `http://www.enzolifesciences.com/ALX-430-141/bmpo-high-purity` (accessed 02/02/2018).
(102) PBN. Spin trapping reagent. Enzo Life Sciences, `http://www.enzolifesciences.com/ALX-430-082/pbn` (accessed 02/02/2018).
(103) Lerner, C. A.; Sundar, I. K.; Watson, R. M.; Elder, A.; Jones, R.; Done, D.; Kurtzman, R.; Ossip, D. J.; Robinson, R.; McIntosh, S.; Rahman, I. *Environ. Pollut.* **2015**, *198*, 100–107.
(104) Sussan, T. E.; Gajghate, S.; Thimmulappa, R. K.; Ma, J.; Kim, J.-H.; Sudini, K.; Consolini, N.; Cormier, S. A.; Lomnicki, S.; Hasan, F.; Pekosz, A.; Biswal, S. *PLOS ONE* **2015**, *10*, e0116861.
(105) Maskos, Z.; Dellinger, B. *Energy & Fuels* **2008**, *22*, 382–388.
(106) Khan, N.; Wilmot, C. M.; Rosen, G. M.; Demidenko, E.; Sun, J.; Joseph, J.; O'Hara, J.; Kalyanaraman, B.; Swartz, H. M. *Free Radic. Biol. Med.* **2003**, *34*, 1473–1481.
(107) Arangio, A. M.; Tong, H.; Socorro, J.; Pöschl, U.; Shiraiwa, M. *Atmos. Chem. Phys.* **2016**, *16*, 13105–13119.
(108) Huang, C.-H.; Shan, G.-Q.; Mao, L.; Kalyanaraman, B.; Qin, H.; Ren, F.-R.; Zhu, B.-Z. *Chem. Commun.* **2013**, *49*, 6436–6438.
(109) Counts, M. E.; Morton, M. J.; Laffoon, S. W.; Cox, R. H.; Lipowicz, P. J. *Regul. Toxicol. Pharmacol.* **2005**, *41*, 185–227.
(110) Purkis, S.; Intorp, M. *Beitr. Tabakforsch. Int.* **2014**, *26*, 57–73.
(111) Margham, J.; McAdam, K.; Forster, M.; Liu, C.; Wright, C.; Mariner, D.; Proctor, C. *Chem. Res. Toxicol.* **2016**, *29*, 1662–1678.
(112) Kálai, T.; Altman, R.; Maezawa, I.; Balog, M.; Morisseau, C.; Petrlova, J.; Hammock, B. D.; Jin, L.-W.; Trudell, J. R.; Voss, J. C.; Hideg, K. *Eur. J. Med. Chem.* **2014**, *77*, 343–350.
(113) Gehling, W.; Dellinger, B. *Environ. Sci. Technol.* **2013**, *47*, 8172–8178.
(114) Gehling, W.; Khachatryan, L.; Dellinger, B. *Environ. Sci. Technol.* **2014**, *48*, 4266–4272.
(115) Pope, C. A.; Burnett, R. T.; Krewski, D.; Jerrett, M.; Shi, Y.; Calle, E. E.; Thun, M. J. *Circulation* **2009**, *120*, 941–948.
(116) Tsuchiya, K.; Yoshizumi, M.; Houchi, H.; Mason, R. P. *J. Biol. Chem.* **2000**, *275*, 1551–1556.